

UNIVERSAL AQUEOUS-BASED ANTIFOULING COATINGS FOR MULTI-MATERIAL DEVICES

By
SHARON C. M. GOH
B.Sc. (Hons)

A Thesis Submitted to the School of Graduate Studies in Partial Fulfillment
of the Requirements for the Degree Master of Applied Science

McMaster University
© Copyright by Sharon C. M. Goh, April 2017

MASTER OF APPLIED SCIENCE (2016)

McMaster University

(School of Biomedical Engineering)

Hamilton, Ontario

TITLE: A universal aqueous-based antifouling coating for multi-material devices

AUTHOR: Sharon C. M. Goh,
B. Sc. (Hons) (McMaster University)

SUPERVISORS: Professor Qiyin Fang
Professor John L. Brash

NUMBER OF PAGES: xii, 97

ABSTRACT

Biofouling is an ongoing problem in the development and usage of biomaterials for biomedical implants, microfluidic devices, and water-based sensors. Antifouling coatings involving surface modification of biomaterials is widely utilized to reduce unwanted protein adsorption and cell adhesion. Surface modification strategies, however, are reliant on the working material's chemical properties. Thus, published procedures are often not applicable to a wide range of material classes. This constitutes a serious limitation in using surface modification on assembled multi-material devices, i.e on whole device modification. The objective of this research is to develop an antifouling coating with non-aggressive reaction conditions that can universally modify polymers and other material classes. Two strategies using polydopamine (PDA) as an anchor for polyethylene glycol (PEG) surface attachment were investigated: (1) PDA-PEG backfilled with bovine serum albumin (BSA), and (2) PDA-PEG with light activated perfluorophenyl azide (PFPA) conjugated to the PEG. Three materials varying in surface wettability were studied to evaluate the coatings for multi-material applications: porous polycarbonate membrane (PC), polydimethyl siloxane (PDMS), and soda lime glass cover slips.

Atomic force microscopy (AFM) and ellipsometry studies revealed substantial structural differences of PDA. Differences in PDA surface roughness affected PEG grafting in solution (the first method), with higher PEG coverage achieved on PC with intermediate surface roughness to PDMS and glass. Radiolabeled Fg adsorption and *E. coli* adhesion experiments showed reduced fouling on all PDA-PEG modified materials when backfilled with BSA. The ability for BSA to penetrate the PEG layer indicated that low PEG grafting densities were achieved using this grafting-to approach. The use of a photoactive labeling agent, PFPA, to tether PEG was proposed

to improve PEG grafting on PDA. The PFPA-PEG modification protocol was optimized by quantifying Fg adsorption. Two treatments of PFPA-PEG were required to fully block PDA active sites. Fg adsorption was not significantly improved on PFPA-PEG modified PC and glass when backfilled with BSA, indicating sufficient PEG coverage of PDA. High Fg adsorption on PFPA-PEG surfaces indicate that high density PEG brushes were still not achieved with this method. PDMS surfaces were damaged with this procedure due to increased surface handling in the protocol. This is the first, to our knowledge, successful demonstration of PFPA modification on PDA surfaces. Photopatterning of polymer-based materials can be achieved, providing opportunities for utilising new materials in cell patterned platforms. Due to low PEG coverage on PDA surfaces from solution and using PFPA, ultra-low protein adsorption cannot be achieved using these aqueous-based methods. Antifouling modifications using PDA and PEG should be applied for short-term cell studies.

ACKNOWLEDGEMENTS

I would like to thank many of my colleagues, friends, and family for their support and guidance throughout my time at McMaster University. Firstly, I would like to thank my supervisors, Dr. Fang and Dr. Brash, for all their support for the past three years. Dr. Fang, thank you for all the endless opportunities, providing a wonderful learning environment, and for training me to become a better engineer. Your work which facilitates collaboration between engineers and biologists is the true definition of biomedical research. Dr Brash, thank you for your extreme passion for biomaterials research which has prevented you from fully retiring and giving me the opportunity to work alongside a renowned professional in the field. I would also like to thank my advisory committee, Dr. Chen, Dr. Geng, Dr. Selvaganapathy and Dr. Schellhorn, for all their valuable suggestions and comments throughout my project. Dr. Chen, thank you for taking me into your lab group at Suzhou University and pairing me with wonderful students to help me with my project.

To Allison Yeh and Anthony Tsikoras, thank you for having confidence in me as a colleague and hiring me as an undergraduate research assistant in the summer of 2013. Without you two, I would not have been able to work with Dr. Fang's group nor developed interest in biomedical engineering. Thank you, Eric Mahoney, for lending your ear to hear my lab woes and for offering many suggestions for improvement. To Leo Hsu and Nehad Hirmiz, thank you for offering training and advice multiple times throughout my graduate studies. To Rena Cornelius, thank you for having so much patience with me when I first started lab work and for training me on many essential lab skills. Thank you Darren Sandejas for keeping me company in the lab and for radiolabelling for me during my pregnancy.

To the many graduate students involved in my project, Xiaojing Wang, Yafei Luan, Hui Du, and Deepinder Sharma, thank you for all your hard work and for pushing with me to finish this project. Your experience, emotional support, and much needed suggestions during our experiment woes were invaluable. I could not have completed my thesis without any of you.

Finally I would like to thank my family members for all their emotional and financial support. To mom, dad, and my lifelong partner Kevin Yi Zhang, thank you for all your words of wisdom and for giving me the confidence to complete my master's degree. You all saw greater things in me that I could not see in myself. To my monkey child still in the womb, Zachary Tianming Zhang, thank you for being such a good baby and for making my last year at McMaster so memorable.

ABSTRACT	ii
ACKNOWLEDGEMENTS	iv
LIST OF FIGURES	ix
LIST OF TABLES	xi
LIST OF ABBREVIATIONS	xii
1. INTRODUCTION AND OBJECTIVES	1
2. LITERATURE REVIEW	4
2.1 THE BIOFOULING PROBLEM.....	4
2.1.1 <i>Marine Biofouling</i>	4
2.1.2 <i>Biofouling of Water Quality Monitoring Devices</i>	5
2.1.3 <i>Biofouling in Biomedical Applications</i>	7
2.2 PROTEIN ADSORPTION.....	8
2.2.1 <i>Electrostatic Attraction</i>	8
2.2.2 <i>Protein Orientation on Solid Surfaces</i>	9
2.2.3 <i>Mixed Protein Adsorption</i>	10
2.3 ANTIFOULING STRATEGIES	11
2.3.1 <i>Hydrophilic Polymers</i>	11
2.3.2 <i>Grafting Hydrophilic Polymers</i>	12
2.3.3 <i>Limitations of Hydrophilic Polymers</i>	14
2.4 POLYDOPAMINE: A UNIVERSAL “BIO GLUE”	15
2.4.1 <i>Dopamine Polymerization on Surfaces</i>	16
2.4.2 <i>Post-modification of PDA</i>	17
2.4.3 <i>PDA-PEG Antifouling Surfaces</i>	23
2.4.4 <i>Limitations of PDA-PEG</i>	23
2.5 BLOCKING PROTEINS	25
3. MATERIALS AND METHODS	27
3.1 MATERIALS	27
3.2 METHODS.....	27

3.2.1 Substrate Preparation	27
3.2.2 PDA Surface Preparation.....	28
3.2.3 PEG Grafting on PDA.....	28
3.2.4 BSA Blocking of PDA	28
3.2.5 PDA-PEG/BSA and PDA-BSA/PEG Modification.....	29
3.2.6 Water Contact Angles.....	29
3.2.7 X-ray Photoelectron Spectroscopy (XPS)	29
3.2.8 Atomic Force Microscopy (AFM)	30
3.2.9 Ellipsometry.....	31
3.2.10 Protein Radiolabelling	32
3.2.11 Stability of BSA Modified Surfaces in Contact with PBS, BSA, and FBS	32
3.2.12 BSA Adsorption	33
3.2.13 Fibrinogen Adsorption	33
3.2.14 E. coli Adhesion.....	33
3.3 STATISTICAL ANALYSIS	34
4. PC, PDMS, AND GLASS SURFACES MODIFIED WITH PEG AND BSA USING POLYDOPAMINE AS A BIO GLUE.....	35
4.1 RESULTS AND DISCUSSION	35
4.1.1 Stability of BSA Attached to PDA Coated Surfaces	36
4.1.2 BSA Adsorption	40
4.1.3 Optimization of PEG Modification.....	44
4.1.4 Water Contact Angles.....	46
4.1.5 XPS Analysis.....	48
4.1.6 PDA Thickness and Roughness	52
4.1.7 PDA Particle Analysis.....	56
4.1.8 Fg Adsorption.....	60
4.1.9 E. coli Adhesion.....	62
4.2 CONCLUSION	65
5. LIGHT ACTIVATED PFPA-PEG ON PDA COATED SURFACES	68
5.1 INTRODUCTION.....	68

5.1.1 Attachment of PFPAs to Surfaces.....	69
5.1.2 Limitations of PFPAs	70
5.1.3 PDA as a Bio Glue for PFPA-PEG.....	70
5.2 MATERIALS AND METHODS	71
5.2.1 Materials.....	71
5.2.2 PFPA-PEG Synthesis	72
5.2.3 PFPA-PEG Surface Preparation	72
5.3 RESULTS AND DISCUSSION	73
5.3.1 PFPA-PEG Concentration Optimization.....	73
5.3.2 PFPA-PEG Adsorption vs. Dip Coating Method for Modification.....	74
5.3.3 PFPA-PEG Drying Test.....	76
5.3.4 Water Contact Angles.....	77
5.3.5 Fibrinogen Adsorption	78
6. SUMMARY AND CONCLUSIONS	81
6.1 SUMMARY	81
6.2 RECOMMENDATIONS FOR FUTURE WORK.....	83
6.2.1 Structure of PDA Deposits on Materials.....	83
6.2.2 Optical Properties of PDA	83
6.2.3 Quantitative Analysis of PEG Surface Density	84
6.2.4 PFPA-PEG and Photopatterned Surfaces.....	85
REFERENCES.....	87
APPENDIX A: Making PDMS Samples SOP	98
APPENDIX B: PDA, PEG, and BSA Modification SOP	99
APPENDIX C: PFPA-PEG Modification of PDA Coated Surfaces SOP.....	101
APPENDIX D: I¹²⁵ Protein Radiolabeling SOP.....	103
APPENDIX E: Quantifying I¹²⁵ Radiolabeled Protein Adsorption SOP	107
APPENDIX F: Quantifying <i>E. coli</i> Adhesion SOP	110

LIST OF FIGURES

Figure 1. Schematic of the biofouling process in marine environments. (Figure from [1]).

Figure 2. The pathway for blood coagulation. Damaged endothelial cells release a network of collagen and von Willebrand factors (VWF) that attract the initial, weak adhesion of platelets. The release of tissue factors initiates conformational changes to platelet cells and activates thrombin to cleave fibrinogen and form fibrin. Fibrins cross-link to stabilise platelet cells, forming a blood clot. (Figure from [26]).

Figure 3. Proposed structure of PDA involving a) covalent linkage of monomers, b) combination of supramolecular and covalent linkages, or c) supramolecular bonding interactions. (Figure from [8]).

Figure 4. Proposed cyclisation route for dopamine determined by ToF-SIMS analysis [7] and post-modification route for thiol- or amine- terminated compounds via Schiff-base or Michael addition chemistries. (Figure from [7] supporting information).

Figure 5. Preparation protocol for the surface modification of PC, PDMS, and glass. PEG is shown in the diagram as a stretched polymer chain.

Figure 6. BSA stability on PDMS surfaces modified with: A) PDA, B) BSA/PEG, and C) PEG/BSA in contact with protein solutions and buffer solutions over two days. Means \pm SD, $n=3$. ($pI_{PDA} = 9.7$; $pI_{BSA}=4.7$)

Figure 7. BSA adsorption on modified PDMS surfaces from: A) BSA and B) FBS solution, both made in pH 7.4 PBS buffer. Means \pm SD for $n=3$ trials.

Figure 8. BSA adsorption on modified PC surfaces from BSA solution (3 mg/mL in PBS buffer, pH 7.4) and 10% FBS solution (PBS buffer, pH 7.4). Means \pm SD, $n=3$.

Figure 9. Comparison of Fg adsorption on M-PEG-NH₂ and NH₂-PEG-NH₂ modified PDA coated PC, PDMS, and glass. Means \pm SD, $n=6$ for PC and PDMS, $n=3$ for glass.

Figure 10. Photograph of unmodified and PDA modified PC, PDMS, and glass samples. Samples were tinted with a distinctive brown colour after 3 h dopamine polymerization at room temperature. Samples remained brown after subsequent modifications with PEG and BSA.

Figure 11. AFM topology images of unmodified and PDA modified PC, PDMS, and glass samples.

Figure 12. a) Large 20x20 μm AFM height scan of PDMS-PDA revealing cracks in the PDA layer. b) Vertical distance map across the white boxed area in AFM image a). PDA thickness = 25.5 nm.

Figure 13. Fg adsorption on a) PC, b) PDMS and c) glass modified materials. Fg adsorption time = 2 h in 1 mg/mL Fg solution (21°C, PBS pH 7.4). Data are mean \pm SD, n=3. * Significant differences (p<0.05).

Figure 14. *E. coli* adhesion on a) PC, b) PDMS and c) glass modified materials. *E. coli* seeding numbers were 2×10^8 cells on PC (4 h), and 2×10^7 cells on PDMS (4 h) and glass (5 h) in PBS (pH 7.4). Data are mean \pm SD, n=3. * Significant differences (p<0.05).

Figure 15. Bright-field and fluorescence images of *E. coli* on a scratched PDMS-PDA-PEG/BSA surface. *E. coli* cells show preferential adhesion to scratch area and low cell adhesion on the adjacent PDA-PEG/BSA modified area.

Figure 16. Chemical structure of PFPAs. R is a customizable group.

Figure 17. Process for the modification of PDA coated surfaces with PFPA-PEG, showing proposed point (NH) for insertion of PFPA-PEG into PDA. C=C insertion may also occur with PDA in the π -stack configuration (not depicted here) [7,8].

Figure 18. Fibrinogen adsorption on PFPA-PEG-modified surfaces prepared at different concentrations of PFPA-PEG. Samples were dip-coated in 10.5 mg/mL (C1), 21 mg/mL (C2), and 31.5 mg/mL (C3) PFPA-PEG solution prior to UV activation. UV activation was for 2 min per side. Means \pm SD, n=3.

Figure 19. Optimizing the PFPA-PEG modification procedure for fibrinogen resistance. Samples were incubated for 1 h (A1-A3) or dip coated (D1-D3) in 10.5 mg/mL PFPA-PEG solution prior to UV activation. The numbers 1, 2, and 3 indicate the number of treatments in PFPA-PEG solution. UV activation time was 5 min per side. Means \pm SD, n=3.

Figure 20. Optimizing temperature used for sample drying. PC samples were dried at room temperature overnight (RT) or at 60°C for roughly 3 h (HT). Samples were treated with PFPA-PEG once or twice. Means \pm SD, n=3.

Figure 21. Fg adsorption on modified PC, PDMS, and glass. PDA coated samples were modified with one, two or three (T1, T2, & T3) treatments of PFPA-PEG. Adsorption time, 2 h in 1 mg/mL Fg solution (PBS, pH 7.4) at room temperature. Data are mean \pm SD, n=3.

LIST OF TABLES

Table 1. List of materials modified with PDA and post-modified in various ways. *P/O* indicates PDA only modification.

Table 2. List of alkaline pH sensitive materials and compounds [67]. The listed materials may be incompatible with PDA modification due to the requirement for dopamine polymerization at alkaline pH. The pH compatibility range is approximate and manufacturer specific.

Table 3. Water contact angles of modified PC, PDMS, and glass. Sessile water contact angles of 6 μ l drops were taken after 2 min of surface contact. Mean \pm SD for n=3 samples.

Table 4. XPS elemental composition of PC, PDMS, and glass surfaces modified with PDA, PEG and BSA.

Table 5. Surface characteristics of PDA deposited on PC, PDMS, and glass as determined by ellipsometry and AFM. The average image RMS surface roughness and grain characteristics are reported for three 2x2 μ m scans. AFM scans are shown in Figure 10. Data are means \pm SD for n=3 measurements or images.

Table 6. Water contact angles (degrees) on modified PC, PDMS, and glass. Sessile drop water contact angles using 6 μ L drops were measured after 2 min surface contact. Means \pm SD, n=3.

LIST OF ABBREVIATIONS

AFM	Atomic force microscopy
BSA	Bovine serum albumin
DA	Dopamine
<i>E. coli</i>	Escherichia coli
FBS	Fetal Bovine Serum
Fg	Fibrinogen
FTIR	Fourier Transform infrared Spectroscopy
HCS	High-content screening
I-125	Iodine-125
PBS	Phosphate buffered saline
PC	Polycarbonate
PDA	Polydopamine
PDMS	Polydimethylsiloxane
PEG	Polyethylene glycol
PFPA	Perfluorophenyl azide
PVP	Polyvinylpyrrolidone
QCM-D	Quartz Crystal Microbalance with Dissipation Monitoring
Tof-SIMS	Time-of-Flight Secondary Ion Mass Spectrometry
UV	Ultraviolet
XPS	X-Ray Photoelectron Spectroscopy

1. INTRODUCTION AND OBJECTIVES

Preventing unwanted protein adsorption on biomedical devices is important to improve biocompatibility, reduce biofouling, and control cell adhesion. As new materials are developed for biomedical applications, antifouling strategies applicable to the new materials are constantly being investigated. Some antifouling strategies include mechanical cleaning, antifouling paints, chemical sprays, and surface modification [1]. Surface modification is the preferred method for creating long-lasting, non-toxic coatings on biomaterials by changing the materials' surface chemistry for desired applications. Surface modification methods are customizable, allowing opportunities for the user to enhance their biomaterials' properties for creating biofunctional surfaces [2], antibacterial surfaces [3], biosensing [4], and cell-based assays [5].

Polymer-based materials are of great interest for their structural versatility and low cost in the development of multi-functional microfluidic assay platforms, implants, and biosensing [6]. Surface modification is needed to enhance these materials' biocompatibility and surface properties by reducing biofouling. A major challenge in modifying polymers is that they are highly sensitive to organic solvents and harsh reaction conditions, which are required in many surface modification protocols. Structural damage, degradation, and swelling are an issue when chemically treating polymers.

In addition, biomedical devices are often composed of multiple classes of materials to enhance their functionality. Surface modification of materials is dependent on the substrates' initial surface chemistry and tolerance of harsh reaction conditions. Thus, antifouling protocols need to be chosen while considering the chemical compatibility of the substrate and, consequently, a method that works on one type of material may not be suitable for others. This

may limit the utility of a successful antifouling strategy to individual materials and prevents modification of pre-assembled multi-material devices. The cost to modify individual materials is high as processes, equipment, and the reagents needed may vary. Furthermore, some integrated devices cannot be modified in pieces due to the possible destruction of the coating during moulding, manufacturing, machining, and assembly. Therefore, a single antifouling method suitable for multi-material, whole device modification is highly desirable [5,7].

Dopamine has received a lot of attention in biomaterials research over the last decade due to its ability to polymerize and adhere strongly on virtually all types of materials under mild reaction conditions [8,9]. Materials that have been modified with dopamine include metals, oxides, ceramics, semiconductors, and polymers [7,8,10]. In addition, dopamine is water soluble, stable in aqueous and mild redox environments, and post-modifiable by bonding to free amine or thiol groups in bioactive molecules [8]. This makes dopamine an attractive reagent for post-modification of a wide variety of materials. For example, aqueous-based antifouling coatings using amine-terminated polyethylene glycol (PEG) bonded to the surface via polydopamine (PDA) have been widely reported in the literature [7,11-14]. The use of PDA for surface modification is favorable since it can be applied to virtually any material and the reaction conditions are mild. However, due to the ability of PDA to bond to free amino groups, PDA coated surfaces generally show enhanced protein adsorption and cell adhesion [15]. Indeed, cell viability has been reported to increase by as much as 50% on PDA coated polyethylene membranes [16]. When PEG grafting is conducted from solution using pre-formed PEG chains (i.e. grafting-to method), the packing density of PEG is limited by the excluded volume effect [2,13], leading to areas of exposed PDA available for protein binding and cell adhesion. Therefore although useful as an aqueous-based anchor for the attachment of anti-fouling

molecules (proteins, polymers), PDA is essentially a “double edged sword” due to its tendency to adsorb proteins which may enhance fouling. For example, Miller et al. [12] reported that PDA-PEG coated polysulfone ultrafiltration membranes (PSF) did not resist bacteria fouling after just three to four days in a continuous biofouling environment.

The goal of this thesis is to improve the antifouling properties of PDA-PEG coated surfaces using two approaches: (1) using bovine serum albumin (BSA) to block protein adsorption to exposed PDA (i.e. PDA not “covered” by PEG), and (2) improving the attachment of PEG to PDA using a light-activated PEG derivative. The research described in this thesis demonstrates for the first time (to our knowledge) the successful use of a protein to “backfill” a PEG-modified surface. We also demonstrate for the first time the stable attachment of light activated perfluorophenyl azide (PFPA) derivatives on PDA coated materials. Furthermore, these antifouling coatings were applied to three materials (polycarbonate (PC), polydimethyl siloxane (PDMS), and glass) to demonstrate the coatings’ applicability to multi-material medical devices.

2. LITERATURE REVIEW

2.1 The Biofouling Problem

2.1.1 Marine Biofouling

Biofouling is described as the unwanted accumulation of proteins, cells, and fouling organisms on wetted surfaces [1,17]. Marine biofouling is a phenomenon that costs millions of dollars in damage and maintenance of oceanic equipment, as well as environmental damage due to the introduction of invasive species and increased fossil fuel consumption by ships due to hydro-dynamic drag [1]. The process of marine biofouling is shown schematically in **Figure 1**. Biofouling begins with the early adsorption of proteins on a submerged surface in protein-containing media. The adsorbed proteins facilitate the attachment of bacteria and other cells and development of a biofilm. The biofilm is rich in sessile microorganisms and an extracellular polysaccharide (EPS) matrix which attracts fouling organisms, leading to the growth of a fouling community on the surface [1,18]. These fouling organisms can exist on the underlying surface indefinitely if undisturbed, causing bio-corrosion and permanent damage to the structure beneath.

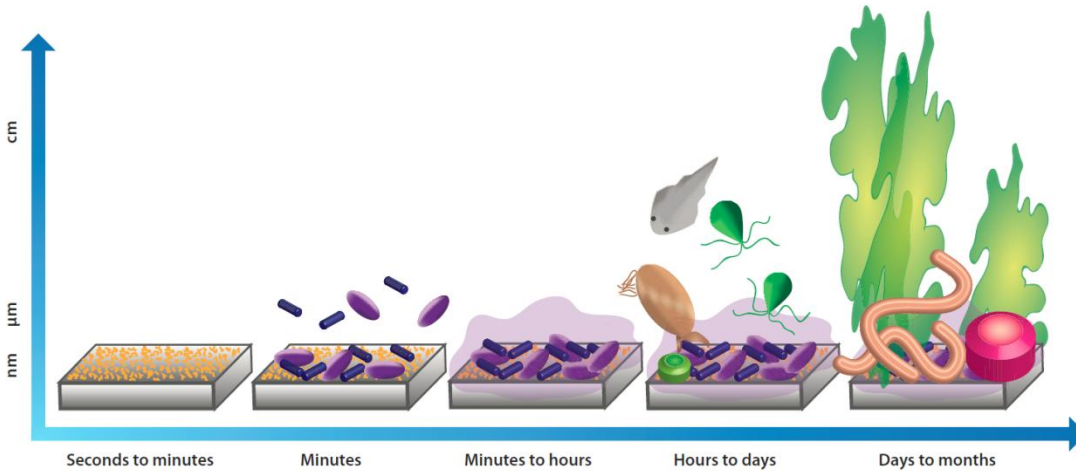


Figure 1. Schematic of the biofouling process in marine environments. (Figure from [1]).

2.1.2 Biofouling of Water Quality Monitoring Devices

Biofouling has had a huge impact on the operation of long-term water quality monitoring. Water quality assessment is vital for natural water preservation and to eliminate the risk of water-related diseases. Failure to detect water contaminants in a timely manner may delay remedial action and prolong public exposure to severe health risks. With the advancement of technologies for long-range communication, network capabilities, and improved sensor technologies, water monitoring is now possible via continuous uninterrupted logging of data pertaining to chemical and biological quality [19]. New monitoring devices are composed of multiple sensors to collect spatially and temporally varying information on water pH, turbidity, conductivity, temperature, dissolved oxygen, and nitrate and phosphate concentration [20]. Wireless technologies allow real-time continuous gathering of water quality data, revealing trends that cannot be seen by spot sampling [19]. Furthermore, wireless systems facilitate information collection from multiple sites remotely, allowing sampling over larger areas for longer periods of time and contributing to reduced monitoring costs [19,21].

Biofouling continues to limit the implementation of these long-term monitoring systems by impairing sensor accuracy and longevity by physical, chemical, and optical obstruction of sensor technology [19,22,23]. In a study by Kerr et al. [23], the effects of biofouling on a fluorometer and transmissometer used for measuring chlorophyll- α concentration and water clarity, respectively, were studied in a natural seawater environment. Chlorophyll- α has the same absorption window (~670 nm) as photosynthetic bacteria. The performance of these sensors began to deteriorate after 200 and 150 hours, with limiting fouling being reached after 11 (fluorometer) and 9 (transmissometer) days of continuous monitoring. The adhesion of bacteria cells and other photosynthetic organisms led to the failure of these optics-based sensors primarily by loss of light via scattering and absorption. Limits may be different in different bodies of water or during different seasons as the fouling rate is dependent on the water conditions at any given time. The concentration of bacteria is crucial. The critical fouling limit of both sensors was reached once a bacteria population above 10^5 cells/mm² had accumulated on the optical window. Of interest, the authors reported that the optical windows of these sensors consisted of a type of acrylic (unspecified by manufacturer) and glass, suggesting the critical importance of optical sensor functionality at this bacteria concentration [23].

Sensors are externally composed of multi-materials such as glass, acrylic polymers, stainless steel, and titanium. Cleaning is conducted either manually or chemically. Manual cleaning and recalibration needs to be conducted frequently on continuous monitoring systems to ensure that the information collected remains representative of the conditions [19,22]. The use of harsh chemical disinfectants such as chlorine and base to prevent biofilm formation in marine applications is typical, but not ideal as a long term solution due to high environmental pollution [24].

2.1.3 Biofouling in Biomedical Applications

Although biofouling is mostly recognized in the context of marine fouling, controlling protein adsorption and cell adhesion is equally important for preserving the functionality and longevity of biomedical devices. Adsorption of proteins on implant materials (e.g. from blood and tissue) is rapid and ubiquitous, and may cause protein denaturation, leading to foreign body reactions that lower the success of implant acceptance by the host [25]. In addition, blood coagulation and thrombosis around blood-contacting materials may occur due to protein adsorption and platelet adhesion, resulting in the need to remove and replace the implanted device [6]. Other consequences of implant failure are unwanted immunogenic responses such as infections and inflammation in the surrounding tissue [25].

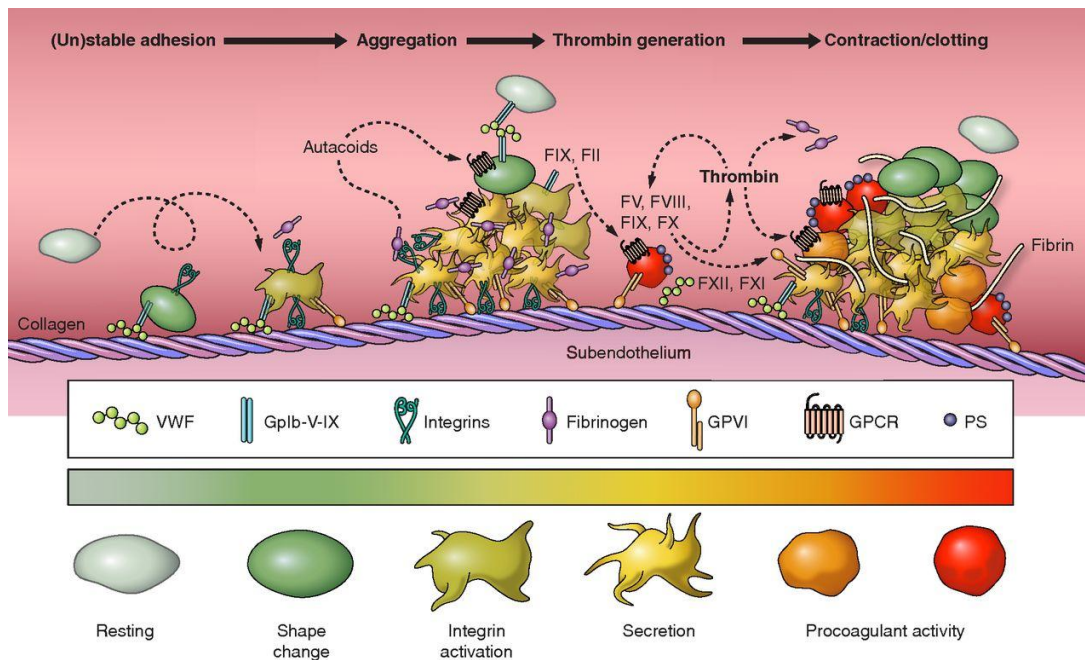


Figure 2. The pathway for blood coagulation. Damaged endothelial cells release a network of collagen and von Willebrand factors (VWF) that attract the initial, weak adhesion of platelets. The release of tissue factors initiates conformational changes to platelet cells and activates thrombin to cleave fibrinogen and form fibrin. Fibrins cross-link to stabilise platelet cells, forming a blood clot. (Figure from [26]).

Promoting favorable protein-material interactions is also important in the development of bioanalytical assays. Production of cytocompatible surfaces through the adsorption of cell adherent proteins is necessary to promote cell proliferation, differentiation, and enhance cell morphology for cell-related studies [27-29], tissue engineering [30-32], and cell-based biosensors [33-36]. Controlling cell adhesion, such as with patterned surfaces, offers distinct advantages by allowing mimicry of *in vivo* cellular environments and allowing single cell analysis for more detailed studies of cellular interactions [27].

2.2 Protein Adsorption

Inhibiting the first stage of biofouling – protein adsorption – is crucial in preventing the progression of the biofouling cascade. The presence of cell adhesive proteins on surfaces is necessary to assist cell adhesion, spreading, normal morphology and cell-to-cell communication [15,37]. These functions are required for normal cellular activity, membrane transport, and cell proliferation [15,37]. Thus, protein resistant surfaces often show impaired cell adhesion and growth [38,39].

2.2.1 Electrostatic Attraction

Since all proteins are surface active, protein adsorption in biofluids is ubiquitous and generally non-specific. The extent of adsorption is dependent on the material's surface properties such as charge. Proteins tend to adhere to charged surfaces via electrostatic interactions between charged amino acid residues and charges of opposite polarity in the substrate surface. By the same token when the protein and substrate charges are of matching polarity adsorption is inhibited. Solution conditions such as pH and ionic strength also play an important role in

adsorption. For example, when the solution pH matches the isoelectric point (pI) of the protein, i.e. when the net charge on the protein is zero, higher protein packing densities are possible due to reduced electrostatic protein-protein repulsion [17] and to the minimum in conformational change (maximal internal coherence) at zero net charge [40]. In addition, environments with high concentrations of dissolved ions (ionic strength) can facilitate protein adsorption on like-charged substrates [17].

2.2.2 Protein Orientation on Solid Surfaces

In early adsorption, the orientation of proteins adsorbed to a surface can occur via end-on and side-on configurations. The protein orientation is dependent on adsorption time and the position of the proteins as they approach the surface [41,42]. End-on adsorption leads to higher protein quantities on the surface. For example, a tight monolayer of fibrinogen (Fg) ($5.0 \times 5.0 \times 47$ nm) in the end-on configuration has estimated adsorption of 1.57-2.26 $\mu\text{g}/\text{cm}^2$, and the side-on configuration has estimated adsorption of 0.21-0.24 $\mu\text{g}/\text{cm}^2$ [42,43]. For smaller bovine serum albumin (BSA) ($4.0 \times 4.0 \times 14$ nm) proteins, tight end-on packing would yield estimated adsorptions of 0.72 $\mu\text{g}/\text{cm}^2$ while side-on adsorption would be 0.21 $\mu\text{g}/\text{cm}^2$ [42]. Surface wettability has been shown to have negligible influence on the rate of protein adsorption and protein orientation in early adsorption, since initial adsorption occurs non-specifically upon surface contact [42]. Proteins are generally held weakly at the surface in early adsorption, allowing desorption [41] or protein exchange to occur [44].

With longer adsorption times, proteins are able to spread or re-orientate themselves to establish more favorable protein-surface interactions. Protein spreading is influenced by substrate wettability, with greater protein spreading on hydrophobic surfaces due to the

hydrophobic dehydration effect [17,40,45]. The hydrophobic surface causes protein denaturation and non-polar functional groups of the adsorbed proteins to dehydrate [40,45]. Water is released, creating a large increase in entropy [40,45] and thereby making protein adsorption on hydrophobic surfaces more entropically favorable. Protein spreading promotes stronger binding to the hydrophobic surfaces as there are more interactions between protein residues and the surface, contributing to the irreversibly bound protein state [40,46]. Therefore, proteins generally have higher affinity to hydrophobic surfaces than hydrophilic ones. Protein spreading has been found to increase with time, and level off after 2 h [42]. Late adsorption on hydrophilic surfaces causes proteins to re-orientate from end-on to side-on configurations rather than spread since it is not favorable to increase surface contact with hydrophilic residues at the expense of internal hydrophobic interactions [41].

2.2.3 Mixed Protein Adsorption

In mixed protein solutions, there may be greater surface affinity for one protein over another. Smaller proteins diffuse to the surface faster, pre-occupying the surface early in the process [17,46]. However, larger proteins adsorb more strongly due to their size and the large number of sites available for protein-surface interaction [17,46]. Thus, larger incoming proteins of higher affinity can displace initially adsorbed proteins of lower affinity. This exchange is referred to as the Vroman effect in recognition of L. Vroman's contribution [44]. The tendency for protein exchange to occur is dependent on the affinity of the early adsorbers, as well as how long they had to inhabit the surface. As discussed previously, the longer a protein is resident on the surface, the more likely it is to “relax” and undergo conformational changes to increase their molecular footprint such that exchange can no longer occur [46]. BSA that has been pre-

adsorbed to a surface and allowed to spread has been shown to slow the rate of adsorption of larger Fg proteins [42].

2.3 Antifouling Strategies

It is apparent that inhibiting protein adsorption and cell adhesion is important for many applications involving biomaterials. Both environmental and substrate effects have a strong influence on protein adsorption, but it is neither necessarily useful nor appropriate to change the material's environment to inhibit protein adsorption. Indeed control of solution effects may not be possible at all, such as in the case of contact with blood or a natural water environment. Thus efforts to control, and in particular to inhibit, adsorption has been focused on modification of the surface itself.

Many strategies for reducing biofouling have been reported. Kirschner and Brennan [1] described three major categories of bio-inspired antifouling strategies involving material surface modification. Physical strategies involve creating surface textures and topographies that deter colonization by fouling organisms. Stimuli-responsive coatings disrupt fouling species in response to an external stimulus such as temperature or pH. Nevertheless, manipulation of material surface chemistry to mimic natural antifouling mechanisms is by far the most common and most successful approach to antifouling surfaces [1].

2.3.1 *Hydrophilic Polymers*

Surface grafting of hydrophilic polymers is one of the most widely practiced antifouling strategies due to its relative simplicity, versatility, and customizability to many types of

materials. Since protein adsorption occurs preferentially on hydrophobic materials, increasing the substrate water wettability has been found to be effective in reducing non-specific protein adsorption [47]. Hydrophilic polymers used for grafting generally consist of chains of varying length, with a functional group at one end for attachment to the surface, and a distal end group that may be used to immobilize bioactive molecules to promote specific interactions [2,5]. Examples include polyethylene glycol/polyethylene oxide (PEG/PEO), polyvinylpyrrolidone (PVP), polyhydroxyethylmethacrylate (PHEMA), poly(2-(dimethylamino)ethylmethacrylate) (PDMAEMA), poly(N-isopropylacrylamide) (PNIPAM), and more [5]. The two main properties of the grafted surface that influence resistance to protein adsorption are polymer chain length and polymer chain density on the surface. In the case of PEG in antifouling surfaces, chain density has been shown to be more important [48-50], although some studies also report strong differences in antifouling capabilities of PEGs of varying molecular weight [24].

The architecture of the polymer dictates the material's behaviour with respect to fouling. Hydrophilic polymers with a simple end group (e.g. hydroxyl) are primarily designed for protein and cell resistance. Biopolymers are available that are cell destructive, trigger-responsive, and that promote specific protein adsorption and cellular responses depending on the bioactivity of the biopolymer [6,25]. Major applications for biofunctional polymer brushes are in the areas of biomedicine, biosensors, bioanalytical assays, enzyme reactors, food packaging, and textiles [6].

2.3.2 Grafting Hydrophilic Polymers

The mechanism of protein resistance of grafted hydrophilic polymers is highly dependent on the grafting density and the chain configuration on the surface. Measuring the grafting density is crucial for determining the efficacy of the modification reaction and for predicting the degree

of protein resistance to be expected. Polymer brushes, i.e. structures in which the polymer chains are extended, are structures of high chain density and, in the case of hydrophilic polymers such as PEG, high water content [38,51,52]. This hydrophilic brush is associated with an “osmotic barrier” that leads to a decrease in entropy as protein molecules approach, thereby inhibiting protein adsorption [6,13,52]. At lower grafting densities, polymer chain configurations are closer to a “mushroom” regime and resist protein adsorption primarily by lacking ionic interactions and blocking attractive van der Waals forces on the underlying substrate [52]. Interfacial water barriers can be formed in the mushroom configuration [48], although they may not be as effective as in the brush conformation. Very low grafting densities are arguably non-functional as protein resistant surfaces due to the proteins’ ability to penetrate the sparsely distributed polymer chains [52]. Generally, surfaces with higher polymer grafting densities resist protein adsorption to a greater extent, with the brush conformation ideal for highly protein and cell resistant surfaces.

There are three major approaches to attaching hydrophilic polymers to a surface: (1) physisorption, (2) “grafting-to” and (3) “grafting-from” [5,52]. Physisorption of diblock copolymers was one of the earlier methods that are now rarely used due to the instability of the adsorbed polymers in different solvents, and their easy displacement by other adsorbents [52]. Chemisorption methods such as grafting-to and grafting-from offer greater stability by covalently bonding the polymer chains to the surface. In grafting-to, pre-formed chain-end functionalized polymers are attached to the surface via reaction with complementary functional groups under appropriate conditions [52]. The grafting density in “grafting to” is sterically limited by previously attached chains (excluded volume effect) and the availability of reactive

groups on the surface [13,52]. This reduces the achievable polymer density on the surface, making this approach less than ideal for creating highly protein resistant surfaces.

The grafting-from approach is more laborious and involves the *in situ* polymerization of a suitable monomer from an initiator on the surface. The chain length and density can be controlled by adjusting the polymerization conditions (time, monomer concentration) and the initiator density respectively [5]. Higher grafting densities can be achieved by the grafting-from approach due to the reduced excluded volume effect, allowing the formation of true polymer brush surfaces [13,52]. This makes the grafting-from approach much more attractive for creating highly protein resistant surfaces and has led to the development of several successful grafting-from techniques including atom-transfer radical polymerization (ATRP), reversible addition-fragmentation chain-transfer (RAFT) polymerization, nitroxide mediated polymerization (NMP), and iniferter polymerization [5,53].

2.3.3 Limitations of Hydrophilic Polymers

A major limitation in the use of hydrophilic polymers in antifouling coatings is that published protocols are often designed only for the specific material in the study. Firstly, grafting is reliant on the availability of appropriate reactive sites on the substrate surface, either intrinsic to the material or incorporated chemically, that can tether the polymer chains. Certainly, not all materials have appropriate intrinsic surface chemistry. Frequently, inert surfaces need to be modified with appropriate functional groups before grafting. Typical functional groups include OH, COOH, and NH₂ which may be incorporated using wet chemical methods or high energy ionized gas treatments [6,54]. Apparent limitations with these methods include lack of stability

of the modified surface, generation of hazardous chemical waste, and surface etching due to the harsh reaction conditions [6,16].

Harsh reaction conditions are not suitable for all types of materials. Polymer-based materials are an important material class for biomedical device design due to their low cost and structural versatility. However, they may experience extensive structural damage when exposed to organic solvents including swelling, degradation, and other functional damage. Thus, surface functionalization is limited by the material's tolerance to specific chemical treatments and must be customized for each material. Thus polymer brush grafting as a solution for biofouling on biomedical implants, sensors, and microfluidic devices composed of multi-materials has challenges. Parts made from different materials would need to be individually modified causing increased manufacturing time, increased cost, and possibly damage to the surface modified parts during assembly. It is apparent that a universal antifouling method suitable for whole device, multi-material modification is highly desired for biomedical applications [5,7].

2.4 Polydopamine: A Universal “Bio Glue”

The first requirement in designing a universal antifouling protocol is the ability to pre-functionalize a variety of materials using the same method. The chemistry for attaching hydrophilic polymers or other biological agents to the surface would then be the same. Dopamine is a unique water soluble compound that has recently attracted a lot of interest as a chemical linker for the surface modification of biomaterials [8]. Originally inspired by the mechanism of mussel adhesion, the oxidized dopamine monomers can strongly self assemble from solution onto virtually all types of material, including polymers, metals, and composites

[8,13,15]. Under constant stirring in an oxygenated environment, dopamine forms an insoluble polymer, polydopamine (PDA), which is highly stable in aqueous environments, strong acids, and mild redox environments for extended periods of time [8,55]. PDA coatings are favorable for surface modification because they are non-toxic, involve solvent-free processes, and are reactive with a wide range of biomolecules for post-modification [15]. The thickness of the PDA layer can be controlled by adjusting the dopamine concentration, deposition time, oxygenation/stirring, and temperature [56].

2.4.1 Dopamine Polymerization on Surfaces

PDA formation on surfaces occurs via two mechanisms (1) polymerization onto the surface and/or (2) adsorption of dopamine-melanin particles formed in solution [13]. The strength of the PDA bond to the substrate surface is dependent on the reactivity of the PDA subunits in forming coordination bonds with surface metal oxides or covalent bonds with nucleophilic groups [13]. Otherwise, PDA attraction to the surface occurs via weaker interactions such as hydrogen bonding, van der Waals interactions, and hydrophobic interactions [8,13]. Dopamine has also been reported to polymerize readily onto electrodes by electrochemical oxidation [57]. Thus, PDA bonding tends to occur more strongly on electrodes and metallic surfaces. Once cyclised intermediates of dopamine are established on the surface, polymerization and growth of the PDA film may occur through the formation of covalent linkages between monomers [58], or through hydrogen bonding, π -stacking, charge transfer and ionic interactions [8]. While the actual structure of PDA remains elusive [8], proposed structures of polymerized dopamine are shown in **Figure 3** based on the possible interactions that may occur between cyclised dopamine intermediates.

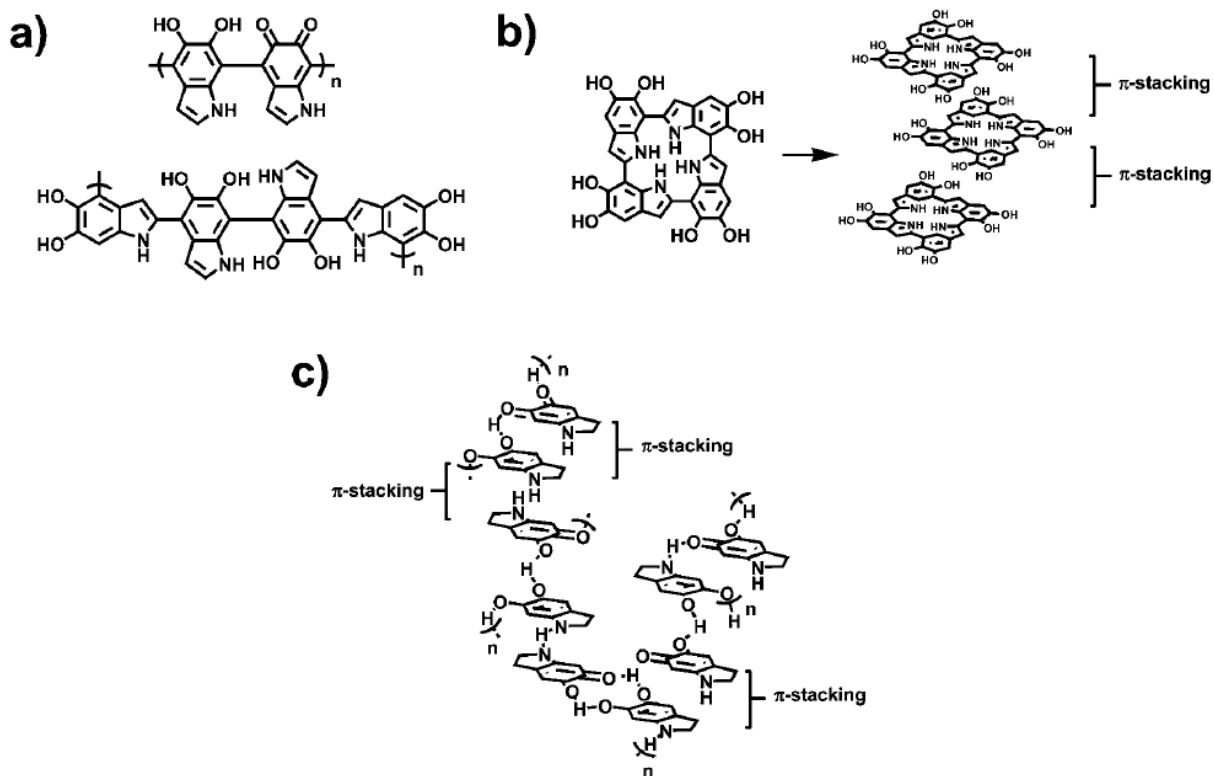


Figure 3. Proposed structure of PDA involving a) covalent linkage of monomers, b) combination of supramolecular and covalent linkages, or c) supramolecular bonding interactions. (Figure from [8]).

2.4.2 Post-modification of PDA

The quinone groups on PDA act as intermediary binding sites to anchor biomolecules containing amino or thiol groups through Michael addition or Schiff base-type reactions (**Figure 4**) [7,8,59]. However, Lee et al. [7] found that PDA had higher coupling efficiency and higher PEG grafting density using amine-terminated PEG compared to thiol-terminated PEG, resulting in greater antifouling resistance. A list of materials successfully modified with dopamine and post-modified in various ways is shown in **Table 1**. PDA coated surfaces have been used as a cytocompatible surface with strong protein adsorption and cell adhesion [15,16,60], as a linker to tether hydrophilic polymers in the construction of bioinert surfaces [11,13,61], as well as

coupling biomolecules in the development of bioactive surfaces for biomimetic strategies [62,63].

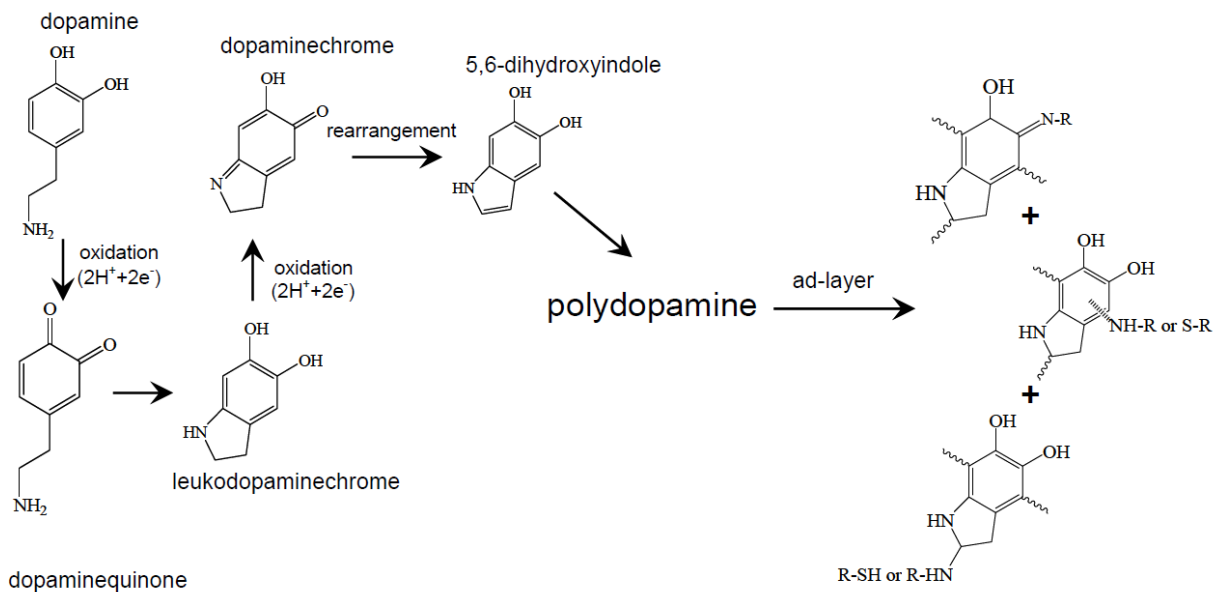


Figure 4. Proposed cyclisation route for dopamine determined by ToF-SIMS analysis [7] and post-modification route for thiol- or amine- terminated compounds via Schiff-base or Michael addition chemistries. (Figure from [7] supporting information).

Table 1. List of materials modified with PDA and post-modified in various ways. *P/O* indicates PDA only modification.

Class	Substrate	Protein Studies	Cell Studies	Post-Modification
Metals	Copper (Cu)	N	N	Alkanethiol [7]
	Gallium Arsenide (GaAs)	N	N	<i>P/O</i> [7]
	Gold (Au)	Y [11,13]	Y [7,64]	mPEG-SH [7], PEG-NH ₂ [11], PEO-NH ₂ [13], PEI-g-PEG [64]
	Nickel Titanium Alloy (NiTi)	N	N	<i>P/O</i> [7]
	Niobium Pentoxide (Nb ₂ O ₅)	N	N	<i>P/O</i> [7]
	Palladium (Pd)	N	N	<i>P/O</i> [7]
	Platinum (Pt)	N	N	<i>P/O</i> [7]
	Quartz	N	N	<i>P/O</i> [7]
	Sapphire (Al ₂ O ₃)	N	N	<i>P/O</i> [7]

	Silicon Dioxide (SiO ₂)	N	N	Alkanethiol [7], PEO-NH ₂ [13]
	Silicon Nitride (Si ₃ N ₄)	N	Y	mPEG-SH [7]
	Silver (Ag)	N	N	<i>P/O</i> [7]
	Stainless Steel	N	N	<i>P/O</i> [7]
	Titanium Dioxide (TiO ₂)	N	Y	Alkanethiol, mPEG-SH [7]
Polymers	Polycarbonate (PC)	N	Y [3]	Alkanethiol [7], mPEG-SH [3]
	Polydimethylsiloxane (PDMS)	N	Y [15]	<i>P/O</i> [7,15,64]
	Polyethersulfone (PES)	Y [65]	N	PEGDA [61], PEG-NH ₂ [65]
	Polyethylene (PE)	N	Y [15,64]	<i>P/O</i> [7,15,64]
	Polyethylene Terephthalate (PET)	N	Y [64]	<i>P/O</i> [7,64], PEO-NH ₂ [13]

Poly(L-lactide) (PLLA)	N	N	PEO-NH ₂ [13]
Polymethyl Methacrylate (PMMA)	N	Y	PEI-g-PEG, PEI-g-biotin [66]
Polypropylene (PP)	N	Y	<i>P/O</i> [64]
Polystyrene (PS)	Y [66]	Y [7,64,66]	PEG-NH ₂ , PEI-g-PEG, PEI-g-biotin [66], mPEG-SH [7], PEO-NH ₂ [13], PEI-g-PEG [64,66]
Polysulfone (PSF)	Y [12]	Y [12,66]	PEI-g-PEG, PEI-g-biotin [66], PEG-NH ₂ [12], PEGDA [61]
Polytetrafluoroethylene (PTFE)	Y [15]	Y [7,15]	mPEG-SH [7], <i>P/O</i> [15]
Polyurethane (PU)	N	Y	PEI-g-PEI, PEI-g-biotin [66], mPEG-SH [7]
Polyvinylidene Fluoride (PVDF)	N	Y [64]	PEGDA [61], <i>P/O</i> [64]

Composites	Bare Fused-Silica Capillary	Y	N	PEG-NH ₂ [11,55]
	Glass	N	Y	mPEG-NH ₂ , m-PEG-silane, m-PEG-SH [7], PEI-g-PEG [64], <i>P/O</i> [15]
	Nitrocellulose (NC)	N	N	Alkanethiol [7]
	Silicone Rubber	N	Y	<i>P/O</i> [15]

2.4.3 PDA-PEG Antifouling Surfaces

Multiple studies have employed amine- and thiol-terminated polyethylene glycol (PEG) to post-modify PDA for multi-material antifouling applications. PEG is an extensively utilised antifouling hydrophilic polymer in biomaterials research for biomedical applications in part because it is water soluble and non-toxic [6]. The use of PDA-PEG coatings as a universal antifouling method offers many advantages including simple modification procedures, mild reaction conditions, no requirement for organic solvents, and high stability. Haeshin et al. [7] first demonstrated the utility of PDA in developing multifunctional coatings by anchoring SH-PEG and NH₂-PEG derivatives on virtually any substrate type. The substantial reduction in protein adsorption and mammalian cell adhesion on a variety of PDA-PEG coated materials inspired many researchers to use this method; e.g to modify membranes for food protein analysis [11,55] and water filtration [12,61], in bioassays and cell patterning [64,66], and for antibacterial surfaces [3].

2.4.4 Limitations of PDA-PEG

There are several challenges associated with using PDA in the development of antifouling coatings for multi-materials. Firstly, since dopamine solution at pH 8.5 is required to initiate polymerization, alkaline pH sensitive materials are not suitable for PDA modification [67]. Materials that may not be appropriate for PDA modification are listed in **Table 2**. Secondly, PDA can be removed by strong base [8], thus limiting the types of biological assays that can be conducted on a PDA coated surface.

Table 2. List of alkaline pH sensitive materials and compounds [67]. The listed materials may be incompatible with PDA modification due to the requirement for dopamine polymerization at alkaline pH. The pH compatibility range is approximate and manufacturer specific.

Material	Damage in Alkaline Solution	pH Compatibility Range
Polyester (PET)	Erosion, Degradation	pH = 5-7.5 [68,69]
Phenolic Resin	Degradation	pH = 3-7 [70]
Proteins (<i>Surfaces with</i>)	Denaturation	Protein specific
pH Sensitive Gel	Gel Failure	pH = 3-8 [71]
pH Sensitive Filter Membrane	Membrane Failure	pH = 3-8 [71]

Another challenge stems from the ability of PDA to react with free amino groups, which promotes protein adsorption and subsequently cell adhesion on PDA coated surfaces [15,16,60]. Thus, the effectiveness of using PDA as a post-modifiable surface for antifouling purposes is limited by the achievable graft density of the post-modifier, e.g hydrophilic polymer. Any exposed PDA on the post-modified surface enhances protein fouling and negates the effects of the antifouling layer. Achieving sufficient density of PEG on PDA coated materials poses challenges when grafting from aqueous solution since PEG tethering becomes dependent on steric effects and monomer orientation. Miller et al. [12] investigated the antifouling performance of PSF filtration membranes modified with PDA-PEG, specifically with respect to long-term biofouling. While bacterial adhesion was reduced in the early stages of bio-exposure, the anti-fouling effect was insufficient after 3 days [12]. Unfortunately, the PEG graft density

was not determined in this study. It seems likely that proteins and bacteria cells were able to penetrate gaps in the PDA-PEG layer.

2.5 Blocking Proteins

Immobilization of a known protein to solid surfaces is commonly practiced to block non-specific protein adsorption in solid phase immunoassays. Solid phase immunoassays provide quantitative measurements of a target molecule by colorimetric detection of the target binding to ligands adhered to the solid phase [72]. Non-specific protein adsorption is undesirable as it impairs the sensitivity and specificity of the assay in detecting the target substance [72]. Blocking proteins are chosen mainly due to their inactivity in the specific immunochemical reaction [73]. Blocking agents include bovine serum albumin (BSA) [74-76], casein, milk, blood serums, gelatins, and high-density lipoproteins [73].

BSA is a water soluble protein that has also been used to reduce non-specific mammalian [77-80] and bacterial cell adhesion [81,82]. It is the most abundant protein in serum, making it easily attainable and affordable [83]. It is proposed that amphiphilic BSA negates adhesion of negatively charged bacterial cells by electrostatic and steric repulsion, low surface interaction energy, or BSA folding into an inactive conformation upon adsorption onto substrates [81,82]. Furthermore, saturated BSA monolayers inhibit further adsorption of cell adhesive proteins [42,79,81] which may contribute to reduced cell adhesion. Indeed, Zhu et al. [16] demonstrated a ~20% decrease in cytocompatibility on PDA-modified polyethylene membranes (PE) blocked with BSA.

In the work reported in this thesis we propose using BSA as a blocking agent for exposed PDA after PEG attachment. Preliminary “fouling” of the surface by BSA is expected to limit the adsorption of cell adhesive proteins in subsequent bio-exposure. BSA can be covalently immobilised on PDA coated materials through its free amino groups (e.g. on lysine residues) [16,67]. The formation of stable bonds between BSA and the PDA surface prevents protein exchange between BSA and unwanted proteins in solution. In the work reported we evaluated the antifouling performance of this novel polymer-protein composite and demonstrate its application for multi-materials.

3. MATERIALS AND METHODS

3.1 Materials

Sylgard® 184 silicone elastomer kit was purchased from Dow Corning (Midland, MI) to prepare the PDMS surfaces. Hydrophilic polycarbonate track etch membranes with 0.01 µm pore size were purchased from Sterlitech Corporation (Kent, WA). Square soda lime glass cover slips (5x5 mm) were purchased from Haimen Aibende Experiment Equipment Co. Ltd. (Nantong, P. R. China). Methoxy-PEG-amine (MW 5000 Da) and amine-PEG-amine (MW 5000 Da) were purchased from Jenkem Technology USA Inc. (Plano, TX). Dopamine hydrochloride and BSA (>98%, lyophilized powder) were purchased from Sigma-Aldrich (Oakville, ON). Qualified fetal bovine serum (FBS) was purchased from Life Technologies (Burlington, ON). Human fibrinogen (Fg) was purchased from Enzyme Research Laboratories (South Bend, IN). AG® 1-X4 Resin was purchased from Bio-Rad (Mississauga, ON). Sodium iodide-125 (Na^{125}I) isotope was purchased from the McMaster Nuclear Reactor (McMaster University, Hamilton, ON) was used to label BSA and fibrinogen (Fg). Slide-A-Lyzer dialysis cassettes were purchased from Thermo Fisher Scientific (Mississauga, ON). Disodium hydrogen phosphate (Na_2HPO_4) was purchased from Caledon Laboratories Ltd. (Georgetown, ON) and potassium acid phthalate BDH buffer (pH 4) was purchased from VWR International (Mississauga, ON). Organic solvents of analytical grade were used as received. 10X Phosphate buffered saline (PBS) from BioShop Canada Inc. (Burlington, ON) at pH 7.4 was diluted to 1X strength using Milli-Q water (18.2 MΩ.cm) from Millipore Co. The pH of PBS was raised to 8.5 using sodium hydroxide (NaOH).

3.2 Methods

3.2.1 Substrate Preparation

Polydimethyl siloxane (PDMS) approximately 1 mm thick was prepared using a Sylgard® 184 silicone elastomer kit according to the manufacturer's instructions. The base and curing agent were mixed well in a 10:1 ratio by weight and cured at 60°C for 4 h. The substrates were then punched into 6 mm diameter discs. Round polycarbonate membranes (PC) of 25 mm diameter were divided and cut into 8 triangular pieces each of area 1.23 cm². Glass samples were used as received (Haimen Aibende Experiment Equipment Co. Ltd., Nantong, P. R. China). All substrates were rinsed with 95% ethanol and Milli-Q water before surface modification.

3.2.2 PDA Surface Preparation

PC, PDMS, and glass samples with dimensions previously noted were immersed in a 2 mg/mL dopamine solution freshly prepared from dopamine hydrochloride in PBS adjusted to pH 8.5 with NaOH. The samples were shaken in an open glass dish at room temperature for 3 h. The newly modified surfaces were thoroughly rinsed with Milli-Q water. All dopamine-coated surfaces were stored in fresh Milli-Q water to prevent transfer of the polydopamine modification onto the storage container. PDA is stable in water and water protects the PDA layer from cracking or transferring onto its contacting surface during the drying process [84].

3.2.3 PEG Grafting on PDA

PDA coated PC, PDMS and glass surfaces were shaken for 24 h at 37°C in 5 mg/mL PEG. PEG solution was prepared in PBS adjusted to pH 8.5 using NaOH. Surfaces were thoroughly rinsed and stored in Milli-Q water.

3.2.4 BSA Blocking of PDA

PDA coated PC, PDMS, and glass surfaces were shaken for 24 h at 21°C in 10 mg/mL BSA made from PBS (pH 7.4) in a closed glass dish. Surfaces were thoroughly rinsed and stored in Milli-Q water.

3.2.5 PDA-PEG/BSA and PDA-BSA/PEG Modification

PDA-PEG treated surfaces were backfilled with BSA using the conditions as previously described. BSA coated surfaces were backfilled with PEG using the conditions previously described. The surfaces were once again rinsed and stored in Milli-Q water before experimentation. These operations are shown schematically in **Figure 5**.

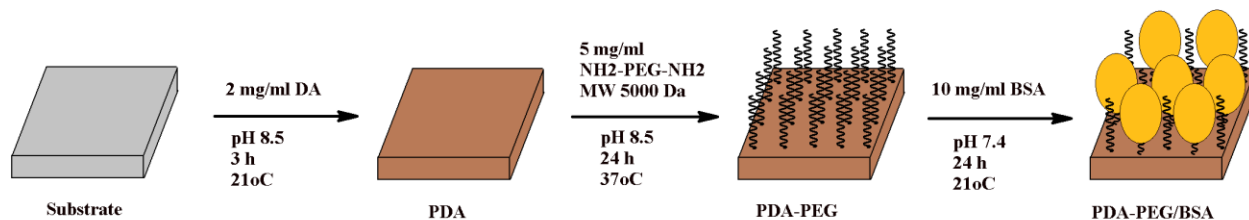


Figure 5. Preparation protocol for the surface modification of PC, PDMS, and glass. PEG is shown in the diagram as a stretched polymer chain.

3.2.6 Water Contact Angles

Samples were air dried before measurement. Water drops of 6 μL were dispensed on the surface and advancing contact angles were measured after 2 min using a Krüss DSA100 goniometer (Hamburg, Germany) at room temperature. Contact angles for $n=3$ samples per modification were recorded.

3.2.7 X-ray Photoelectron Spectroscopy (XPS)

XPS spectra were recorded using a Physical Electronics (PHI) Quantera II spectrometer. X-rays were generated with an aluminum anode source and focussed with a quartz crystal monochromator. The monochromatized aluminum $K\alpha$ X-ray source at 1486.7 eV was operated at 50W,15kV. A dual beam charge compensation system was used for neutralization of all samples. Survey spectra were obtained with 280 eV pass energy at a 45° take off angle. Elemental compositions of the surfaces were determined from low resolution scans for C, O, N and Si. Data treatment was performed using PHI MultiPak Version 9.4.0.7 software. One measurement per sample type was carried out at two surface locations with a spot size of 200 μm .

3.2.8 Atomic Force Microscopy (AFM)

AFM height images of PDA modified surfaces were taken using a Veeco Dimension Icon AFM (Plainview, NY). The AFM images were taken in air under ambient conditions using ScanAsyt mode with PeakForce tapping. The silicon nitride cantilever (spring constant k : 0.4 N/m) was automatically adjusted to a scan rate of 1Hz and set to acquire 512 samples/line. NanoScope Analysis software ver.1.5 by Bruker Corporation was used for image analysis. PDA particle analysis was conducted on features above the surface. Threshold height values were set to incorporate the maximum number of PDA particles for analysis. Surface roughness was reported as the average root mean square (R_{rms}) roughness taken over the entire image. The roughness parameter was defined as the root mean square average of the height deviations taken from the mean data plane as described by **Equation (1)**,

$$R_{rms} = \sqrt{\frac{1}{N} \sum_{i=1}^N (h_i - \bar{h})^2} \quad (1)$$

where \bar{h} is the mean data plane height, h_i is the current height value, and N is the number of points within the selected image region [85]. AFM values were reported as mean \pm SD for three $2 \times 2 \mu\text{m}$ images.

3.2.9 Ellipsometry

Dopamine layer thickness was determined using a variable angle spectroscopic ellipsometer (J.A. Woollam Co., Lincoln, NE). PDMS was cured onto 1 mm thick glass slides and modified with PDA as described. PC-PDA samples were placed on top of silicon wafers to improve the optical contrast of the sample pores. Glass slides were modified with PDA as described. Measurements were performed over a wavelength range of $\lambda = 245\text{-}1700$ nm at angles of incidence 55, 60, 65, and 70° for PDMS and glass. For PC, measurements were performed over a wavelength range of $\lambda = 1000\text{-}1700$ nm since complete depolarization of the incident light occurred below 1000 nm. PC measurements were conducted at angles of incidence 70° and 75°, which provided the greatest signal intensity. Ellipsometry data were modelled using CompleteEASE software v.4.65 developed by J. A. Woollam Co. The Cauchy model was used as the base for glass. PDMS and PC base were modelled using the B-Spline layer. Due to the porous nature of PC, anisotropic B-Spline was applied with refractive index $n_{PC}=1.625$ and 1.58 as specified by the manufacturer. The PDA layer was modelled using the Cauchy model and refractive index set to $n=1.45$ [84,86] with the absorption coefficient determined to be $k=0.01399$. A graded model was applied for the PDA layer on glass with an average inhomogeneity of $-41.8 \pm 11.9\%$. The average thickness and roughness of PDA were reported for

n=3 measurements with modelling confidence specified by $MSE_{PC}<6$, $MSE_{PDMS}<2$, and $MSE_{glass}<8$.

3.2.10 Protein Radiolabelling

BSA and Fg were radiolabeled with $Na^{125}I$ using the iodine monochloride method [87]. The radioactive BSA solution was transferred to a Slide-A-Lyzer dialysis cassette and dialyzed against isotonic Tris-buffered saline (pH 7.4) with 4 changes of buffer over 24 h. The radioactive Fg solution was passed through a column of AG 1X4 anion exchange resin to remove unbound iodide ion. Tests were conducted to determine residual free iodide. Briefly, labelled protein was precipitated in trichloroacetic acid (TCA) and centrifuged. The suspension containing free iodide ion was counted on a Wizard Automatic Gamma Counter (Perkin Elmer, Boston, MA) and levels below 1% were deemed acceptable.

3.2.11 Stability of BSA Modified Surfaces in Contact with PBS, BSA and FBS

The stability of the BSA-modified PDMS surfaces was investigated. PDA and PEG modifications were conducted as described using M-PEG-NH₂. A 10 mg/mL BSA solution containing 10% I-125-labelled BSA was used for the modification procedure. The surfaces were thoroughly rinsed and dried, then individually submerged in counting vials containing 1 mL of either PBS (pH 7.2), 3 mg/mL BSA, 10% FBS, or buffers at pH 4, 7, and 11 (n = 3 for each condition). Buffers of pH 7 and 11 were prepared by dissolving Na₂HPO₄ in Milli-Q water to a final concentration of 0.1 M and adjusted using NaOH. Buffer of pH 4 was prepared by diluting a pH 4 reference buffer to 0.1 M and adjusting with HCl. The samples were counted on a gamma counter at t = 0, 2, 24, and 48 h. At each time point, the samples were removed from solution and

placed in a clean vial for γ -counting. Once counted, the samples were placed in a new vial with fresh buffer or protein solution.

3.2.12 BSA Adsorption

The surfaces were incubated in BSA solutions prepared in PBS or in 10% FBS. These preparations contained I-125-labelled BSA at the 5-10% level. The BSA concentrations in PBS were 0.05, 0.1, 0.5, 1.5, and 3 mg/mL. The stock labeled FBS was serially diluted to 1, 2, 5, 7.5, and 10%. Samples were incubated for 2 h at room temperature and surface radioactivity was determined by γ -counting. The mass density of protein on the surface was calculated by comparing the surface radioactivity to that of a solution of labelled BSA of known concentration. The experiments were repeated three times using three different batches of samples modified independently.

3.2.13 Fibrinogen Adsorption

The surfaces were incubated fibrinogen solutions containing 5% I-125-labelled fibrinogen and diluted in PBS to a final concentration of 1 mg/mL. After a 2 h incubation at room temperature, the surfaces were rinsed three times in PBS (pH 7.4). Surface radioactivity was determined by γ -counting. The mass density of protein on the surface was calculated by comparing the surface radioactivity to that of a solution of labelled fibrinogen of known concentration. The experiments were repeated three times using three different batches of samples modified independently.

3.2.14 E. coli Adhesion

Substrates were sterilized with 70% EtOH and rinsed in Milli-Q water prior to cell seeding. *E. coli* K12 stably transfected with GFP from plasmid was inoculated from agar into LB media

supplemented with 25 µg/mL Kanamycin antibiotics. The culture was allowed to grow until an optical density of 0.4 was reached; it was then centrifuged and the pellet re-suspended in PBS (pH 7.4) to remove the LB media. PDMS and PC samples were incubated in 1 mL of medium containing 2×10^7 cells/mL and 2×10^8 cells/mL, respectively, for 4 h in a 200 RPM rotary shaker at 37°C. Glass samples were incubated in 1mL of medium containing 2×10^7 cells/mL for 5 h in a stationary incubator at 37°C. PDMS and PC samples were gently rinsed three times (5 min each time) with PBS before imaging on an Evos FL Auto epifluorescence microscope (Life Technologies, United States) equipped with a YFP LED light cube (Ex. 500/24nm; Em. 524/27nm) at 20x objective. Glass samples were not rinsed prior to imaging due to weak cell adhesion on this surface. Cells were counted using ImageJ particle analysis software.

3.3 Statistical Analysis

Student t-tests were conducted on all data sets with a significance level set at $p < 0.05$. Data analysis was performed in Microsoft Excel 2007 using the Data Analysis ToolPak.

4. PC, PDMS, AND GLASS SURFACES MODIFIED WITH PEG AND BSA USING POLYDOPAMINE AS A BIO GLUE

4.1. Results and Discussion

PC and PDMS were first investigated in earlier studies. These materials were chosen to investigate the feasibility of an aqueous-based coating method for universal modification of multiple materials of varying wettability. Polydimethylsiloxane (PDMS) is a hydrophobic material ($\theta \sim 120^\circ$) widely used in the production of biomedical microfluidic devices [33] and water monitoring sensors [4] due to its non-toxic, non-immunogenic, and gas permeability properties. The second material, polycarbonate (PC) membrane, is used for filtration [16,61] and in optical sensors [88]. The PC membrane used in this study is pre-coated with polyvinylpyrrolidone (PVP) by the manufacturer to make the surface hydrophilic and improve its compatibility in aqueous environments. The PC membrane was found to have a water contact angle of $\theta = 66 \pm 2^\circ$, indicating hydrophilicity at an “intermediate” level.

Minimizing the surface roughness of the formed PDA layer has been recommended to improve the post-modification of PDA surfaces [13]. Over time, the polymerized dopamine begins to aggregate in solution and form colloidal dopamine-melanin particles of increasing size [13,84]. These particles can spontaneously adsorb to the material surface at any time during dopamine polymerization, generating an uneven surface. High surface roughness caused by the adsorption of large PDA particles may limit the coverage of PDA by PEG and BSA in subsequent treatments. The optimal PDA thickness to give a hole-free layer while maintaining minimal surface roughness was found to be in the 10-20 nm range, and was achieved after 2-4

hours of PDA exposure at room temperature on various polymers [13]. Thus, a PDA deposition time of 3 h was chosen for this study.

4.1.1 Stability of BSA Attached to PDA Coated Surfaces

Following the pioneering PDA-PEG studies of Lee et al. [7], methoxy-PEG-amine (M-PEG-NH₂) of molecular weight 5000 Da was used to post-modify PDA coated surfaces. In preliminary studies, poor Fg resistance was found on PC and PDMS surfaces modified with PDA-PEG (data not shown). We hypothesized that BSA could be used as a backfill on PDA-PEG surfaces to block free PDA binding sites and reduce Fg adsorption. However, the interaction between BSA, PEG, and the PDA surface is unclear. Ideally, BSA would be interacting with the substrate-PDA, granted that brush densities allow sufficient diffusion. However, at higher grafting densities, covalent bonding of BSA to PDA, as proposed by Zhu et al. [16], may be hindered in the presence of PEG. Consequently, if BSA attaches to the surface by physisorption, the BSA may be displaced by other proteins (possibly cell adhesive proteins) in solution which have greater affinity to the surface [17]. Electrostatic bonding between BSA and PDA is also not favourable since some applications may involve environments of changing pH, such as in natural and waste water quality monitoring and biological or chemical assays in cell culture platforms.

To determine whether the bond between BSA and PDA was stable, the loss of protein from PDMS-PDA discs modified with radiolabeled BSA was monitored over two days. Samples were incubated in buffer solutions at pH above and below the isoelectric points (pI) of PDA (pI_{PDA} = 9.7) and BSA (pI_{BSA} = 4.7) to investigate the possibility of electrostatic interactions. If BSA is interacting with the surface electrostatically, altering the solution pH may modify the

interaction such that BSA release occurs. Specifically, BSA and PDA will carry a net negative charge when the solution $\text{pH} > \text{pI}$, and a net positive charge when $\text{pH} < \text{pI}$. The PDA surface will repel the incoming protein when the charges of BSA and PDA match. Equilibration after a change of pH may take as long as 12 h [89]. Surfaces were also incubated in BSA solutions and fetal bovine serum (FBS) to observe protein loss/exchange. Gradual BSA loss from the surface would also be observed over time if protein release/exchange is occurring, although the exact rate of protein exchange will depend on the strength of protein-substrate interactions and the affinity of other proteins in solution for the surface [46].

The results of these experiments are summarized in **Figure 6**. PDA-BSA*/PEG surfaces showed no significant loss of BSA* under all solution conditions after 48 h ($p < 0.05$). Only PDA-BSA* in BSA solution ($p = 0.01$), and PDA-PEG/BSA* in PBS ($p = 0.02$) and pH7 buffer ($p = 0.04$) showed significant BSA* loss after 48 h. Some BSA loss occurred for the other conditions but was not statistically significant. It is likely that the small BSA losses observed may have been caused by sample handling at each time point rather than by exchange with other proteins or changes in solution pH .

Accepting this to be true, then we may conclude that protein loss/exchange over 48 h in the protein solutions and buffers were insignificant. Also it is likely that the BSA will remain on the surface over longer periods of time. It has been shown that protein desorption and exchange are less and less likely to occur the longer the adsorbed protein is in contact with the surface [46]. Proteins that have had sufficient contact time with the surface establish strong contact with the surface during spreading and transform into un-exchangeable conformations [40]. This was likely the case with BSA on PDA as it was allowed to adsorb to the surface for 24 h during post-modification of PDMS-PDA. In addition, due to the insignificant loss of BSA from the modified

surfaces in contact with buffers and protein solutions, we can assume that BSA did not bond to the PDA-modified surface electrostatically or by other weak attractive forces. From these results it may be concluded only that BSA adsorbed strongly to the surface, but whether BSA is bonded to PDA covalently remains unclear.

An interesting result is that no significant difference was seen in the quantities of BSA adsorbed to the PDA-BSA, PDA-BSA/PEG, and PDA-PEG/BSA surfaces. This suggests that the density of PEG on the surface was insufficient to completely prevent adsorption or affect the mechanism by which BSA interacted with PDA. If higher grafting densities of PEG on the PDA surface were achieved, it is probable that BSA quantities would be lower in PDA-PEG/BSA modifications compared to PDA-BSA. BSA interactions with PDA may be changed with the higher PEG density. The relatively high BSA adsorption seen on the PEG modified surfaces also further emphasizes the need to cover exposed PDA on PDA-modified surfaces.

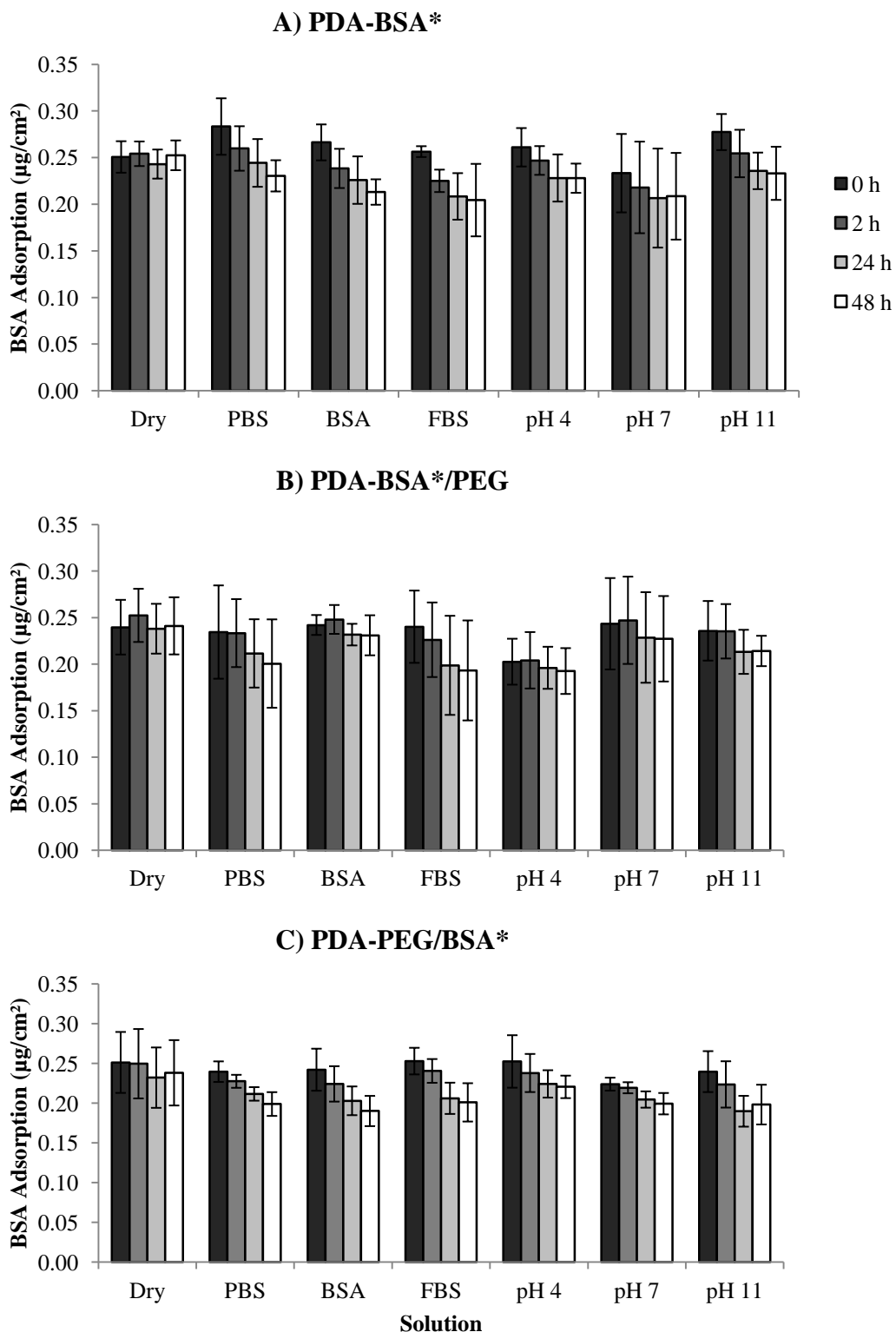


Figure 6. BSA stability on PDMS surfaces modified with: A) PDA, B) BSA/PEG, and C) PEG/BSA in contact with protein solutions and buffer solutions over two days. Means \pm SD, $n=3$. ($pI_{PDA} = 9.7$; $pI_{BSA}=4.7$)

4.1.2 BSA Adsorption

BSA was used as a model protein to measure the fouling resistance of each surface. The quantities of BSA adsorbed to PDMS and PC are shown in **Figures 7** and **8**, respectively. Adsorption experiments were completed for 2 h in single protein (BSA) solutions and mixed protein (FBS) solutions. For comparison purposes it is noted that 10% FBS contains approximately 2.3 mg/mL of BSA [90].

As expected, PDA-modified PDMS and PC adsorbed significantly more BSA compared to the unmodified surfaces ($p_{PDMS}=0.001$; $p_{PC}=0.00007$) from BSA solution. PDA modification increased BSA adsorption by 43% and 38% on PDMS and PC, respectively. However, comparable BSA adsorption was observed in 10% FBS solution on unmodified and PDA-modified materials. In fact, there was notably less BSA adsorption on all modified PDMS and PC surfaces from FBS solution compared to single BSA protein solution. Competing proteins in FBS may have either dominated early adsorption events or displaced BSA via a Vroman-type effect, thereby reducing BSA adsorption. The relative extent to which these two phenomena occur will depend on differences in protein-substrate interactions on the different surfaces.

Nevertheless, trends in the data were similar for PDMS and PC in BSA and FBS solutions. The modification of PDA surfaces with PEG reduced the number of PDA sites available for BSA adsorption. PEG modification reduced BSA adsorption more so on PC-PDA (reduction in 3 mg/mL BSA = 80% and 10% FBS = 52%) compared to PDMS-PDA (reduction in 3 mg/mL BSA = 50% and 10% FBS = 39%). This suggests that higher PEG grafting densities (and greater PDA coverage) were achieved on PC-PDA compared to PDMS-PDA. However, high BSA adsorption to PDA-PEG modified PC and PDMS suggests that grafting densities were

not high enough to prevent BSA from penetrating the PEG layer. Dense PEG brush configurations were likely not achieved on PC-PDA and PDMS-PDA surfaces.

Consequently, the reduction in BSA adsorption on PDA-PEG was not nearly as much as PDA-BSA. The higher BSA adsorption on PDA-PEG surfaces suggested that active PDA sites were not as well blocked by PEG and thus emphasized the need to improve this PDA-PEG method. Significantly lower protein adsorption to PDA with BSA compared to PEG in BSA solution ($p_{PDMS}=0.005$; $p_{PC}=0.02$) and FBS ($p_{PDMS}=0.008$; $p_{PC}=0.0002$) was likely due to the much larger BSA molecules providing more surface coverage.

BSA adsorption on PDMS modified PDA-BSA, PDA-BSA/PEG, and PDA-PEG/BSA were not significantly different. This validates the explanation (section 4.1.1) of the observation that the similar quantities of BSA on PDA-BSA, PDA-BSA/PEG, and PDA-PEG/BSA were likely due to poor PEG coverage on the PDMS surface. PC-PDA surfaces on the other hand reported significantly lower BSA adsorption with PEG/BSA compared to BSA/PEG in BSA solution ($p=0.006$). Better protein reduction on PC-PDA-PEG/BSA was likely due to greater PEG coverage and reduced need for BSA to cover free PDA sites. BSA adsorption on PC-PDA modified with BSA/PEG and PEG/BSA was not significant in FBS, but this may be a consequence of FBS proteins outcompeting BSA and masking these differences as was seen with unmodified and PDA surfaces.

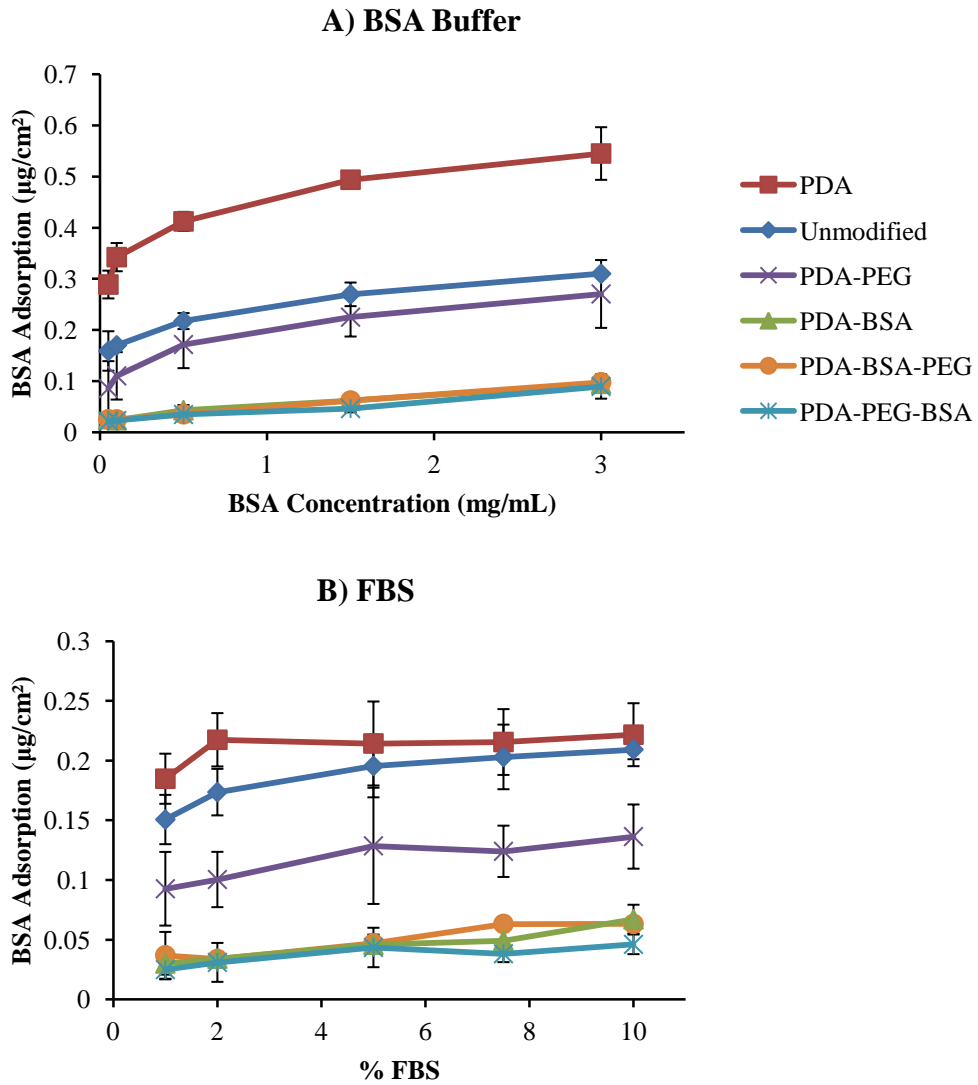


Figure 7. BSA adsorption on modified PDMS surfaces from: A) BSA and B) FBS solution, both made in pH 7.4 PBS buffer. Means \pm SD for n=3 trials.

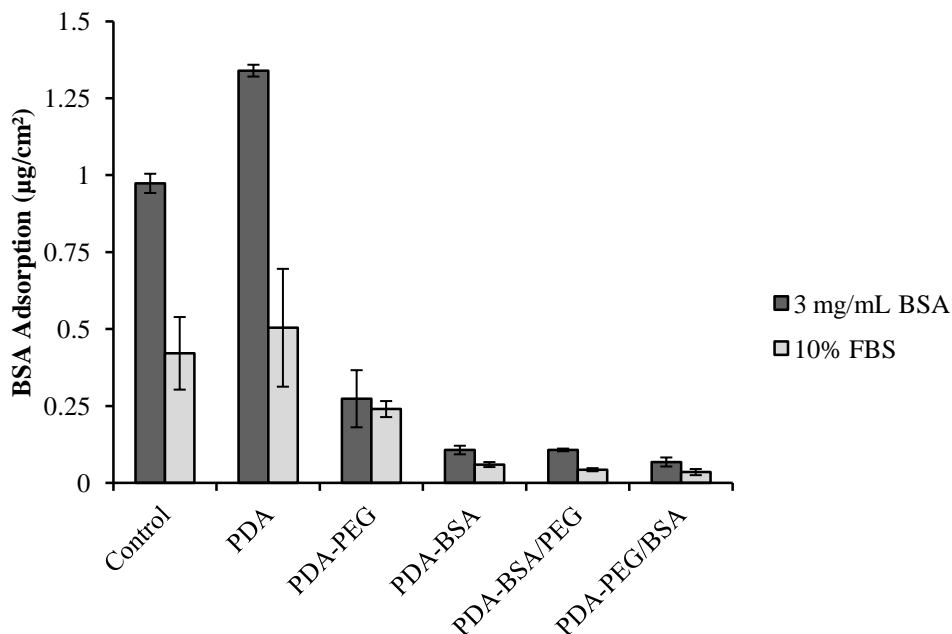


Figure 8. BSA adsorption on modified PC surfaces from BSA solution (3 mg/mL in PBS buffer, pH 7.4) and 10% FBS solution (PBS buffer, pH 7.4). Means \pm SD, n=3.

The results presented so far reveal differences in the antifouling performance of the PDA-PEG/BSA modified PC and PDMS surfaces. These differences are likely a consequence of differences in grafted PEG densities, which may be caused by differences in PDA polymerization that affect PEG grafting. The subsequent studies will assess the quality of the PDA layer, such as whether 3 h polymerization time is sufficient in creating a hole-free layer. PDA thickness and surface roughness will also be quantified. In addition, a third material was added to the study to observe how substrate wettability affects dopamine polymerization. Glass was chosen for its highly hydrophilic properties ($\theta \sim 16^\circ$) and because it is widely used in cell culture, imaging platforms, and sensor technology due to its structural rigidity and optical transparency.

Substantially lower BSA adsorption from FBS provides a strong indication that other proteins in the serum competed effectively for surface sites. This may explain the small, insignificant differences in BSA adsorption observed on substrates incubated in FBS, while significant differences in adsorption from single protein BSA solutions were seen. Different model proteins may show greater differences in resistance to adsorption between the different modified surfaces. Fibrinogen (Fg) was chosen as model protein for subsequent adsorption experiments. Fg is a 340 kDa cell adhesive protein which plays an important role in platelet adhesion and thrombosis on blood contacting surfaces as well as in coagulation. In blood coagulation, fibrinogen is broken down by serine protease thrombin to form insoluble fibrin strands which cross-link to assist platelet adhesion [91]. Fg adsorption is therefore commonly used in the study of antithrombotic surfaces [25]. Since Fg is a much larger protein than albumin, it possesses stronger surface affinity, so that desorption and exchange are expected to be limited.

4.1.3 Optimization of PEG Modification

It was apparent from the BSA adsorption results that improvement in PEG grafting on PDA surfaces to achieve higher protein resistance was needed. As previously mentioned, a dense brush configuration is more ideal for protein repulsion through steric repulsion, osmotic repulsion, and water interactions [53]. However, the results in section 4.1.2 suggest that brush-type configurations are not achievable with amino-PEG at one chain end. To improve PEG binding efficiency and coverage on PDA, difunctional PEG with amino groups at both chain ends may be desirable for surface modification. Yet, due to the high molecular weight of PEG (5000 Da), both terminal amines may bind to the PDA surface forming loops. It is possible that such looped PEG may spatially hinder incoming proteins to the PDA surface, although it is not as repellent as a PEG brush.

Figure 9 compares Fg resistance on PDA-modified PC, PDMS, and glass surfaces post-modified with M-PEG-NH₂ or NH₂-PEG-NH₂. Both PEG types reduced Fg adsorption on all three PDA-modified materials as expected. Significantly less Fg adsorption was seen on all PDA surfaces post-modified with NH₂-PEG-NH₂ compared to M-PEG-NH₂ ($p_{PC} = 0.0005$, $p_{PDMS} = 0.0005$, $p_{Glass} = 0.0008$). These data suggest that greater PEG attachment was achieved with the diamino PEG, and/or the formation of PEG loops allowed for greater coverage and masking of PDA. Based on these results, NH₂-PEG-NH₂ will be referred to as PEG for convenience and used in subsequent experiments.

Adsorption of Fg and BSA was compared on PDMS surfaces at 1 mg/mL protein concentration. BSA adsorption on PDMS was approximated at 1 mg/mL concentration from buffer from the isotherm in **Figure 7**. In converting protein adsorption to pmol/cm², there was more BSA adsorbed to unmodified (3.5 pmol/cm²) and PDA modified PDMS (6.9 pmol/cm²) than Fg (2.5 and 4.2 pmol/cm², respectively). Higher BSA adsorption correlates to the fact that BSA (66.5 kDa) is much smaller than Fg (340 kDa), resulting in greater protein molecules per area (mol/cm²) at reduced weight per area (µg/cm²). Following PDA modification, Fg adsorption increased by 72% and BSA adsorption increased by ~100%. A greater increase in BSA adsorption is again reflective of the smaller BSA size, allowing greater protein coverage on the surface due to reduced steric hindrance. Surfaces modified with M-PEG-NH₂ reported similar protein adsorption of 3.6 pmol/cm² of Fg and 3.0 pmol/cm² of BSA.

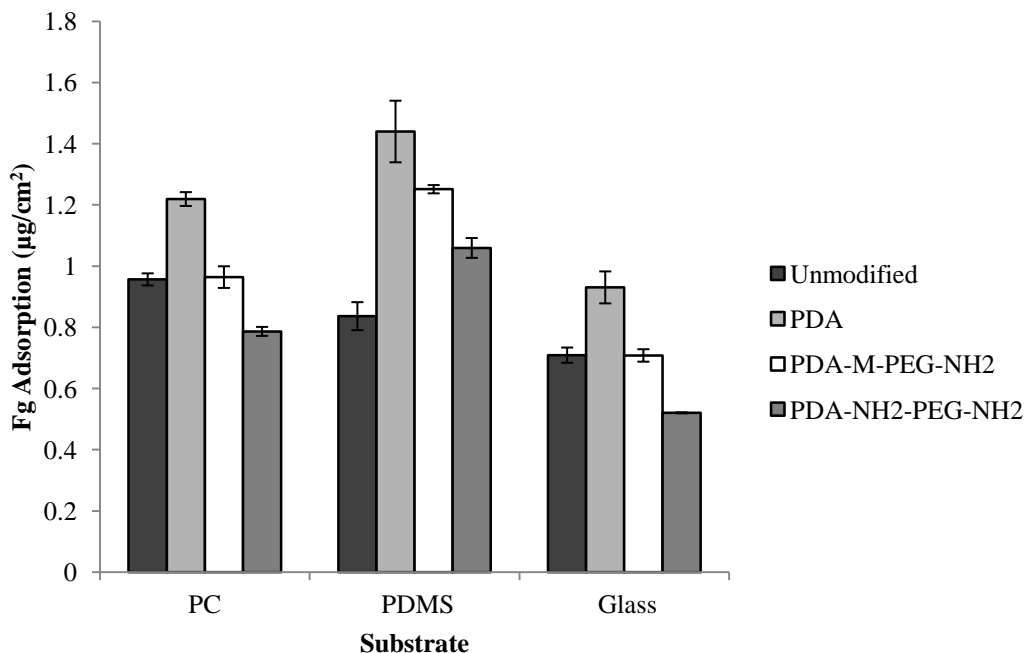


Figure 9. Comparison of Fg adsorption on M-PEG-NH₂ and NH₂-PEG-NH₂ modified PDA coated PC, PDMS, and glass. Means \pm SD, n=6 for PC and PDMS, n=3 for glass.

4.1.4 Water Contact Angles

Water contact angles were measured to verify changes in substrate surface chemistry as reflected in wettability (**Table 3**). Contact angles of PDA-modified surfaces have been reported between 50-65° no matter the underlying substrate after 24 h of dopamine exposure [8,67,84], which corresponds to the formation of a PDA layer greater than 10 nm [7].

After 3 h stirring in dopamine solution, the contact angle of PDMS dropped to 67 \pm 8° while that of glass increased to 41 \pm 4°. Indeed, the contact angles of PDMS and glass were approaching the characteristic wettability of PDA surfaces as previously reported. However, the slightly higher contact angle of PDMS and lower contact angle of glass suggest that the underlying surface was still sensed in the contact angle measurement. This may be due to

incomplete coverage of PDA on the surface. The contact angle of PC decreased slightly to $58\pm 7^\circ$, i.e. within the wettability range of PDA as previously reported. Since unmodified PC showed a contact angle similar to that of PDA, no conclusion regarding PDA coverage could be made.

The water contact angles of the three substrates were reduced on treatment of the PDA surfaces with PEG, while they were increased on treatment with BSA. These results are consistent with the findings of Zhu et al. [16] who reported decreased hydrophilicity of PDA-BSA coated PE membranes ($\theta_i=61.6\pm 3.7$) compared to PDA coated membranes ($\theta_i=46.7\pm 3.8$). The wide range in contact angles after PEG and BSA modifications among the three materials may be due to the differences in initial PDA coverage. The combination of BSA and PEG on the surfaces resulted in contact angles between that of PDA-PEG and PDA-BSA for PDMS and glass surfaces. The high wettability of PDA-BSA/PEG and PDA-PEG/BSA on PC surfaces suggests that the PEG coverage may be greater than that of BSA.

Table 3. Water contact angles of modified PC, PDMS, and glass. Sessile water contact angles of 6 μ l drops were taken after 2 min of surface contact. Mean \pm SD for n=3 samples.

Modification	PC	PDMS	Glass
Unmodified	$66\pm 2^\circ$	$117\pm 3^\circ$	$16\pm 2^\circ$
PDA	$58\pm 7^\circ$	$67\pm 8^\circ$	$41\pm 4^\circ$
PDA-PEG	$38\pm 2^\circ$	$54\pm 3^\circ$	$24\pm 2^\circ$
PDA-BSA	$65\pm 4^\circ$	$72\pm 2^\circ$	$54\pm 1^\circ$
PDA-BSA/PEG	$33\pm 1^\circ$	$72\pm 7^\circ$	$38\pm 3^\circ$
PDA-PEG/BSA	$34\pm 2^\circ$	$60\pm 5^\circ$	$36\pm 2^\circ$

4.1.5 XPS Analysis

The elemental compositions of bare and modified PC, PDMS, and glass surfaces as determined by XPS are presented in **Table 4**. After 3 h dopamine polymerization, the surfaces acquired a distinctive brown tinge known to be characteristic of PDA (**Figure 10**) [8]. The increase in nitrogen (N) signal and decrease in silicon (Si) on PDMS and glass after PDA modification showed that some of the Si signal from the underlying substrate was blocked by PDA. Incomplete quenching of the Si signal native to unmodified PDMS and glass implies that the thickness of the PDA layer after 3 h was less than the sampling depth of XPS (<10 nm) or that PDA coverage was incomplete. This is consistent with the water contact angle data (table 3), suggesting some influence of the bare substrate on the wettability of the PDA modified surfaces. Further PDA surface analysis and characterization by AFM and ellipsometry are discussed in section 4.1.6.

Due to the presence of carbon in the unmodified substrates, the carbon data cannot be used directly to determine whether the N and C signals after PDA modification were consistent with theoretical predictions. **Equation (2)**, adapted from Michel et al. [25], was used to obtain the true signal of an element, X, by correction for an overlayer using a substrate specific signal (in this case, Si) as a reference:

$$X_{True} = X_f - X_i \left(\frac{Si_f}{Si_i} \right) \quad (2)$$

where X_{True} is the corrected element signal, X_f and Si_f are the post-modification signals (atom %), and X_i and Si_i are the signals before modification. Using the corrected values for C, the nitrogen-to-carbon ratio (N/C) was determined to be 0.094 for PDMS and 0.121 for glass. These

values are close to the theoretical N/C ratio of 0.125 for PDA [7]. The uncorrected N/C ratio for PC-PDA was 0.086, suggesting that substrate-specific C may be present in the XPS carbon signal. Due to the lack of substrate specific elements for PC, the actual C and N values contributed by PDA could not be obtained. However, the large increase in N content after PDA modification and the change in substrate colour as shown in **Figure 10** provided evidence that PDA was indeed deposited on the surface.

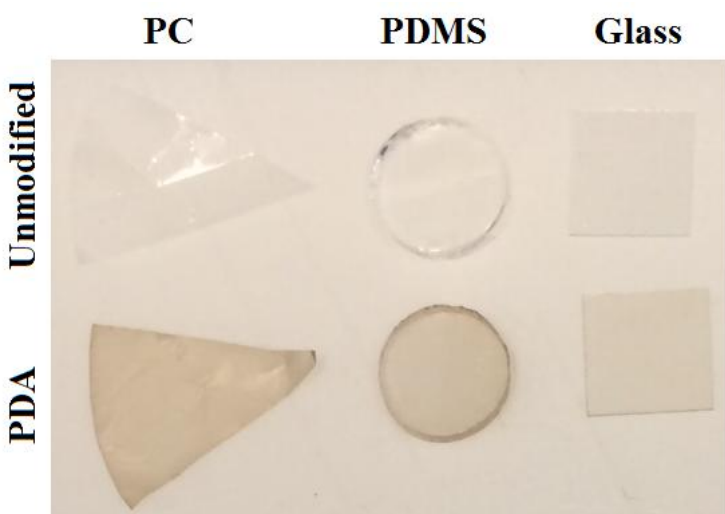


Figure 10. Photograph of unmodified and PDA modified PC, PDMS, and glass samples. Samples were tinted with a distinctive brown colour after 3 h dopamine polymerization at room temperature. Samples remained brown after subsequent modifications with PEG and BSA.

Further increase in N content was observed on PC-PDA surfaces after the attachment of amino-terminated PEG and BSA. The larger increase in N upon treatment with BSA compared to PEG is expected due to the high N content (amide and amino groups) of proteins (BSA, MW=66 kDa). PC modified with PDA-BSA and PDA-BSA/PEG showed similar atomic compositions. Attachment of PEG after BSA treatment was likely difficult due to the large BSA molecules occupying most of the available binding sites on PDA. However, when PEG exposure preceded BSA, the N content was intermediate between that of PDA-PEG and PDA-BSA

surfaces. Greater quantities of PEG were attached to the PDA surface when added before BSA, as indicated by the reduced N content. In addition, since the N-content on PDA-PEG/BSA was not as high as on PDA-BSA but not the same as PDA-PEG, we can conclude that there was indeed a mixture of PEG and BSA on the surface.

The atomic composition of PDMS-PDA was unchanged after PEG modification, and thus could not be used to verify that PEG was attached to the surface. In addition, the atomic composition was similar for PDMS surfaces modified with PDA-BSA, PDA-BSA/PEG, and PDA-PEG/BSA. These data suggest that much of the PDA was not covered by PEG on these surfaces. The water contact angles of the PEG-treated surfaces suggest that some PEG may be present though at lower density thereby allowing high quantities of BSA to penetrate the PEG layer.

Trends in nitrogen content could not be reliably tracked for the glass surfaces due to suspected PDA surface damage. Increase in Si and decrease in N content after PEG and BSA modifications following PDA treatment suggest that PDA was removed during both modifications. Si content was nearly restored to the unmodified glass values after PEG/BSA and BSA/PEG treatments. Mechanical removal of PDA may have occurred via contact with other samples or container walls during treatment. No loss of PDA was observed on PDMS and PC samples after modification, although PDMS is also prone to mechanical damage during sample handling. The contact angle of a PDMS-PDA surface scratched extensively with tweezers is restored almost to that of unmodified PDMS. Due to the delicate nature of the PC membrane, mechanical removal of PDA was not investigated.

Table 4. XPS elemental composition of PC, PDMS, and glass surfaces modified with PDA, PEG and BSA.

Surface	C 1s	N 1s	O 1s	Si 2p
PC-PVP	79.1	0.5	19.5	0.9
PC-PVP-PDA	67.8	5.8	24.0	2.5
PC-PVP-PDA-PEG	69.4	7.3	21.4	1.3
PC-PVP-PDA-BSA	68.0	10.8	20.1	1.1
PC-PVP-PDA-BSA/PEG	69.9	10.0	19.1	1.1
PC-PVP-PDA-PEG/BSA	70.1	8.4	20.0	0.8
PDMS	44.2	0	31.1	24.7
PDMS-PDA	49.8	1.3	28.8	20.1
PDMS-PDA-PEG	51.6	1.4	29.0	18.0
PDMS-PDA-BSA	54.0	3.7	27.0	15.3
PDMS-PDA-BSA/PEG	51.4	3.0	28.7	16.9
PDMS-PDA-PEG/BSA	51.9	3.2	27.8	17.1
Glass	12.7	0	61.4	22.8
Glass-PDA	54.2	6.0	31.0	8.0
Glass-PDA-PEG	45.7	5.0	37.2	11.3
Glass-PDA-BSA	35.4	6.2	42.6	14.7
Glass-PDA-BSA/PEG	20.0	1.0	56.0	22.7
Glass-PDA-PEG/BSA	28.1	3.7	48.8	18.6

Estimated data precision $\pm 0.5\%$

4.1.6 PDA Thickness and Roughness

Data on thickness and surface roughness of PDA layers on modified surfaces as determined by ellipsometry and AFM are summarized in **Table 5**. AFM scans used to determine surface roughness and particle features are shown in **Figure 11**. Roughness measurements for PC could not be determined by ellipsometry due to near complete depolarization and low signal intensity of the reflected light at $\lambda < 1000$ nm. Surface roughness is modelled at shorter wavelengths due to higher scattering of light at those wavelengths [92]. Assuming that the ellipsometer used was operating optimally, common substrate specific causes for depolarization of the incident light include light scattering due to thickness inhomogeneity, backside reflections for weakly absorbing substrates, or large surface roughness [92]. Since strong depolarization was observed on unmodified PC, light depolarization was narrowed to the PC substrate rather than the PDA deposit. Assuming that the supplier of the PC membrane enforces strict quality control, thickness non-uniformity was not questioned. While the PC membrane showed low absorption over the wavelengths used ($k \sim 0$), strong interference caused by backside reflections is not likely as the membrane is quite thin ($t_{PC} = 6 \mu\text{m}$). Backside reflections tend to interfere with the observation of surface features if the substrate is greater than 0.2 mm in thickness [92]. Depolarization caused by surface roughness was also unlikely since the surface roughness of the PC was minimal as determined by AFM ($r_{PC} = 3.0 \pm 1.3$ nm). It is suspected that strong anisotropic light scattering leading to light depolarization was most likely the cause. This effect is due to the birefringent nature of the porous PC membrane ($n_{PC} = 1.625$ and 1.58).

To accurately model the PDA thickness on PC, wavelengths below 1000 nm were eliminated from the analysis. The PDA thickness on PC was determined to be below the sampling depth of XPS ($t_{PC-PDA} = 6.3 \pm 0.1$ nm), confirming that the low N:C ratio determined by

XPS was due to excess carbon signal from the PC substrate rather than from PDA. PDA roughness was determined to be 16.5 ± 4.4 nm from AFM analysis. “Divots” in the PDA surface caused by the pores of the membrane were observed in AFM scans, although the extent of pore coverage by PDA was uncertain. Fluid permeability experiments observing flow rate through the membrane should be conducted to determine changes in membrane performance.

The PDA thickness on PDMS was determined to be 27 ± 5 nm. The Si signals detected in the XPS analysis of PDMS-PDA were therefore most likely caused by gaps in the PDA layer exposing bare PDMS. The larger area AFM scan of PDMS-PDA shown in **Figure 12a)** reveals cracks in the PDA layer. Data from the AFM scan shown in **Figure 12b)** confirm that the thickness of PDA was within the range determined by ellipsometry. This provides strong evidence that the material at the lowest point of the fissure was likely bare PDMS or PDMS minimally covered by PDA, allowing substrate specific Si to be detected. In addition, the slightly low N/C ratio for PDA on PDMS may be due to the substrate carbon signal having a contribution from the cracks. PDA deposit cracking was only observed for PDMS, possibly due to the flexibility of this material. The surface roughness of PDMS also increased after PDA deposition, with feature size of about 7 nm as determined by both AFM and ellipsometry.

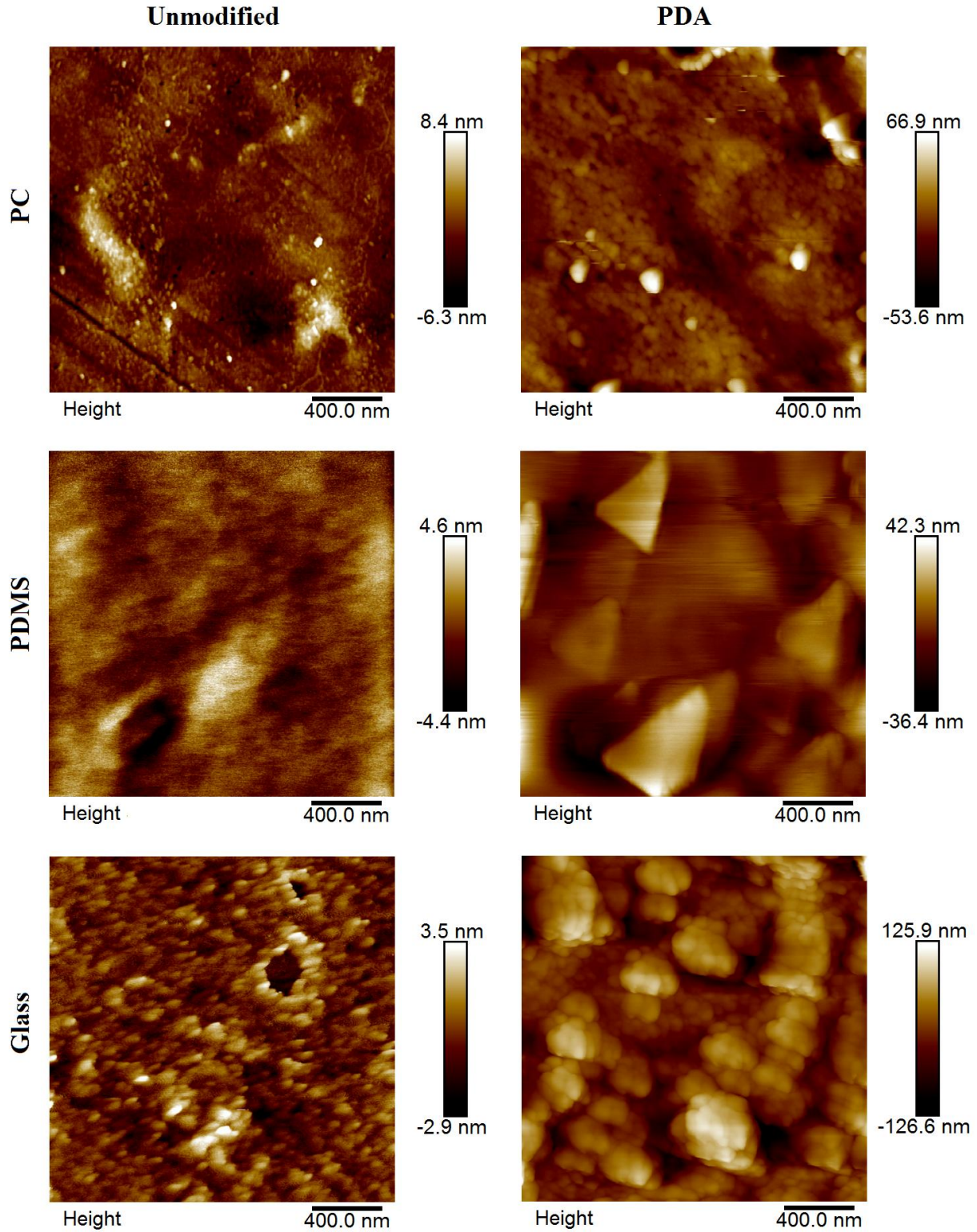


Figure 11. AFM topography images of unmodified and PDA modified PC, PDMS, and glass samples.

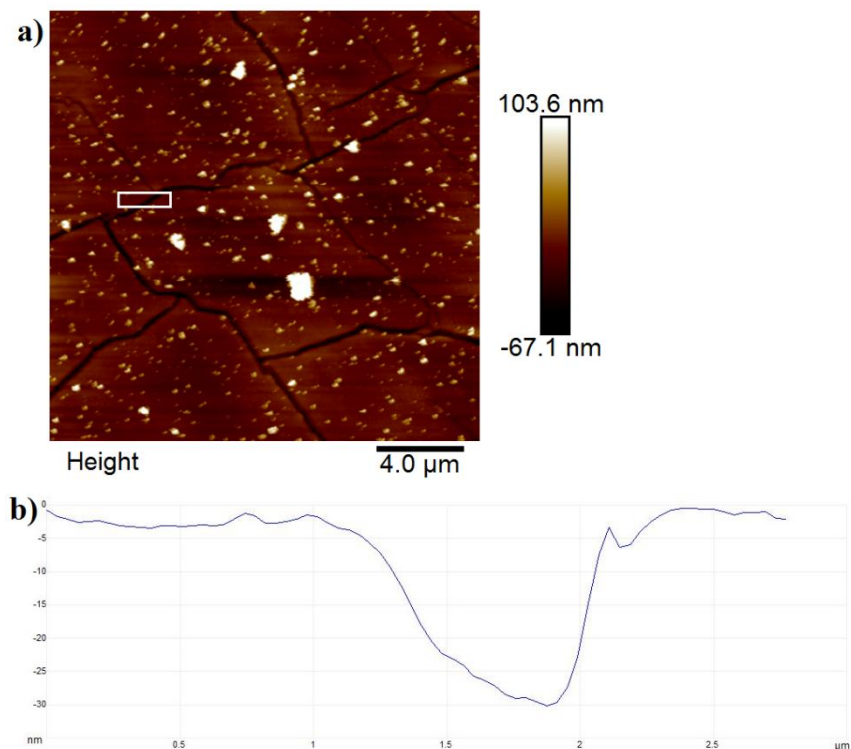


Figure 12. a) Large 20x20 μm AFM height scan of PDMS-PDA revealing cracks in the PDA layer. b) Vertical distance map across the white boxed area in AFM image a). PDA thickness = 25.5 nm.

Ellipsometry measurements on glass-PDA samples showed PDA thickness to be on the order of 10 nm ($t_{\text{glass-PDA}} = 11 \pm 3$ nm), thus supporting the conclusion that the Si signal detected by XPS was due to the thickness of the PDA layer being less than the XPS sampling depth (~10 nm). Despite the fact that glass was the smoothest of the three unmodified substrates, glass-PDA showed the highest roughness of the three modified materials: 36.8 ± 1.4 nm by AFM and 50 ± 13 nm by ellipsometry. The discrepancy between the PDA roughness values determined by the two methods may be due to differences in the samples used in each analysis and/or differences in the sampling area of the two techniques. The spot size for the ellipsometer used was 3x5.5 mm at an angle of incidence of $\theta_i = 57^\circ$ [93], substantially larger than the 2x2 μm scan size used for AFM analysis. Another possible reason for the discrepancy is overestimation associated with

modelling of the ellispometry data. Surface roughness is approximated using the Bruggeman Effective Medium Approximation (EMA) [92,94]. EMA “converts” the real layer into a mixed graded layer consisting of the thin film with 50% void content [92,94]. However, this model is only accurate when the magnitude of the surface roughness is less than the wavelength used. This often corresponds to surface roughness features $< \lambda/10$ or <40 nm since shorter wavelengths are more prone to surface scattering [92,94]. Since the reported surface roughness of PDA based on AFM was close to the limit of the model, the EMA model with 50% void content may not accurately describe the surface roughness.

4.1.7 PDA Particle Analysis

Variability in PDA thickness and roughness on the three materials revealed substantial differences in the way dopamine polymerizes on different substrates. From the AFM scans shown in **Figure 11** it is clear that the PDA particles formed on each material were of very different morphologies. Since colloidal PDA has been reported to increase in diameter over time (2 mg/mL dopamine, 10 mM Tris-HCl pH 8.5) [13], it was decided to undertake PDA particle analysis as a means of probing differences in dopamine polymerization on the three materials.

PDMS-PDA showed the lowest surface density and largest diameter of PDA grains. However, PDA thickness on PDMS was found to be greater than on PC or glass. This suggests that PDA deposition on PDMS may occur primarily by direct polymerization on the surface rather than adsorption/deposition of colloidal particles formed in solution. This leads to a greater packing density of PDA (and hence, a thicker PDA layer) while minimizing PDA surface roughness. The affinity of polydopamine for the hydrophobic PDMS thus appears to be high, causing rapid and extensive adsorption and polymerization of dopamine. Contrary to our original

hypothesis, XPS revealed poor PEG grafting on PDMS-PDA despite having the lowest surface roughness of the three materials. Possibly, the decreased surface area of PDA on PDMS altered the accessibility and reduced the availability of reactive PDA sites for PEG attachment.

AFM images of PC and glass surfaces revealed a greater variety of PDA particle structures. The greater height values for PC and glass compared to PDMS were due to stacking of PDA particles as they adsorbed on the surface. This correlates with the calculated PDA roughness values: glass showed the highest roughness with the greatest height variation. PC-PDA showed the highest grain density with the smallest grain size, indicating that PDA particle deposition on PC was favored early in the process. However, glass-PDA showed, respectively, average grain diameter and grain density almost twice and half those on PC. Since all three materials were modified under the same reaction conditions, PDA particle growth in the solution should be the same.

It appears that the attractive forces between dopamine/PDA and the substrate may influence whether dopamine polymerizes directly on the substrate or if dopamine-melanin particles formed in solution deposit on the surface. PDA attraction to the hydrophilic glass may be weak and require larger PDA particles to stick to the surface. PDA attraction to PC, which has similar water contact angles as PDA, is moderate allowing smaller particles to adsorb to the surface early on. Shearing of the PC-PDA surface due to sample stirring in solution may explain why the particle size did not increase. Finally, strong attraction of dopamine to the hydrophobic PDMS promoted quick adsorption of dopamine oligomers and polymerization from the surface. Since the starting surface roughness values of the three materials were similar, it is not possible to know from our results whether initial surface roughness affects early dopamine polymerization.

The findings in this study are in contrast to those of Pop-Georgievski et al. [13] who found similar PDA growth rates on different materials. These authors also used ellipsometry to determine PDA thickness on gold, silicon, PLLA, and PET substrates. However, their data analysis methods and model choice raise questions over the accuracy of their thickness data. PDA thickness was modelled using a Lorentz oscillator model and led to a model fit giving $MSE=37$ [13]. This high MSE value casts doubt on the choice of model and thus on the reported PDA thicknesses. Indeed, applying the Lorentz oscillator model for PDA to our data, $MSE>50$ was obtained indicating a poor data fit. The Cauchy model for PDA provided a better fit since the PDA layer absorbed only slightly ($k=0.014$). Oscillators are generally used for strongly absorbing films where the dielectric function is unknown and involves more complex parametric dispersion models to describe the absorption behavior [92].

Table 5. Surface characteristics of PDA deposited on PC, PDMS, and glass as determined by ellipsometry and AFM. The average image RMS surface roughness and grain characteristics are reported for three 2x2 μm scans. AFM scans are shown in Figure 10. Data are means \pm SD for n=3 measurements or images.

Surface	PDA Thickness (nm)	Roughness (nm)		Density of Grains (μm^{-2})	Average Grain Height (nm)	Average Grain Diameter (nm)
		<i>Ellipsometry</i>	<i>AFM</i>			
		PC	-			
PC-PDA	6.3 ± 0.1	N/A	16.5 ± 4.4	22 ± 6	17 ± 7	69 ± 25
PDMS	-	0 ± 0	1.3 ± 0.1	-	-	-
PDMS-PDA	27 ± 5	7 ± 1	7.1 ± 3.2	1.2 ± 0.2	15 ± 2	303 ± 67
Glass	-	1.1 ± 0.02	0.8 ± 0.3	-	-	-
Glass-PDA	11 ± 3	50 ± 13	36.8 ± 1.4	7 ± 3	52 ± 1	129 ± 29

4.1.8 Fg Adsorption

Fg adsorption results are presented in **Figure 13**. As expected, high Fg adsorption was observed on all PDA modified materials. Modification with PEG further reduced Fg adsorption on PDA for all materials ($p_{PC}=0.01$; $p_{PDMS}=0.0007$; $p_{Glass}=0.009$). Fg adsorption was reduced by 56% on PC-PDA with PEG treatment, compared to PEG modified PDMS-PDA (40%) and glass-PDA (36%). This confirms XPS and water contact angle data that PEG grafting to PC-PDA was better than the other materials. However, significant reduction in Fg on PDMS-PDA after PEG attachment provided evidence that PEG may still have grafted onto PDMS-PDA in lower densities, despite XPS reporting poor PEG attachment.

Significantly fewer Fg adsorbed to PDA-BSA surfaces compared to PDA-PEG for all three substrates ($p_{PC}=0.003$; $p_{PDMS}=0.00007$; $p_{Glass}=0.004$). This result again indicates that PEG grafting from solution was not complete on PDA, and greater surface coverage of PDA was achieved by the larger BSA molecules. High Fg adsorption on the PDA-PEG modified materials provide evidence that a dense polymer brush was not achieved, allowing BSA molecules to penetrate the polymer layer. Thus, PEG of low density and mushroom-type configuration or looped structures was likely produced.

Fg adsorption was not significantly different between PDA-BSA and PDA-BSA/PEG modified surfaces. PEG attachment was likely hindered by the large BSA molecules resulting in a surface more characteristic of BSA. Addition of PEG prior to BSA (PDA-PEG/BSA) resulted in improved Fg reduction on PC and PDMS compared to PDA-BSA ($p_{PC}=0.02$; $p_{PDMS}=0.01$) and PDA-BSA/PEG surfaces ($p_{PC}=0.01$; $p_{PDMS}=0.02$). Insignificant differences between PDA-

BSA/PEG and PDA-PEG/BSA on glass may be due to surface damage impairing the modification as indicated by XPS.

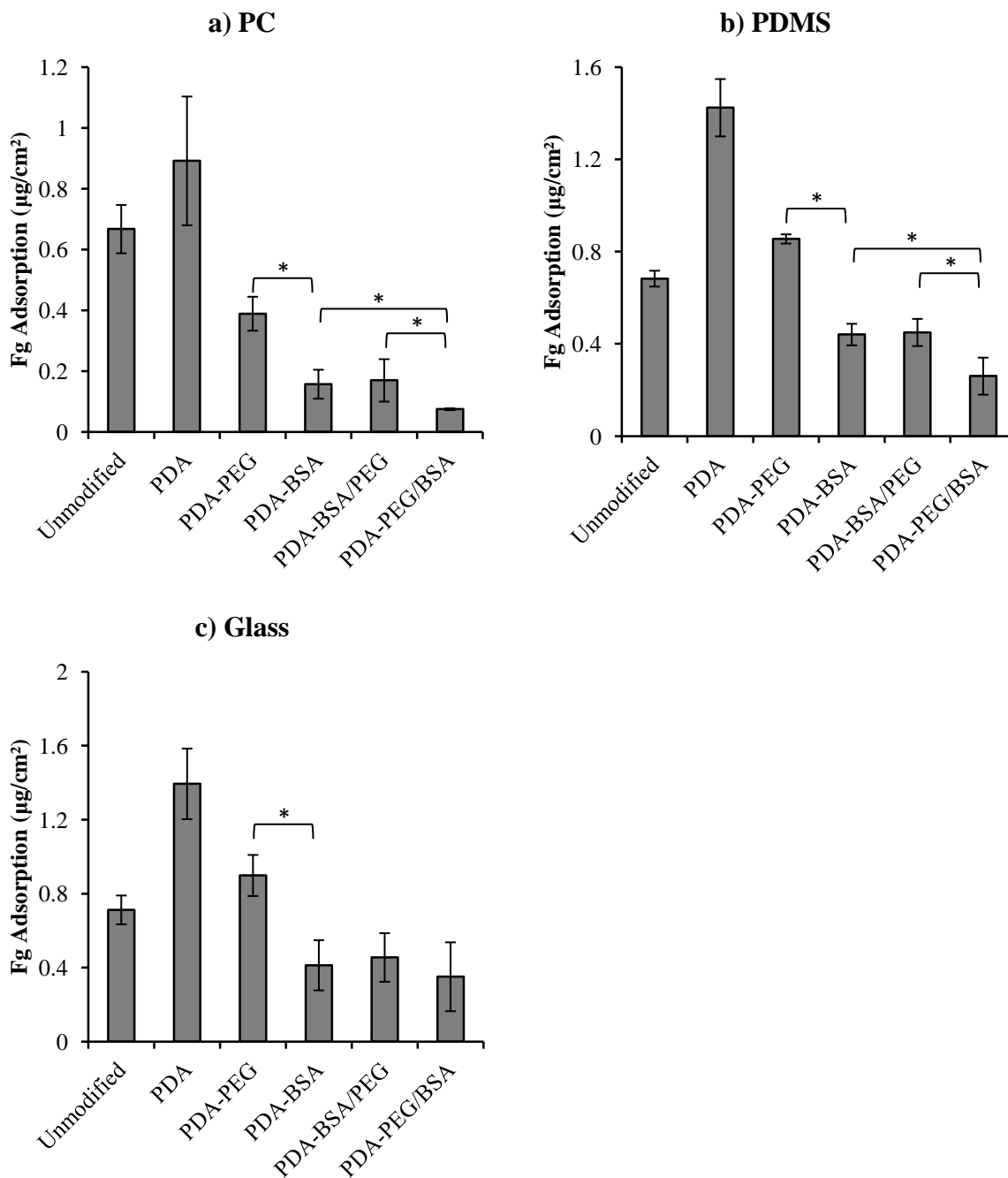


Figure 13. Fg adsorption on a) PC, b) PDMS and c) glass modified materials. Fg adsorption time = 2 h in 1 mg/mL Fg solution (21°C, PBS pH 7.4). Data are mean \pm SD, n=3. * Significant differences ($p < 0.05$).

4.1.9 *E. coli* Adhesion

E. coli adhesion results are presented in **Figure 14**. *E. coli* adhesion experiments were conducted in nutrient deficient medium (PBS buffer) to prevent cell proliferation. In hindsight, quantifying *E. coli* adhesion in protein rich medium would be better to correlate protein and cell results. *E. coli* adhesion occurs in two phases (1) reversible sorption and (2) irreversible sorption [95]. Reversible sorption is the initial, weak attraction of the cells to the surface primarily influenced by cell wall hydrophobicity [96], cell surface electronegativity, and van der Waals attraction [97,98]. Irreversible sorption is the firm adhesion of bacteria to the surface by interaction between cell surface organelles and proteins adsorbed to the substrate. In nutrient poor conditions and absence of proteins, *E. coli* adhesion to the surface is weak and reversible. Therefore, the results presented in **Figure 14** represent the change in *E. coli* adhesion with respect to the reduction in initial cell attraction to the surface. Cell sorption in this case occurs by the weak attractions previous stated, as well as cell settling, flagellar mediated motility, and/or curli expression [99,100]. Curli is a cell surface organelle essential in primary surface colonization and is expressed predominantly in nutrient poor conditions [99,100]. Since *E. coli* adhesion was strong and highest on PDA coated surfaces, we propose that curli may be able to interact with the PDA layer and promote cell adhesion. This suggests that the PDA layer may act as an adhesive platform for cell surface proteins, although this is speculative.

E. coli adhesion was highest on PDA coated surfaces, validating that the PDA layer may act as an adhesive platform for cell surface proteins. Addition of PEG and BSA reduced *E. coli* fouling on PDA. Repulsion of *E. coli* on PDA-BSA surfaces are due to a combination of reduced PDA binding sites and repulsion between the negatively charged BSA and *E. coli* surface. Interestingly, *E. coli* adhesion on PDA-PEG and PDA-BSA modified PC and PDMS were not

significantly different. The presence of PEG may have spatially hindered the cell surface organelles from interacting with PDA, causing “whole particle” repulsion. We suspect that *E. coli* adhesion would be higher on PDA-PEG surfaces if proteins were present in medium. As indicated by Fg results, proteins in solution are able to penetrate the PEG layer which may then aid *E. coli* adhesion. *E. coli* adhesion on PDA-PEG was significantly higher than PDA-BSA modified glass ($p_{Glass}=0.009$), although it is unclear whether this result is due to sparse PEG allowing *E. coli* to interact with PDA and/or damage to the surface during modification.

For PC and PDMS, PDA-PEG surfaces backfilled with BSA had reduced cell adhesion compared to PDA-BSA ($p_{PC}=0.0009$; $p_{PDMS}=0.005$). Thorough coverage of remaining free PDA unblocked by PEG was achieved by BSA. *E. coli* adhesion on PDA-BSA/PEG and BSA-PEG/BSA was weakly significantly different on PC ($p_{PC}=0.048$) and not significantly different on PDMS. *E. coli* adhesion on glass surfaces modified by PDA-BSA, PDABSA/PEG, and PDA-PEG/BSA were not significantly different.

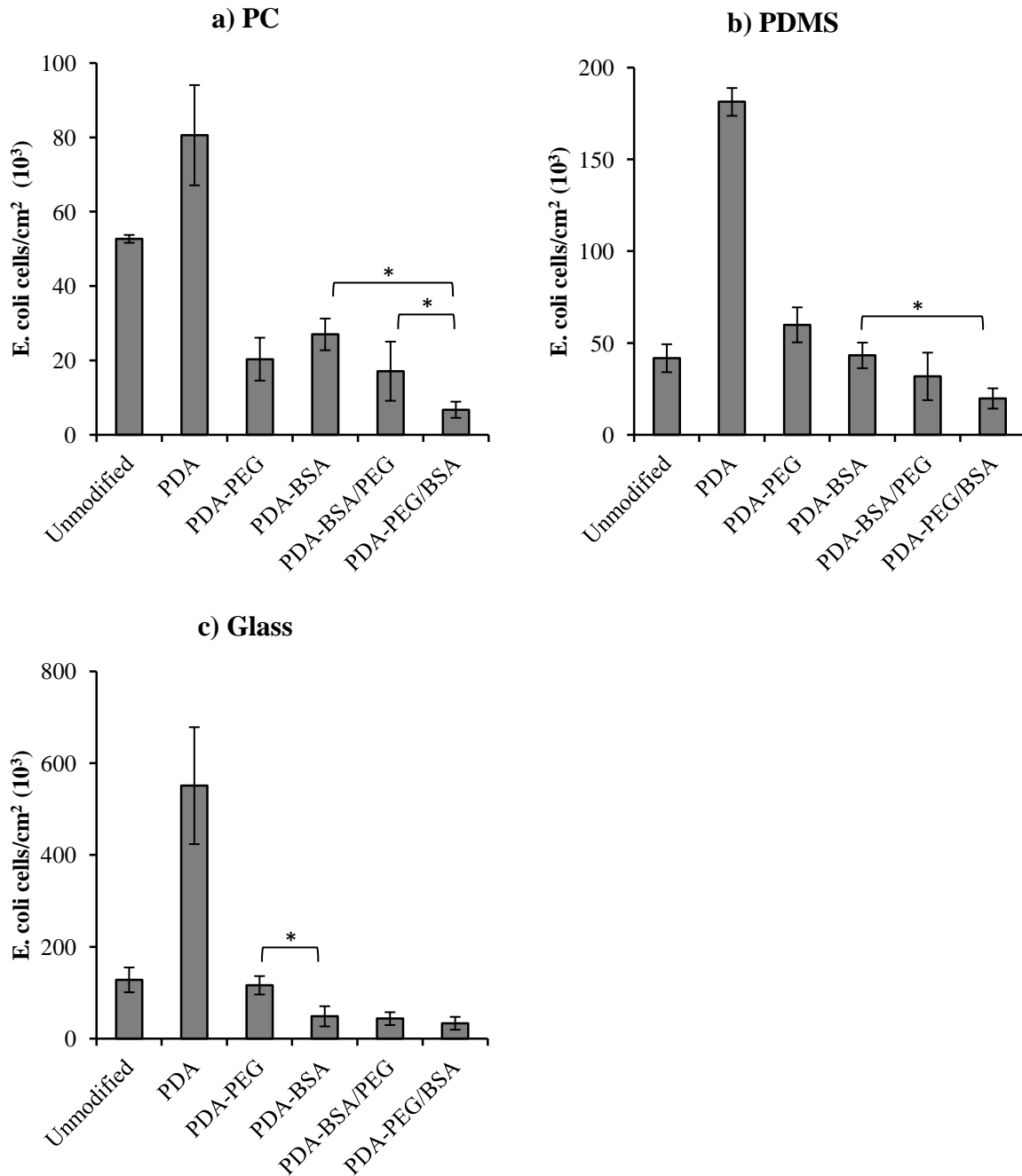


Figure 14. *E. coli* adhesion on a) PC, b) PDMS and c) glass modified materials. *E. coli* seeding numbers were 2×10^8 cells on PC (4 h), and 2×10^7 cells on PDMS (4 h) and glass (5 h) in PBS (pH 7.4). Data are mean \pm SD, n=3. * Significant differences (p<0.05).

In a simple experiment to investigate the role of defects in the modifying layers, PDMS surfaces modified with PDA-PEG/BSA were scratched with forceps to reveal bare PDMS prior to cell seeding. As shown in **Figure 15**, *E. coli* cells adhered preferentially to the scratched area compared to the modified area. This observation emphasizes the need to protect the PDA-modified surfaces from damage if it is to be used as a bio glue. This is especially important for PDMS and glass surfaces which exhibit easy PDA removal with abrasion and scratching.

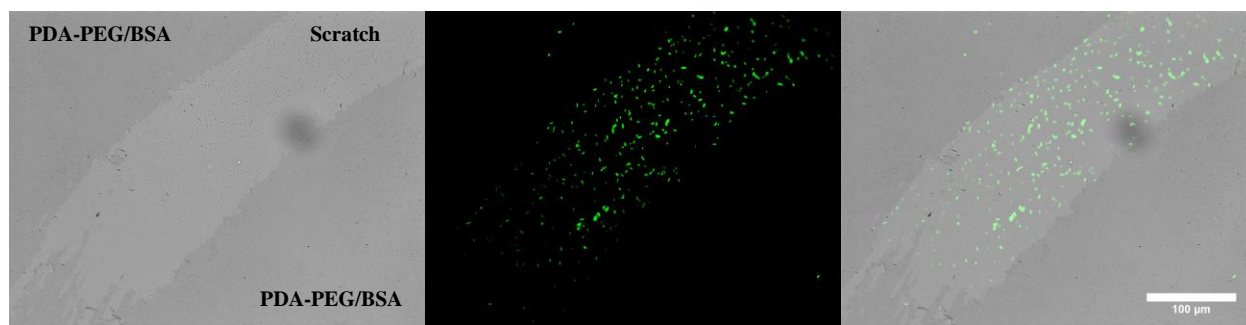


Figure 15. Bright-field and fluorescence images of *E. coli* on a scratched PDMS-PDA-PEG/BSA surface. *E. coli* cells show preferential adhesion to scratch area and low cell adhesion on the adjacent PDA-PEG/BSA modified area.

4.2 Conclusion

In this work, we sought to improve the widely published aqueous based antifouling protocol (based on PEG) by backfilling PDA-PEG surfaces with a blocking protein, BSA, to fill gaps that may be present in the PEG layer. In addition, two approaches to improve PEG attachment to PDA were investigated: (1) reducing the dopamine polymerization time to 3 h to decrease surface roughness, and (2) using $\text{NH}_2\text{-PEG-NH}_2$ to promote more extensive PEG bonding to PDA. Surface characterization showed differences in dopamine polymerization on PC, PDMS, and glass substrates. PDA attraction to the surface was dependent on the surface wettability, with stronger PDA attraction to hydrophobic PDMS and weaker attraction to hydrophilic glass. This resulted in differences in the polymerization mechanism (i.e. direct

polymerization or adsorption of PDA particles) on the three materials, which altered the achievable PDA thickness and surface roughness with 3 h of PDA deposition. Contrary to our original hypothesis, PEG grafting was not as efficient on PDMS-PDA surfaces despite reporting the smoothest PDA layer. Reduced surface area of PDA may have lessened the amount of available PDA post-modification sites. Glass-PDA also reported high PDA surface roughness and poor PEG grafting (as indicated by Fg adsorption and *E. coli* presence), although the result may be in contribution to surface damage. PC-PDA with intermediate surface roughness reported the best PEG coverage based on high reduction in Fg and *E. coli* fouling. It appears that PEG grafting is best on surfaces with similar wettability to PDA (50-65°), which can promote dopamine polymerization with intermediate roughness values.

The inability to control PDA thickness and surface roughness on different substrates under the same reaction conditions poses additional challenges in using PDA as a bio glue for the modification of materials varying in surface wettability. In addition, due to the apparent mechanical removal of PDA from PDMS and glass surfaces during processing, it is recommended to use this method under conditions where precautions are taken to minimize surface damage. Consequently, results for glass surfaces were inconclusive due to suspected modification removal as indicated by XPS results.

PC and PDMS surfaces reported lower Fg adsorption and *E. coli* presence on PDA-PEG surfaces backfilled with BSA. The need for BSA to further block exposed PDA after PEG grafting confirms that low PEG graft density was achieved on the PDA modified surfaces. Low achievable PEG density with this method may be, in part, due to the ability of diamino PEG to form looped structures and difficulty in PEG grafting from solution using pre-formed chains. Higher PEG grafting densities is needed to achieve brush-configurations and lower fouling.

Removal of the second amino group on PEG would be needed to achieve extended chains required for brush configurations. However, earlier Fg studies revealed that the second amine on PEG was needed to promote PEG attachment to the surface. It appears that PEG grafting from solution has low potential for achieving highly protein and cell resistant surfaces. Strategies to promote better PEG grafting on PDA is needed.

5. LIGHT ACTIVATED PFPA-PEG ON PDA COATED SURFACES

5.1 Introduction

It is apparent from the studies reported in Chapter 4 that higher grafting densities of PEG are required to further reduce protein and cell fouling. Complete PEG coverage of PDA may not be achievable by relying on solution kinetics to promote PEG grafting, i.e. optimizing time, concentration and temperature in the grafting process. However, the use of a chemically reactive biological agent to tether PEG (or other hydrophilic polymers) to the surface may have potential for achieving higher grafting densities.

Perfluorophenyl azides (PFPA) are a type of photoaffinity labeling reagent that uses light activation for surface functionalization [101]. The general structure of PFPA is shown in **Figure 16**. The fluorinated azide limits ring expansion after UV activation, preventing the conversion of singlet phenyl nitrene to the less reactive dehydroazepine alternate [101,102]. Thus, the labeling efficiency of fluorinated azides is much greater than their non-fluorinated analogues [101,102]. PFPA contains a customizable functional group (R, **Figure 16**) and a highly reactive light-activated azido moiety, allowing PFPA to be exploited as heterobifunctional coupling agents in surface functionalization [103]. PFPA has been used to tether hydrophilic polymers on surfaces to reduce cell adhesion [24,104], control protein leaching from latex [105], and to reduce non-specific protein adsorption [106]. McVerry et al. [24] showed that *E. coli* adhesion on a commercial reverse osmosis polyamide membrane was reduced from 22% to <1% coverage by modification of PFPA-PEG (PFPA pre-functionalized to PEG). In addition, significantly less *E. coli* adhesion was found on PFPA-PEG surfaces using PEG of molecular weight 5000 Da compared to 550 Da and 1000 Da PEG [24]. Patterned surfaces can also be achieved with PFPA using a photomask [104], since PFPA show virtually

no coupling to surfaces in the dark, allowing non-activated material to be washed away with water [24]. This is useful in developing biological platforms for single-cell analysis where researchers are interested in studying individual cell interactions and functions, including cell geometry, morphology, differentiation and proliferation [27]. Another advantage is that PFPAs are highly soluble in water, thus eliminating the need for harsh solvents and reaction conditions [24].

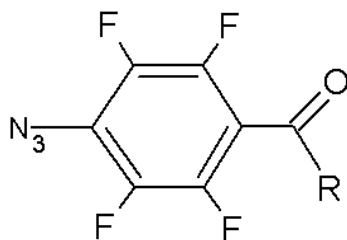


Figure 16. Chemical structure of PFPAs. R is a customizable group.

5.1.1 Attachment of PFPAs to Surfaces

Coupling of PFPAs to a surface can occur in two ways: (1) by surface-specific coupling of the functional group R [104,106,107] or (2) through insertion of the reactive azide [24,105]. The aforementioned method is not suitable for simultaneous modification of multiple materials as the R-group would need to be customized to react with functional groups on the substrate of interest [106]. In addition, stable covalent coupling of PFPA via the R-group to a surface is hard to achieve without harsh chemical reaction conditions or laborious procedures. Often, the R-group is charged for attachment to surfaces via electrostatic interactions [104,107], which, as discussed in earlier chapters, is non-ideal for applications in environments where the pH may vary.

Surface functionalization with PFPA via the azide group is preferred. Irradiation of the azide group with shortwavelength UV light forms a reactive singlet nitrene that readily inserts into CH, NH, and C=C bonds, forming stable covalent bonds [101,103]. This makes it a widely applicable coupling agent for various materials [103], especially high molecular weight polymers [24,104-106]. In addition, surface attachment via the azide frees PFPAs to tether other molecules, such as PEG, to expand their applications as a photolabel.

5.1.2 Limitations of PFPAs

UV-sensitive and photodegradable materials such as organic compounds, plastics, selected polymers, and materials containing dyes and pigments may not be suitable for this modification method [108,109]. Some UV-sensitive materials may be able to withstand low power UV irradiation for a short time. PFPA derivatives have previously been reported to be activated with UV light intensity as low as 0.06 mW/cm^2 at 254 nm for 5 min [104]. Verifying the UV sensitivity of interested substrates prior to PFPA modification is recommended. In regards to the materials used in this thesis, cured PDMS and glass are not photodegradable upon UV exposure. Polycarbonates are known to discolour via the photo-Fries reaction especially at short wavelengths (<290 nm) [110]. The resistance of PC to photodamage is effectively unknown. Heat can also be used to activate PFPAs for applications where UV-sensitive materials are required. Temperatures of 70-140°C and longer exposure times (>20min) are required to activate PFPAs by heat [106,111,112]. Since heat activation is more time consuming and limits applications to whole surface modification, light activation is often preferred.

5.1.3 PDA as a Bio Glue for PFPA-PEG

Pre-functionalizing surfaces with PDA may allow PFPA-PEG attachment via photoactivation of the azide on substrates that do not contain or have limited available CH, NH, or C=C bonds. For example, PDA would be needed as a base for PFPA-PEG attachment on glass and metals. The work reported in this thesis is, to our knowledge, the first demonstration of PFPA attachment to PDA. It is proposed that PFPA inserts into the NH or C=C bonds of PDA (**Figure 17**), and based on the high reactivity of the azido moiety it is hypothesized that a high density of PFPA and consequently a high density of PEG on PDA-modified surfaces should be achieved.

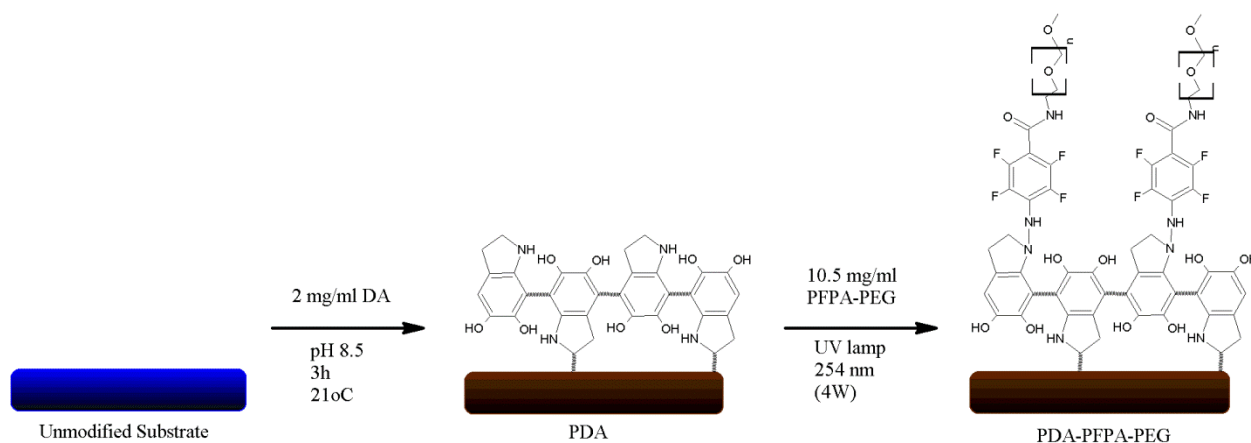


Figure 17. Process for the modification of PDA coated surfaces with PFPA-PEG, showing proposed point (NH) for insertion of PFPA-PEG into PDA. C=C insertion may also occur with PDA in the π -stack configuration (not depicted here) [7,8].

5.2 Materials and Methods

5.2.1 Materials

Sodium Azide (NaN_3) purchased from Solarbio (Shanghai, P. R. China) and methyl pentafluorobenzoate purchased from Sigma Aldrich (Shanghai, P. R. China) were used to

synthesize perfluorophenyl azide (PFPA). Organic solvents of analytical grade were used as received. See Chapter 3 for complete materials list.

5.2.2 PFPA-PEG Synthesis

PFPA-PEG was synthesized as previously described [24,105] and provided by Dr. Hong Chen's research group at Soochow University. Briefly, sodium azide and methyl pentafluorobenzoate (mol ratio 1:3) were refluxed for 8 h in a 8:3 mixture of acetone and water. Ester hydrolysis of the purified product, methyl-4-azido-2,3,5,6-tetrafluorobenzoate, was carried out in methanol-sodium hydroxide with continuous stirring for 20 h at room temperature. The carboxylic acid group was then chlorinated to form 4-azido-2,3,5,6-tetrafluorobenzoyl chloride in a 36 h reflux reaction in dichloromethane and thionyl chloride. Finally, one equivalent of 4-azido-2,3,5,6-tetrafluorobenzoic chloride was combined with 0.9 equivalent of $\text{NH}_2\text{-PEG-O-CH}_3$ (MW 5000 Da) in chloroform-triethylamine, and reacted overnight at room temperature in the dark. The final product was dialysed against Milli-Q water for two days and dried, yielding PFPA-PEG conjugate. Intermediate products were extracted with diethyl ether and dried over magnesium sulfate. Fourier transform infrared (FTIR) spectra were taken on a Nicolet 6700 spectrometer (Thermo Fisher Scientific, Beijing, P. R. China).

5.2.3 PFPA-PEG Surface Preparation

Surfaces were prepared as previously described in sections 3.2.1 and 3.2.2. Two methods for PFPA-PEG modification were tested. For adsorption experiments, samples were submerged in 10.5 mg/mL PFPA-PEG solution prepared in Milli-Q water and incubated for 1 h. For the dip coat method, samples were quickly (~3 sec) dipped in 10.5 mg/mL PFPA-PEG solution as previously described [24,105]. Adsorbed and dipped samples were then dried in the dark

overnight in ambient conditions or at 60°C for 3 h. Dried samples were then irradiated with a Mineralight UV lamp UVG-11 ($\lambda = 254$ nm) for 5 min on each side. The average power of the lamp was determined to be 1.12 mW/cm² at 254 nm using a 1830-C Newport optical power meter (Newport Inc., Irvine, CA). Un-reacted PFPA-PEG was washed off with Milli-Q water. The PFPA-PEG treatment was repeated up to 3 times. For repeat treatments using the 1 h adsorption method, samples were incubated in fresh PFPA-PEG solution each time. BSA backfilled samples (PDA-(PFPA-PEG)/BSA) were prepared after three treatments of PFPA-PEG by incubation in BSA solution (10 mg/mL, PBS, pH 7.4) for 24 h at room temperature.

5.3 Results and Discussion

5.3.1 PFPA-PEG Concentration Optimization

Following the protocol for PFPA treatment previously published [24,105], PDA modified samples were dip coated in PFPA-PEG solution and dried in ambient conditions prior to UV activation. Drying the samples prior to light activation is essential to ensure that the activated azide is in close proximity to the substrate surface thus optimizing the coupling efficiency while reducing cross-reactions with other activated PFPA by free-radical addition. Preliminary results showed very little reduction in Fg adsorption on PFPA-PEG-treated PC-PDA and PDMS-PDA surfaces versus the unmodified PDA precursors (data not shown). It was then decided to investigate whether increasing the concentration of PFPA-PEG would improve PEG density on the surface. Fg adsorption on PC-PDA and PDMS-PDA surfaces dip coated in PFPA-PEG solutions showed no significant difference for PFPA-PEG concentrations over a three-fold range (10.5, 21 and 31.5 mg/mL) (**Figure 18**). Moreover, the reduction in adsorption was no greater than for surfaces prepared by solution-based grafting of PEG on PDA. These results suggest that

PEG coverage of PDA was not improved with the PFPA when modifying surfaces with this protocol.

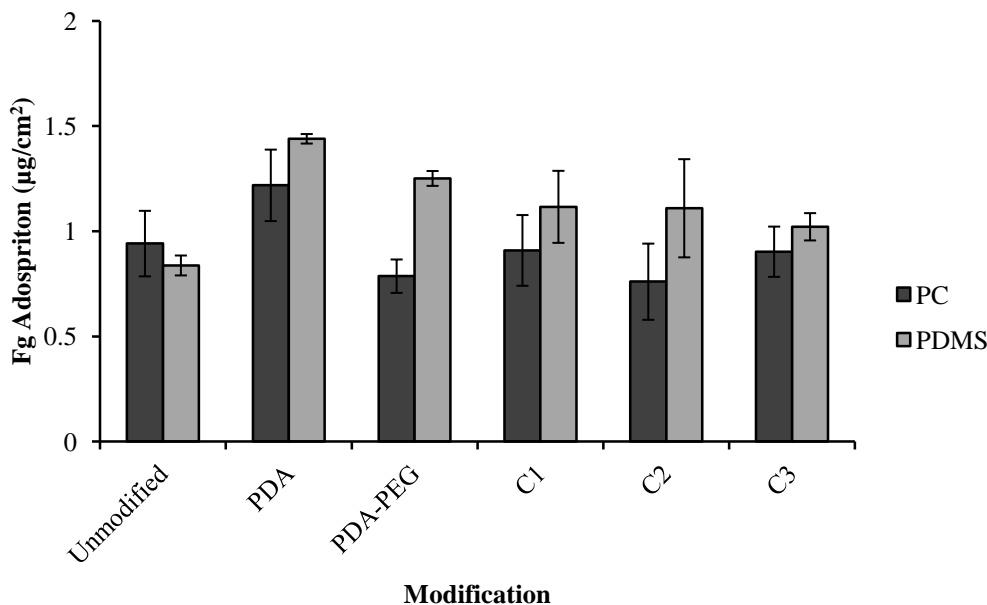


Figure 18. Fibrinogen adsorption on PFPA-PEG-modified surfaces prepared at different concentrations of PFPA-PEG. Samples were dip-coated in 10.5 mg/mL (C1), 21 mg/mL (C2), and 31.5 mg/mL (C3) PFPA-PEG solution prior to UV activation. UV activation was for 2 min per side. Means \pm SD, n=3.

5.3.2 PFPA-PEG Adsorption vs. Dip Coating Method for Modification

It was then decided to investigate whether incubating samples in PFPA-PEG solution for a longer time (as opposed to dip coating) would improve attachment of PFPA-PEG molecules to the surface and thus increase PEG density. Also, surfaces were modified with repetitive treatments of PFPA-PEG to test for improved PEG coverage and Fg reduction. Additional modifications with PFPA-PEG may block free PDA untargeted by the previous coating. Surfaces prepared with a longer UV activation time (5 min/side) to ensure more complete PFPA activation were also investigated. Since no improvement was achieved using higher concentrations of PFPA-PEG, a concentration of 10.5 mg/mL was used in these subsequent experiments.

Fg adsorption data for surfaces prepared using the modified PFPA-PEG protocols are presented in **Figure 19**. A significant reduction in Fg adsorption on PC was seen for surfaces dip coated once in PFPA-PEG solution compared to the analogous surfaces in **Figure 18** ($p=0.01$), indicating that activation of PFPA-PEG with 2 min UV exposure may have been less complete than with 5 min. Surfaces prepared by 1 h incubation were less performing than those that were dip coated. It appears as though PFPA-PEG were not able to adsorb to the PC-PDA and PDMS-PDA surfaces. The reason for this difference is unclear. However, it is apparent that multiple treatments with PFPA-PEG greatly improved surface coverage for both the adsorption and dip coating methods. Significantly less Fg was adsorbed to PC with each successive PFPA-PEG treatment ($p_{1to2}=0.007$ and $p_{2to3}=0.03$). In the case of PDMS, no additional effect was seen after two treatments ($p_{1to2}=0.009$; $p_{2to3}=0.45$).

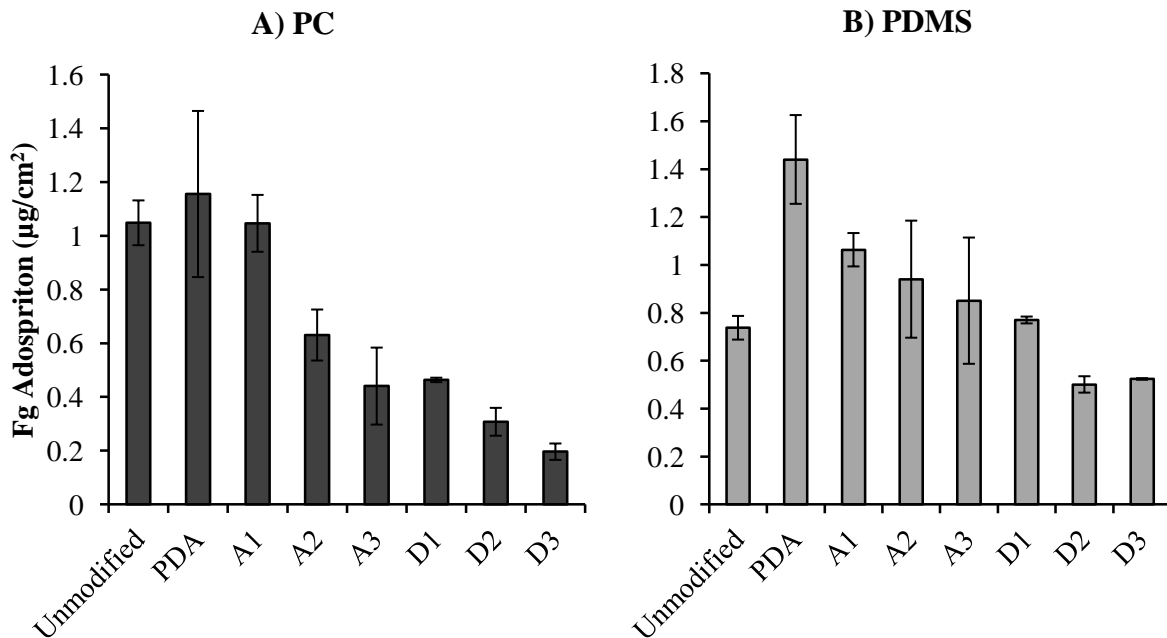


Figure 19. Optimizing the PFPA-PEG modification procedure for fibrinogen resistance. Samples were incubated for 1 h (A1-A3) or dip coated (D1-D3) in 10.5 mg/mL PFPA-PEG solution prior to UV activation. The numbers 1, 2, and 3 indicate the number of treatments in PFPA-PEG solution. UV activation time was 5 min per side. Means \pm SD, $n=3$.

5.3.3 PFPA-PEG Drying Test

Multiple treatments of PFPA-PEG resulted in more complete coverage of PDA. However, this modification protocol is very time consuming with the added drying time after each treatment. Since heat has also been reported to activate PFPA-PEGs [106,111,112], we investigated whether increasing the drying temperature (to reduce drying time) would reduce the reaction efficiency due to activation of PFPA-PEG while the sample is still wet. Fg adsorption data comparing sample drying at room temperature overnight (RT) versus at 60°C for 3 h (HT) are shown in **Figure 20**. After one treatment with PFPA-PEG, Fg adsorption on HT samples were slightly higher than RT dried samples, although the significance was weak ($p=0.044$). Differences may be more of a consequence of light contamination, sample variability, or sample handling. After two treatments there was no significant difference between the drying temperatures ($p=0.11$). These results indicate that drying the samples at 60°C for 3 h does not materially reduce the coupling efficiency of PFPA-PEG to the substrate.

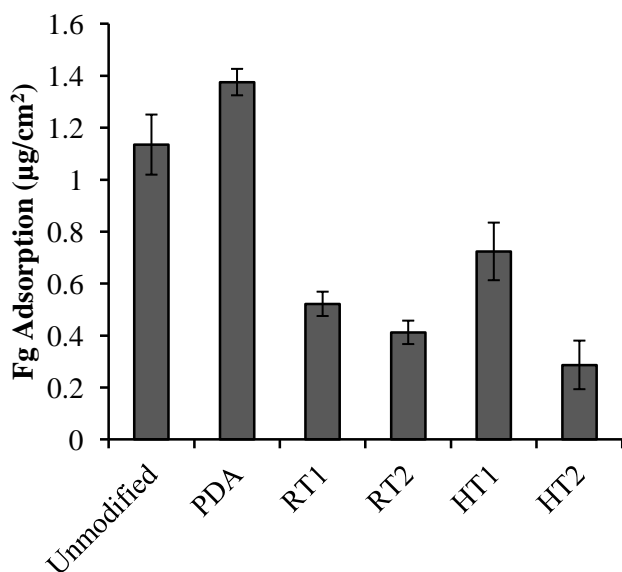


Figure 20. Optimizing temperature used for sample drying. PC samples were dried at room temperature overnight (RT) or at 60°C for roughly 3 h (HT). Samples were treated with PFPA-PEG once or twice. Means \pm SD, $n=3$.

5.3.4 Water Contact Angles

Using the optimized PFPA-PEG protocol (3 treatments of PFPA-PEG with 3 h drying at 60°C after each treatment), a full set of samples was prepared on PC, PDMS, and glass surfaces. Water contact angles measured using the sessile drop method is presented in **Table 6**. Treatment with PFPA-PEG increased the hydrophilicity of the PDA coated PC and glass surfaces. BSA backfilled surfaces (T3/BSA) again reported an intermediate contact angle to BSA and PEG, suggesting that a mixture of PEG and BSA may be present on the surface. In contrast, contact angles on PDMS-PDA were higher after PFPA-PEG treatment. It is noted that the angle on PDMS-PDA surface was the same as for similar samples prepared independently (**Table 3**) (73 ± 5 vs $67\pm 8^\circ$) so it is unlikely that differences in PDA deposition was responsible for this unexpected result. Rather, PDA may have been removed during modification as the protocol for PFPA-PEG modification requires much more sample handling. Contact angles on PDMS-PDA-BSA were much higher than reported in Table 3 (102 ± 4 vs $72\pm 2^\circ$). It is suspected that the surfaces in these experiments were damaged during processing.

Although the PDMS surfaces were clearly not “well behaved”, some general trends in the data can be discerned. For all three materials, the second treatment with PFPA-PEG increased the wettability compared to the first treatment. The third treatment provided no additional improvement, suggesting that all available PDA groups were reacted after the second treatment. Exposure to BSA after the third treatment with PFPA-PEG resulted in a contact angle between PEG and BSA, consistent with the data presented in Chapter 4, and providing some evidence that there may be a mixture of PEG and BSA on the surface. The large error bars on the contact angle data raise concerns about the consistency of the modification procedure, and are likely due to

differences in manipulation of the surfaces during sample handling and ensuring sufficient UV exposure.

The contact angles on the glass surfaces are inconclusive as to whether the PDA coating was compromised as was observed in earlier experiments (see Chapter 4). After three treatments with PFPA-PEG, the contact angle was the same as that for unmodified glass. The glass surfaces retained the brown tint characteristic of PDA, although partial thinning of the coating may still have occurred. XPS and AFM analysis will be required to elucidate these observations.

Table 6. Water contact angles (degrees) on modified PC, PDMS, and glass. Sessile drop water contact angles using 6 μ L drops were measured after 2 min surface contact. Means \pm SD, n=3.

Modification	PC	PDMS	Glass
Unmodified	66 \pm 2	117 \pm 3	16 \pm 2
PDA	55 \pm 2	73 \pm 5	36 \pm 5
PDA-BSA	61 \pm 4	102 \pm 4	53 \pm 4
T1	34 \pm 5	96 \pm 10	20 \pm 1
T2	23 \pm 10	80 \pm 7	17 \pm 3
T3	33 \pm 10	83 \pm 9	16 \pm 2
T3/BSA	39 \pm 9	107 \pm 6	45 \pm 10

5.3.5 Fibrinogen Adsorption

Fg adsorption data are presented in **Figure 21**. For PDMS, as might be predicted from the water contact angles, modification with PFPA-PEG did not reduce Fg adsorption greatly. While

the T1 surfaces showed lower Fg adsorption than the precursor PDA, additional treatments with PFPA-PEG (T2, T3) did not reduce adsorption further. Of all the PDMS surfaces PDA-BSA and T3/BSA showed the lowest Fg adsorption. Based on the water contact angles and the protein adsorption data, the T3/BSA surfaces probably “presented” mainly BSA molecules rather than PEG. As mentioned previously, it was suspected that these surfaces were damaged during PFPA-PEG modification since the contact angles for T3/BSA were close to that of unmodified PDMS. It is also possible that PFPA-PEG grafting on PDA was hindered in the same way as observed for PEG grafting from solution (Chapter 4), with reduced surface roughness limiting available post-modifiable PDA sites.

For PC and glass, Fg adsorption on PDA-BSA was significantly lower than on surfaces treated once with PFPA-PEG ($p_{PC}=0.004$, $p_{Glass}=0.02$), indicating the presence of free PDA on the T1 surfaces. Fg adsorption was further reduced with two treatments of PFPA-PEG compared to one treatment ($p_{PC}=0.003$, $p_{Glass}=0.01$). There was no statistically significant difference in adsorption between the T2 and T3 surfaces, suggesting that maximum surface coverage of PFPA-PEG was achieved after just one additional PFPA-PEG treatment on PC and glass. In addition, no additional improvement to T3 PC and glass surfaces was found when backfilled with BSA. This provides strong evidence that the majority of the PDA was covered by PFPA-PEG, rendering the BSA backfill redundant. This assertion is supported in that the differences between T2, T3, and T3/BSA surfaces were not significantly different.

These results support the hypothesis that higher PEG grafting densities and PDA coverage may be achievable with the PFPA labeling reagent. However, Fg adsorption on the T2 and T3 PC and glass surfaces were comparable to PDA-BSA. While maximum coverage of PDA was probably achieved, the grafting density of PFPA-PEG on PDA may be limited by the

availability, accessibility, and density of modifiable PDA functional groups. Further XPS analysis would be required to determine the extent of PEG grafting on these surfaces. Although *E. coli* adhesion experiments were not done on these surfaces, it is probable that the higher PEG grafting density on the PDA base would lead to reduced *E. coli* adhesion compared to PDA-BSA.

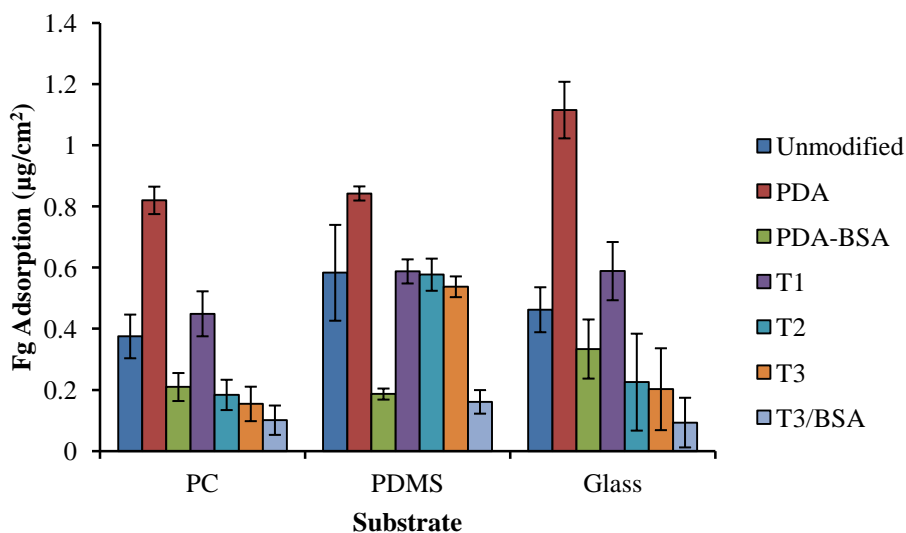


Figure 21. Fg adsorption on modified PC, PDMS, and glass. PDA coated samples were modified with one, two or three (T1, T2, & T3) treatments of PFPA-PEG. Adsorption time, 2 h in 1 mg/mL Fg solution (PBS, pH 7.4) at room temperature. Data are mean \pm SD, n=3.

6. SUMMARY AND CONCLUSIONS

6.1 Summary

Aqueous based antifouling strategies are desirable for modifying the surfaces of multi-material devices and biosensors. PDA-PEG has garnered much interest as a potential universal antifouling coating due to its simplicity, the fact that it can be implemented under mild reaction conditions in aqueous solution, and its applicability to a wide variety of polymers, metals, and composites. However, it is apparent from the work reported in this thesis that in PEG grafting from solution to PDA-coated materials, it is difficult to achieve complete coverage of PDA. The conjugation of PEG to PDA using pre-formed PEG chains requires favorable reaction conditions, including minimal steric exclusion/hindrance effects [13]. Since PDA exhibits extensive protein and cell fouling, ensuring complete coverage of PDA during post-modification is essential to create an antifouling surface.

We first investigated the use of a blocking protein, BSA, to fill gaps in the PDA layer not covered by PEG. Ideally, the surface should be PEG-dominated with BSA as a supplementary component to maximize non-fouling. XPS, water contact angle and protein adsorption studies revealed substantial differences in PEG grafting efficiency on PC, PDMS, and glass substrates. Differences in dopamine polymerization based on the substrate wettability resulted in varying PDA surface roughness. PEG grafting was the most efficient on PC with intermediate PDA roughness, and PDA-PEG/BSA modified PC reported the highest resistance to Fg and *E. coli*. PDMS substrates reported the lowest surface roughness and showed poor PEG grafting, but BSA backfilling gave surfaces with good fouling resistance. Due to surface damage of modified glass surfaces during handling no definitive conclusion for glass based surfaces was possible.

However, significant improvements to PDA-PEG surfaces backfilled with BSA revealed that low PEG densities were achieved on PDA modified surfaces using this approach.

Based on these initial results, it was clear that improved PEG grafting to PDA surfaces was needed to achieve more fouling resistant surfaces. To this end a photo-activated bioconjugate, PFPA-PEG, was developed to enhance PEG attachment to PDA. After trials with several variations of the modification protocol, it was determined that two treatments with PFPA-PEG were sufficient to maximize attachment to PDA on PC and glass. Insignificant differences between surfaces treated with PFPA-PEG twice (T2), three times (T3), and three times with BSA backfill (T3-BSA) support the conclusion that most of the free PDA was blocked by PFPA-PEG, making the BSA backfill redundant. To our knowledge, this is the first successful demonstration of the modification of a PDA coating by PFPA-conjugated PEG. PFPA-PEG modification of PDMS-PDA surfaces was found to be poor, probably due to excessive surface damage during sample handling, or simply to inherently inefficient PEG grafting on PDMS-PDA surfaces given that PEG grafting via the solution-based method was also poor.

Although considerable progress has been made via the work reported here, challenges remain in surface modification with PDA as a bio glue for antifouling modification. Dense PEG brushes were not able to form on PDA surfaces even with the aid of PFPA. Limited accessibility and availability of PDA reactive sites for PEG tethering may attribute to low attainable grafting densities. However since the detailed structure of the PDA surfaces are still largely unknown, this explanation should be seen as speculative [8]. Mechanical removal of PDA (as seen on PDMS and glass) impacts the usability of PDA coated surfaces in applications where the surface may be susceptible to mechanical “trauma”. Thus it is recommended that PDA coatings should

be limited to applications with minimal surface exposure and where ultra-low fouling is not necessary, such as for cell patterned surfaces and some microfluidic chip applications. PDA-based antifouling coatings are ideal for short-term cell assays on solvent sensitive platforms. These coatings are not ideal for longer antifouling applications such as natural water quality monitoring sensors or implant devices.

6.2 Recommendations for Future Work

6.2.1 Structure of PDA Deposits on Materials

While many studies have proclaimed the versatility of PDA coatings for functionalizing a broad range of materials [7,10,15], comparison of PDA film structure on different materials have not been conducted. As discovered in the present work, dopamine polymerization on PC, PDMS, and glass was not consistent even when carried out under the same conditions. Differences in PDA roughness, surface coverage, and morphology of deposited particles as observed in our work, may influence the quality and reproducibility of subsequent modification, e.g. with PEG. While it appears that substrate wettability greatly influences dopamine polymerization, it would be interesting if this holds true for metals and charged surfaces since PDA deposition on these materials differ. An extensive study on dopamine polymerization on materials varying in wettability, surface charge, and surface roughness is recommended in the further development of PDA as a universal coating for attachment of fouling suppressants or other species.

6.2.2 Optical Properties of PDA

For optical-based sensors, it is necessary to characterize the optical properties of PDA. Any adsorption and scattering of light by PDA would affect the detection of water contaminants with similar optical properties. PDA has similar chemical structures to melanin, which is known to adsorb light over the entire visible spectrum [113]. Ellipsometry modelling of PDA coated glass, PC, and PDMS revealed low adsorption ($k=0.014$), with the thickest PDA layer measuring ~ 30 nm on PDMS. Emission of fluorescence by PDA is unknown and should be measured. The refractive index of PDA is also not well defined, and in this thesis was estimated to be $n=1.45$ based on PDA modelling conducted by previous studies [84,86]. Determination of the true refractive index of PDA is necessary to validate the PDA thicknesses measured by ellipsometry. It is also necessary for sensor design, as light collection by the system would be affected.

6.2.3 *Quantitative Analysis of PEG Surface Density*

To improve the quality of these investigations and validate some of the assumptions therein, it would be desirable to determine quantitatively the PEG grafting density achieved on the PDA coated surfaces. More valid comparisons among the surfaces could then be made. Quantification of the PEG density achieved on the PDA coated materials is also necessary to determine the efficiency of PEG grafting. XPS data could be used to calculate the grafting density of PFPA-PEG using the fluorine signal in the XPS which is unique to the grafting species (theoretical F:C ratio 3.381×10^{-5}). Since PEG and PDA contain the same atoms, the grafting density of PEG cannot be easily determined from XPS data.

Ellipsometry has been used by others to calculate PEG grafting density [13]. However, this method is not suitable for our surfaces since PDA and PEG have very similar refractive indices.

Thus poor optical contrast between PDA and PEG in the surface would prevent accurate quantification of the PEG density.

We did attempt to determine PEG grafting density using the quartz crystal microbalance with dissipation monitoring (QCM-D). QCM-D measures adsorption/desorption gravimetrically at the nanogram level [114]. In the QCM measurement, a shear deformation oscillation is excited in a piezoelectric crystal. Adsorption on the crystal decreases the resonant frequency of the oscillation in a manner related to the mass of adsorbate. Therefore, by measuring the frequency shift, the mass adsorbed can be determined. Since QCM-D chips are gold plated, thin films (<10 μm) of PDMS were spin coated on the chip for adsorption experiments. However the excessive weight of the PDMS and/or the unevenness of the PDMS surface affected the resonant frequency of the chip and measurement of adsorption was not possible.

Fluorescent-based assays offer another method for quantifying PEG density. Since the PEG derivatives used are amine-terminated, fluorescamine could be used to determine left over PEG by reaction with unbound terminal PEG amino groups. Upon reaction with primary amines, fluorescamine generates a fluorescent product that emits light at 480 nm when excited at 390 nm [115]. The fluorescence intensity can be calibrated with known concentrations of PEG. Concentrations of PEG as low as 250 nM can be detected with this assay [115]. In addition, PDA-PEG-modified samples could be fluorescently labelled to determine the configuration of the PEG on PDA, e.g. whether the PEG retains one free end group or forms looped structures on PDA in which both end groups would be reacted.

6.2.4 PFPA-PEG and Photopatterned Surfaces

Since PEG coverage on PDA was improved when conjugated to the PFPA photolabel, it may be worthwhile to develop this method for cell patterning. UV light activation offers a simple and quick way to produce customizable cell patterned surfaces for studying cell-surface interactions and other behaviours. Since this method does not involve solvents or harsh chemical conditions, photopatterning of polymer-based materials could be achieved, providing opportunities for the creation of new cell patterned platforms. A challenge with this method would be the need to synthesize PFPA-PEG in house, a highly time consuming process, or hire a chemical company to custom synthesize the compound. To our knowledge, PFPA-PEG is not a commercially available product.

References

- [1] C. M. Kirschner and A. B. Brennan, "Bio-inspired antifouling strategies," *Annual Review of Materials Research*, vol. 42, pp. 211-229, 2012.
- [2] Y. Qian, Y. Zhang, H. Wang, J. L. Brash and H. Chen, "Anti-fouling bioactive surfaces," *Acta Biomaterialia*, vol. 7, pp. 1550-1557, 2011.
- [3] T. S. Sileika, H.-D. Kim, P. Maniak and P. B. Messersmith, "Antibacterial performance of polydopamine-modified polymer surfaces containing passive and active components," *ACS Applied Materials and Interfaces*, vol. 3, pp. 4602-4610, 2011.
- [4] L. Hsu, P. R. Selvaganapathy, J. L. Brash, Q. Fang, C.-Q. Xu, M. J. Deen and H. Chen, "Development of a low-cost hemin-based dissolved oxygen sensor with anti-biofouling coating for water monitoring," *IEEE Sensors Journal*, vol. 14, no. 10, pp. 3400-3407, 2014.
- [5] M. Krishnamoorthy, S. Hakobyan, M. Ramstedt and J. E. Gautrot, "Surface-initiated polymer brushes in the biomedical field: Applications in membrane science, biosensing, cell culture, regenerative medicine and antibacterial coatings," *Chemical Reviews*, vol. 114, pp. 10976-11026, 2014.
- [6] J. M. Goddard and J. H. Hotchkiss, "Polymer surface modification for the attachment of bioactive compounds," *Progress in Polymer Science*, vol. 32, pp. 698-725, 2007.
- [7] H. Lee, S. M. Dellatore, W. M. Miller and P. B. Messersmith, "Mussel-inspired surface chemistry for multifunctional coatings," *Science*, vol. 318, pp. 426-430, 2007.
- [8] D. R. Dreyer, D. J. Miller, B. D. Freeman, D. R. Paul and C. W. Bielawski, "Perspectives on poly(dopamine)," *Chemical Science*, vol. 4, pp. 3796-3802, 2013.
- [9] B. P. Lee, P. B. Messersmith, J. N. Israelachvili and J. H. Waite, "Mussel-inspired adhesives and coatings," *Annual Review of Materials Research*, vol. 41, pp. 99-132, 2011.
- [10] Q. Wei, K. Achazi, H. Liebe, A. Schulz, P.-L. M. Noeske, I. Grunwald and R. Haag, "Mussel-inspired dendritic polymers as universal multifunctional coatings," *Angewandte Chemie International Edition*, vol. 53, pp. 11650-11655, 2014.
- [11] L. Chen, R. Zeng, L. Xiang, Z. Luo and Y. Wang, "Polydopamine-graft-PEG antifouling coating for quantitative analysis of food proteins by CE," *Analytical Methods*, vol. 4, pp.

2852-2859, 2012.

- [12] D. J. Miller, P. A. Araujo, P. B. Correia, M. M. Ramsey, J. C. Kruithof, M. C. van Loosdrecht, B. D. Freeman, D. R. Paul, M. Whiteley and J. S. Vrouwenvelder, "Short-term adhesion and long-term biofouling testing of polydopamine and poly(ethylene glycol) surface modifications of membranes and feed spaces for biofouling control," *Water Research*, vol. 46, no. 12, pp. 3737-3753, April 2012.
- [13] O. Pop-Georgievski, S. Popelka, M. Houska, D. Chvostova, V. Proks and F. Rypacek, "Poly(ethylene oxide) layers grafted to dopamine-melanin anchoring layer: Stability and resistance to protein adsorption," *Biomacromolecules*, vol. 12, pp. 3232-3242, 2011.
- [14] O. Pop-Georgievski, D. Verreault, M.-O. Diesner, V. Proks, S. Heissler, F. Rypacek and P. Koelsch, "Nonfouling poly(ethylene oxide) layers end-tethered to polydopamine," *Langmuir*, vol. 28, pp. 14273-14283, 2012.
- [15] S. H. Ku, J. Ryu, S. K. Hong, H. Lee and C. B. Park, "General functionalization route for cell adhesion on non-wetting surfaces," *Biomaterials*, vol. 31, pp. 2535-2541, 2010.
- [16] L.-P. Zhu, J.-H. Jiang, B.-K. Zhu and Y.-Y. Xu, "Immobilization of bovine serum albumin onto porous polyethylene membranes using strongly attached polydopamine as a spacer," *Colloids and Surfaces B: Biointerfaces*, vol. 86, pp. 111-118, 2011.
- [17] M. Rabe, D. Verdes and S. Seeger, "Understanding protein adsorption phenomena at solid surfaces," *Advanced Colloid Interface Science*, vol. 162, pp. 87-106, 2011.
- [18] P. J. Molino, S. Childs, M. R. E. Hubbarb, M. A. Burgman and R. Wetherbee, "Development of the primary bacterial microfouling layer on antifouling and fouling release coatings in temperate and tropical environments in Eastern Australia," *Biofouling*, vol. 25, no. 2, pp. 149-162, 2009.
- [19] B. O'Flynn, F. Regan, A. Lawlor, J. Wallace, J. Torres and C. O'Mathuna, "Experiences and recommendations in deploying a real-time, water quality monitoring system," *Measurement Science and Technology*, vol. 21, pp. 124004-124013, 2010.
- [20] A. Whelan and F. Regan, "Antifouling strategies for marine and riverine sensors," *Journal of Environmental Monitoring*, vol. 8, pp. 880-886, 2006.
- [21] O. Korostynska, A. Mason and A. Al-Shamma'a, "Monitoring of nitrates and phosphates in wastewater: current technologies and further challenges," *International Journal on Smart Sensing and Intelligent Systems*, vol. 5, no. 1, pp. 149-176, 2012.

- [22] World Meteorological Organization, "Planning of Water Quality Monitoring Systems, Technical Report Series No. 3," World Meteorological Organization, Geneva, 2013.
- [23] A. Kerr, M. J. Cowling, C. M. Beveridge, M. J. Smith, A. C. Parr, R. M. Head, J. Davenport and T. Hodgkiess, "The early stages of marine biofouling and its effect on two types of optical sensors," *Environment International*, vol. 24, no. 3, pp. 331-343, 1998.
- [24] B. T. McVerry, M. C. Wong, M. L. Kristofer, J. A. Temple, C. Marambio-Jones, E. M. Hoek and R. B. Kaner, "Scalable antifouling reverse osmosis membranes utilizing perfluorophenyl azide photochemistry," *Macromolecular Rapid Communications*, vol. 35, no. 17, pp. 1528-1533, 2014.
- [25] R. Michel, S. Pasche, M. Textor and D. G. Castner, "Influence of PEG architecture on protein adsorption and conformation," *Langmuir*, vol. 21, pp. 12327-12332, 2005.
- [26] H. H. Versteeg, J. W. Heemskerk, M. Levi and P. H. Reitsma, "New fundamentals in hemostasis," *Physiological Reviews*, vol. 93, no. 1, pp. 327-358, 2013.
- [27] A. M. Leclair, S. S. Ferguson and F. Lagugne-Labarhet, "Surface patterning using plasma-deposited fluorocarbon thin films for single-cell positioning and neural circuit arrangement," *Biomaterials*, vol. 32, pp. 1351-1360, 2011.
- [28] G. Salieb-Beugelaar, G. Simone, A. Arora, A. Philippi and A. Manz, "Latest developments in microfluidic cell biology and analysis systems," *Analytical Chemistry*, vol. 82, pp. 4848-4864, 2010.
- [29] J. Zhou, A. V. Ellis and N. H. Voelcker, "Recent developments in PDMS surface modification for microfluidic devices," *Electrophoresis*, vol. 31, pp. 2-16, 2010.
- [30] G.-Q. Chen and Q. Wu, "The application of polyhydroxyalkanoates as tissue engineering materials," *Biomaterials*, vol. 26, no. 33, pp. 6565-6578, 2005.
- [31] D. Seliktar, "Designing cell-compatible hydrogels for biomedical applications," *Science*, vol. 336, no. 6085, pp. 1124-1128, 2012.
- [32] P. A. Gunatillake and R. Adhikari, "Biodegradable synthetic polymers for tissue engineering," *European Cells and Materials*, vol. 5, pp. 1-16, 2003.
- [33] S. Upadhyaya and R. P. Selvaganapathy, "Microfluidic devices for cell based high throughput screening," *Lab on a Chip*, vol. 10, pp. 341-348, 2010.
- [34] R. Cheong, C. J. Wang and A. Levchenko, "High content cell screening in a microfluidic

- device," *Molecular & Cellular Proteomics*, vol. 8.3, pp. 433-442, 2009.
- [35] P. Neuzil, S. Giselbrecht, K. Lange, T. J. Huang and A. Manz, "Revisiting lab-on-a-chip technology for drug discovery," *Nature Reviews*, vol. 11, pp. 620-632, 2012.
- [36] N. Ye, J. Qin, W. Shi, X. Liu and B. Lin, "Cell-based high content screening using an integrated microfluidic device," *Lab on a Chip*, vol. 7, no. 12, pp. 1696-1704, 2007.
- [37] K. Anselme, "Osteoblast adhesion on biomaterials," *Biomaterials*, vol. 21, pp. 667-681, 2000.
- [38] E. Tziampazis, J. Kohn and P. V. Moghe, "PEG-variant biomaterials as selectively adhesive protein templates: model surfaces for controlled cell adhesion and migration," *Biomaterials*, vol. 21, pp. 511-520, 2000.
- [39] M. Zhang, T. Desai and M. Ferrari, "Proteins and cells on PEG immobilized silicon surfaces," *Biomaterials*, vol. 19, pp. 953-960, 1998.
- [40] C. A. Haynes and W. Norde, "Globular proteins at solid/liquid interfaces," *Colloids and Surfaces B: Biointerfaces*, vol. 2, pp. 517-566, 1994.
- [41] C. F. Wertz and M. M. Santore, "Fibrinogen adsorption on hydrophilic and hydrophobic surfaces: geometrical and energetic aspects of interfacial relaxations," *Langmuir*, vol. 18, pp. 706-715, 2002.
- [42] C. F. Wertz and M. M. Santore, "Effect of surface hydrophobicity on adsorption and relaxation kinetics of albumin and fibrinogen: single-species and competitive behaviour," *Langmuir*, vol. 17, pp. 3006-3016, 2001.
- [43] A. Schmitt, R. Varoqui, S. Uniyal, J. L. Brash and C. Pusiner, "Interaction of fibrinogen with solid surfaces of varying charge and hydrophobic-hydrophilic balance," *Journal of Colloid and Interface Science*, vol. 92, no. 1, pp. 25-34, 1983.
- [44] L. Vroman and A. L. Adams, "Adsorption of proteins out of plasma and solutions in narrow spaces," *Journal of Colloids and Interface Science*, vol. 111, no. 2, pp. 391-402, 1986.
- [45] R. D. Tilton, C. R. Robertson and A. P. Gast, "Manipulation of hydrophobic interactions in protein adsorption," *Langmuir*, vol. 7, pp. 2710-2718, 1991.
- [46] I. Lundstrom and H. Elwing, "Simple kinetic models for protein exchange reactions on solid surfaces," *Journal of Colloid and Interface Science*, vol. 136, no. 1, pp. 68-84, 1990.

- [47] G. B. Sigal, M. Mrksich and G. M. Whitesides, "Effect of surface wettability on the adsorption of proteins and detergents," *Journal of the American Chemical Society*, vol. 120, no. 14, pp. 3464-3473, 1998.
- [48] P. Kingshott, H. Thissen and H. J. Griesser, "Effects of cloud-point grafting, chain length, and density of PEG layers on competitive adsorption of ocular proteins," *Biomaterials*, vol. 23, pp. 2043-2056, 2002.
- [49] M. Malmsten, K. Emoto and J. Van Alstine, "Effect of chain density on inhibition of protein adsorption by poly(ethylene glycol) based coatings," *Journal of Colloid Interface Science*, vol. 202, pp. 507-517, 1998.
- [50] S. J. Sofia, V. Premnath and E. W. Merrill, "Poly(ethylene oxide) grafted to silicon surface: grafting density and protein adsorption," *Macromolecules*, vol. 31, pp. 5059-5070, 1998.
- [51] H. Chen, L. Wang, Y. Zhang, D. Li, G. W. McClung, M. A. Brook, H. Sheardown and J. L. Brash, "Fibrinolytic poly(dimethyl siloxane) surfaces," *Macromolecules Bioscience*, vol. 8, pp. 863-870, 2008.
- [52] W. J. Brittain and S. Minko, "A structural definition of polymer brushes," *Journal of Polymer Science: Part A: Polymer Chemistry*, vol. 45, pp. 3505-3512, 2007.
- [53] R. Barbey, L. Lavanant, D. Paripovic, N. Schuwer, C. Sugnaux, S. Tugulu and H.-A. Klok, "Polymer brushes via surface-initiated controlled radical polymerization: synthesis, characterization, properties, and applications," *Chemical Reviews*, vol. 109, pp. 5437-5527, 2009.
- [54] M. Farrell and S. Beaudoin, "Surface forces and protein adsorption on dextran- and polyethylene glycol-modified polydimethylsiloxane," *Colloids and Surfaces B: Biointerfaces*, vol. 81, pp. 468-475, 2010.
- [55] R. Zeng, Z. Luo, D. Zhou, F. Cao and Y. Wang, "A novel PEG coating immobilized onto capillary through polydopamine coating for separation of proteins in CE," *Electrophoresis*, vol. 31, pp. 3334-3341, 2010.
- [56] V. Ball, D. D. Frari, V. Toniazzo and D. Ruch, "Kinetics of polydopamine film deposition as a function of pH and dopamine concentrations: insights in the polydopamine deposition mechanism," *Journal of Colloid and Interface Science*, vol. 386, pp. 366-372, 2012.
- [57] M. D. Hawley, S. V. Tatawawadi, S. Piekarski and R. N. Adams, "Electrochemical studies of the oxidation pathways of catecholamines," *Journal of the American Chemical Society*,

- vol. 89, no. 2, pp. 447-450, 1967.
- [58] M. d'Ischia, A. Napolitano, A. Pezzella, P. Meredith and T. Sama, "Chemical and structural diversity in eumelanins: unexplored bio-optoelectronic materials," *Angewandte Chemie International Edition*, vol. 48, no. 22, pp. 3914-3921, 2009.
- [59] C. Tao, S. Yang, J. Zhang and J. Wang, "Surface modification of diamond-like carbon films with protein via polydopamine inspired coatings," *Applied Surface Science*, vol. 256, pp. 294-297, 2009.
- [60] R. Luo, L. Tang, S. Zhong, Z. Yang, J. Wang, Y. Weng, Q. Tu, C. Jiang and N. Huang, "In vitro investigation of enhanced hemocompatibility and endothelial cell proliferation associated with quinone-rich polydopamine coating," *ACS Applied Materials and Interfaces*, vol. 5, pp. 1704-1714, 2013.
- [61] H. W. Kim, H. D. Lee, S. J. Jang and H. B. Park, "Highly chlorine and oily fouling tolerant membrane surface modifications by in situ polymerization of dopamine and poly(ethylene glycol) diacrylate for water treatment," *Journal of Applied Polymer Science*, p. 41661, 2015.
- [62] K. C. Black, J. Yi, J. G. Rivera, D. C. Zelasko-Leon and P. B. Messersmith, "Polydopamine-enabled surface functionalization of gold nanorods for cancer cell-targeted imaging and photothermal therapy," *Nanomedicine*, vol. 8, no. 1, pp. 17-28, 2013.
- [63] H. Lee, J. Rho and P. B. Messersmith, "Facile conjugation of biomolecules onto surfaces via mussel adhesive protein inspired coatings," *Advanced Materials*, vol. 21, no. 4, pp. 431-434, 2009.
- [64] H.-W. Chien and W.-B. Tsai, "Fabrication of tunable micropatterned substrates for cell patterning via microcontact printing of polydopamine with poly(ethylene imine)-grafted copolymers," *Acta Biomaterialia*, vol. 8, pp. 3678-3686, 2012.
- [65] F. Li, J. Meng, J. Ye, B. Yang, Q. Tian and C. Deng, "Surface modification of PES ultrafiltration membrane by polydopamine coating and poly(ethylene glycol) grafting: morphology, stability, and anti-fouling," *Desalination*, vol. 344, pp. 422-430, 2014.
- [66] W.-B. Tsai, C.-Y. Chien, H. Thissen and J.-Y. Lai, "Dopamine-assisted immobilization of poly(ethylene imine) based polymers for control of cell-surface interactions," *Acta Biomaterialia*, vol. 7, pp. 2518-2525, 2011.
- [67] Q. Wei, F. Zhang, J. Li, B. Li and C. Zhao, "Oxidant-induced dopamine polymerization for

- multifunctional coatings," *Polymer Chemistry*, vol. 1, pp. 1430-1433, 2010.
- [68] Eastman Chemical Company, "Improved hydrolytic stability of waterborne polyester resins with Eastman 1,4-CHDA and Eastman TMPD glycol," 2013. [Online]. Available: http://www.eastman.com/Literature_Center/N/N342.pdf. [Accessed 21 March 2016].
- [69] V. Elias, A. Salman and D. Goulias, "The effect of pH, resin properties, and manufacturing process on laboratory degradation of polyester geosynthetics," *Geosynthetics International*, vol. 5, no. 5, pp. 459-490, 1998.
- [70] Valspar Corporation, "Steel container brochure," 2012. [Online]. Available: <http://www.valsparpackaging.com/assets/files/SteelContainerBrochure05-2012v5.pdf>. [Accessed 21 March 2016].
- [71] Q. Wei, J. Li, B. Qian, B. Fang and C. Zhao, "Preparation, characterization and application of functional polyethersulfone membranes blended with poly (acrylic acid) gels," *Journal of Membrane Science*, vol. 337, no. (1-2), pp. 266-273, 2009.
- [72] M. Steinitz, "Quantitation of the blocking effect of tween 20 and bovine serum albumin in ELISA microwells," *Analytical Biochemistry*, vol. 282, pp. 232-238, 2000.
- [73] R. F. Vogt, D. L. Phillips, O. L. Henderson, W. Whitfield and F. W. Spierto, "Quantitative differences among various proteins as blocking agents for ELISA microtiter plates," *Journal of immunological Methods*, vol. 101, pp. 43-50, 1987.
- [74] D. Zang, L. Ge, M. Yan, X. Song and J. Yu, "Electrochemical immunoassay on a 3D microfluidic paper-based device," *Chemical Communications*, vol. 48, pp. 4683-4685, 2012.
- [75] S. Cesaro-Tadic, G. Dernick, D. Juncker, G. Buurman, H. Kropshofer, B. Michel, C. Fattinger and E. Delamarque, "High-sensitivity miniaturized immunoassays for tumor necrosis factor α using microfluidic systems," *Lab on a Chip*, vol. 4, pp. 563-569, 2004.
- [76] S. Hideshima, R. Sato, S. Inoue, S. Kuroiwa and T. Osaka, "Detection of tumor marker in blood serum using antibody-modified field effect transistor with optimized BSA blocking," *Sensors and Actuators B: Chemical*, vol. 161, no. 1, pp. 146-150, 2012.
- [77] S. A. Michel, M. L. Knetsch and L. H. Koole, "Adsorption of albumin on flax fibers increases endothelial cell adhesion and blood compatibility in vitro," *Journal of Biomaterials Science, Polymer Edition*, vol. 25, no. 7, pp. 698-712, 2014.
- [78] H. Yamazoe and T. Tanabe, "Preparation of water-insoluble albumin film possessing

- nonadherent surface for cells and ligand binding ability," *Journal of Biomedical Materials Research Part A*, vol. 86, no. 1, pp. 228-234, 2007.
- [79] H. Yamazoe, T. Uemura and T. Tanabe, "Facile cell patterning on an albumin-coated surface," *Langmuir*, vol. 24, pp. 8402-8404, 2008.
- [80] A. Revzin, P. Rajagopalan, A. W. Tilles, F. Berthiaume, M. L. Yarmush and M. Toner, "Designing a hepatocellular microenvironment with protein microarraying and poly(ethylene glycol) photolithography," *Langmuir*, vol. 20, pp. 2999-3005, 2004.
- [81] E. Bulard, M.-P. Fontaine-Aupart, H. Dubost, W. Zheng, M.-N. Bellon-Fontaine, J.-M. Herry and B. Bourguignon, "Competition of bovine serum albumin adsorption and bacterial adhesion onto surface-grafted ODT: in situ study by vibrational SFG and fluorescence confocal microscopy," *Langmuir*, vol. 28, pp. 17001-17010, 2012.
- [82] C. Nune, W. Xu and R. D. Misra, "The impact of grafted modification of silicone surfaces with quantum-sized materials on protein adsorption and bacterial adhesion," *Journal of Biomedical Materials Research Part A*, vol. 100A, pp. 3197-3204, 2012.
- [83] X. Zheng, H. Baker, W. S. Hancock, F. Fawaz, M. McCaman and E. Pungor, "Proteomic analysis for the assessment of different lots of fetal bovine serum as a raw material for cell culture. Part IV. Application of proteomics to the manufacture of biological drugs," *Biotechnology Progress*, vol. 22, pp. 1294-1300, 2006.
- [84] J. Jiang, L. Zhu, L. Zhu, B. Zhu and Y. Xu, "Surface characteristics of a self-polymerized dopamine coating deposited on hydrophobic polymer films," *Langmuir*, vol. 27, pp. 14180-14187, 2011.
- [85] S. Sharma, R. W. Johnson and T. A. Desai, "XPS and AFM analysis of antifouling PEG interfaces for microfabricated silicon biosensors," *Biosensors and Bioelectronics*, vol. 20, pp. 227-239, 2004.
- [86] S. Nirasay, A. Badia, G. Leclair, J. P. Claverie and i. Marcotte, "Polydopamine-supported lipid bilayers," *Materials*, vol. 5, pp. 2621-2636, 2012.
- [87] D. M. Doran and I. L. Spar, "Oxidative iodine monochloride iodination technique," *Journal of Immunological Methods*, vol. 39, pp. 155-163, 1980.
- [88] J. S. Taurozzi and V. V. Tarabara, "Silver nanoparticle arrays on track etch membrane support as flow-through optical sensors for water quality control," *Environmental Engineering Science*, vol. 24, no. 1, pp. 122-137, January 2007.

- [89] M. Liu, J. Pi, X. Wang, R. Huang, Y. Du, X. Yu, W. Tan, F. Liu and K. J. Shea, "A sol-gel derived pH-responsive bovine serum albumin molecularly imprinted poly(ionic liquids) on the surface of multiwall carbon nanotubes," *Analytica Chimica Acta*, vol. 932, pp. 29-40, 2016.
- [90] T. Lindl, *Zell-und Gewebekultur* 5ed, Heidelberg: Spektrum Akademischer Verlag, 2002.
- [91] B. Blomback, B. Hessel, D. Hogg and L. Therkildsen, "A two-step fibrinogen-fibrin transition in blood coagulation," *Nature*, vol. 275, pp. 501-505, 1978.
- [92] H. Fujiwara, *Spectroscopic Ellipsometry: Principles and Applications*, Chichester: John Wiley & Sons Ltd., 2007.
- [93] Y.-C. Chang, C.-H. Liu, C.-H. Liu, S. Zhang, S. R. Marder, E. E. Narimanov, Z. Zhong and T. B. Norris, "Realization of mid-infrared graphene hyperbolic metamaterials," *Nature Communications*, vol. 7, 2016.
- [94] I. J. A. Woollam Co., *CompleteEASE Data Analysis Manual v.3.65*, Lincoln: J. A. Woollam Co., Inc. , 2008.
- [95] C. E. ZoBell, "The effect of solid surfaces upon bacterial activity," *Journal of Bacteriology*, vol. 46, pp. 39-59, 1943.
- [96] M. C. van Loosdrecht, J. Lyklema, W. Norde, G. Schraa and A. J. Zehnder, "The role of bacterial cell wall hydrophobicity in adhesion," *Applied and Environmental Microbiology*, vol. 53, no. 8, pp. 1893-1897, 1987.
- [97] K. C. Marshall, R. Stout and R. Mitchell, "Mechanism of the initial events in the sorption of marine bacteria to surfaces," *Journal of General Microbiology*, vol. 68, pp. 337-348, 1971.
- [98] P. Gilbert, D. J. Evans, E. Evans, I. Duguid and M. R. Brown, "Surface characteristics and adhesion of *Escherichia coli* and *Staphylococcus epidermidis*," *Journal of Applied Bacteriology*, vol. 71, pp. 72-77, 1991.
- [99] C. Prigent-Combaret, G. Prensier, T. T. L. Thi, O. Vidal, P. Lejeune and C. Dorel, "Developmental pathway for biofilm formation in curli-producing *Escherichia coli* strains: role of flagella, curli and colanic acid," *Environmental Microbiology*, vol. 2, no. 4, pp. 450-464, 2000.
- [100] A. Olsen, A. Jonsson and S. Normark, "Fibronectin binding mediated by a novel class of surface organelles on *Escherichia coli*," *Nature*, vol. 338, pp. 652-655, 1989.

- [101] J. F. W. Keana and S. X. Cai, "New reagents for photoaffinity labeling: Synthesis and photolysis of functionalized perfluorophenyl azides," *Journal of Organic Chemistry*, vol. 55, pp. 3640-3647, 1990.
- [102] K. A. Schnapp, R. Poe, E. Leyva, N. Soundararajan and M. S. Platz, "Exploratory photochemistry of fluorinated aryl azides. Implications for the design and photoaffinity labeling reagents," *Bioconjugate Chemistry*, vol. 4, pp. 172-177, 1993.
- [103] L.-H. Liu and M. Yan, "Perfluorophenyl azides: New applications in surface functionalization and nanomaterial synthesis," *Accounts of Chemical Research*, vol. 43, no. 11, pp. 1434-1443, 2010.
- [104] O. Sterner, M. Giazzon, S. Zurcher, S. Tosatti, M. Liley and N. D. Spencer, "Delineating fibronectin bioadhesive micropatterns by photochemical immobilization of polystyrene and poly(vinylpyrrolidone)," *ACS Applied Materials & interfaces*, vol. 6, pp. 18683-18692, 2014.
- [105] M. Yan, "Covalent functionalization of natural rubber latex," *Reactive and Functional Polymers*, vol. 45, pp. 137-144, 2000.
- [106] H. Wang, J. Ren, A. Hlaing and M. Yan, "Fabrication and anti-fouling properties of photochemically and thermally immobilized poly(ethylene oxide) and low molecular weight poly(ethylene glycol) thin films," *Journal of Colloid and Interface Science*, vol. 354, pp. 160-167, 2011.
- [107] O. Sterner, A. Serrano, S. Mieszkin, S. Zurcher, S. Tosatti, M. E. Callow, J. A. Callow and N. D. Spencer, "Photochemically prepared, two-component polymer-concentration gradients," *Langmuir*, vol. 29, pp. 13031-13041, 2013.
- [108] M. Zayat, P. Garcia-Parejo and D. Levy, "Preventing UV-light damage of light sensitive materials using a highly protective UV-absorbing coating," *Chemical Society Reviews*, vol. 36, pp. 1270-1281, 2007.
- [109] P. Garcia-Parejo, M. Zayat and D. Levy, "Highly efficient UV-absorbing thin-film coatings for protection of organic materials against photodegradation," *Journal of Materials Chemistry*, vol. 16, pp. 2165-2169, 2006.
- [110] A. L. Andradý, K. Fueki and A. Torikai, "Spectral sensitivity of polycarbonate to light-induced yellowing," *Journal of Applied Polymer Science*, vol. 42, no. 7, pp. 2105-2107, 1991.

- [111] M. Yan and J. Ren, "Covalent immobilization of ultrathin polymer films by thermal activation of perfluorophenyl azide," *Chemical Materials*, vol. 16, pp. 1627-1632, 2004.
- [112] M. Yan and J. Ren, "Covalent immobilization of polypropylene thin films," *Journal of Materials Chemistry*, vol. 15, pp. 523-527, 2005.
- [113] P. Meredith and T. Sarna, "The physical and chemical properties of eumelanin," *Pigment Cell Research*, vol. 19, no. 6, pp. 572-594, 2006.
- [114] K. Reimhult, K. Petersson and A. Krozer, "QCM-D analysis of the performance of blocking agents on gold and polystyrene surfaces," *Langmuir*, vol. 24, pp. 8695-8700, 2008.
- [115] X. Xia, M. Yang, y. Wang, Y. Zheng, Q. Li, J. Chen and Y. Xia, "Quantifying the coverage density of poly(ethylene glycol) chains on the surface of gold nanostructures," *ACS Nano*, vol. 6, no. 1, pp. 512-522, 2012.

APPENDIX A: Making PDMS Samples SOP

A.1 Purpose

To make PDMS disc samples for antifouling experiments.

A.2 Materials

- Sylgard 184 Silicone Elastomer Kit (Dow Corning, Midland, MI)
- 4 Petri Dishes
- Scale
- Transfer Pipette
- Tri-pour
- 10 mL Syringe

A.3 Methods

1. Using a scale, measure and mix 24g of PDMS base and 2.4 g of curing agent (10:1) in a tri-pour.
2. Stir for 5 min until mixture turns opaque and bubbly.
3. Using a syringe, draw 6 mL of PDMS mixture and dispense into 10 cm dish. Repeat until 4 dishes are made. PDMS will be approximately 1 mm thick.
4. Cover petri dishes with lid and leave the dishes overnight on a leveled* table to remove air bubbles. OR use a vacuum chamber to remove air bubbles if PDMS is needed same day.
5. Put the PDMS plates in a 60°C oven for 2 h. Check if PDMS is dry.
6. Let samples cool down, then punch discs using a 6 mm diameter punch.
7. Wash PDMS discs in 95% ethanol or 100% isopropanol. Can wash samples in an ultrasound bath for 5 min if samples are very dirty.
8. Rinse samples in Mili-Q water.
9. Cover samples and store away.

A.4 Hazard Identification and Risk of Exposure to Hazards

- High heat when curing PDMS

A.5 Exposure Controls specific to Above Risk of Exposure

- Wear gloves and use forceps to remove PDMS dishes

A.6 Biological Waste Disposal Methods

- Non-toxic. Dispose in regular waste.

A.7 Spill Response Procedures

Wipe with paper towels, and/or allow PDMS to cure in open air. Peel the PDMS off once it has cured and discard in regular waste.

A.8 Biosafety Training Requirements

- All required McMaster safety courses for workers.
- Biosafety level 1 (BSL-1)

APPENDIX B: PDA, PEG, and BSA Modification SOP

B.1 Purpose

To modify samples using polydopamine (PDA), polyethylene glycol (PEG) and bovine serum albumin (BSA).

B.2 Materials

- Hydrophilic polycarbonate track etch membranes (PC, d = 25mm, 0.01 μm pore) (Sterlitech Corporation, Kent, WA)
 - Samples cut into 8 triangles
- Glass samples (Haimen Aibende Experiment Equipment Co. LTD., Nantong, China)
- PDMS discs (see PDMS samples sop)
- Bovine serum albumin (>98% lyophilized powder) (Sigma-Aldrich, Oakville, ON)
- Dopamine (Sigma-Aldrich, Oakville, ON)
- NH_2 -PEG- NH_2 (MW 5000 Da) (JenKem Technology USA Inc., Plano, TX)
- 10X phosphate buffered saline (PBS), pH 7.4 (BioShop Canada Inc., Burlington, ON)
 - Diluted to 1X PBS using Milli-Q water (18.2 $\text{M}\Omega\cdot\text{cm}$) from Millipore Co.
 - 1X PBS adjusted to pH 8.5 using NaOH
- 100 mL Pyrex glass dishes
- Tweezers
- Graduated cylinder

B.3 Methods

B.3.1 PDA Modification

1. PC, PDMS, and glass samples were washed in 95% ethanol and rinsed thoroughly before use.
2. Prepare 100 mL of 2 mg/mL dopamine solution in PBS pH 8.5 at room temperature.
3. Dissolve dopamine powder then quickly pour 50 mL of dopamine solution into two glass dishes.
4. Add PC, PDMS, and glass samples to the dopamine solution. Make sure that the samples do not overlap and are submerged. Place PDMS samples one by one while stirring the dopamine solution to prevent PDMS samples from sticking together. Do not place PDMS and PC samples together in the same dish (since PC can stick to PDMS).
5. Place dishes in an open shaker. Allow samples to stir for 3 h at 80 RPM in room temperature. Do not cover the dish.
6. Discard PDA solution in the sink and flush with lots of water.
7. Rinse samples 3x thoroughly with Milli-Q water.
8. Store samples in 96-well plate (one sample per well).

B.3.2 BSA Modification

1. Prepare 40 mL of 10 mg/mL BSA solution in PBS pH 7.4. Pour solution into a glass dish.
2. Place PDA-modified samples in the glass dish and seal the opening with parafilm. Stir at 80 RPM for 24 h at room temperature.
3. Discard BSA solution in the sink and flush with lots of water.
4. Rinse samples 3x thoroughly with Milli-Q water.
5. Store samples in 96-well plate (one sample per well).

B.3.3 PEG Modification

1. Prepare 40 mL of 5 mg/mL PEG solution in PBS pH 8.5. Pour solution into a glass dish.
2. Place PDA-modified samples in the glass dish and seal the opening with parafilm. Stir at 80 RPM for 24 h at 37°C.
3. Discard PEG solution in the sink and flush with lots of water.
4. Rinse samples 3x thoroughly with Milli-Q water.
5. Store samples in 96-well plate (one sample per well).

B.3.4 BSA and PEG Backfill (PDA-BSA/PEG and PDA-PEG/BSA Samples)

1. PDA-BSA samples were modified in PEG solution as previously described.
2. PDA-PEG samples were modified in BSA solution as previously described.

B.4 Hazard Identification and Risk of Exposure to Hazards

- Base burns when adjusting buffer pH with NaOH
- Risk of exposure during: spills, inhalation

B.5 Exposure Controls specific to Above Risk of Exposure

- Wear appropriate PPE

B.6 Biological Waste Disposal Methods

- PDA, PEG, and BSA solution may be flushed down the drain with lots of running water.
- Modified surfaces are disposed in biohazardous waste.

B.7 Spill Response Procedures

For PDA, PEG, or BSA solution spills, wipe up with paper towels and dispose in biohazardous waste.

B.7.1 Small Spills of NaOH

Use a chemical spill kit and follow instructions.

B.7.2 Large Spills of NaOH

Notify safety office at x24956, or x88 (security) after hours.

B.8 Biosafety Training Requirements

- All required McMaster safety courses for workers.
- Biosafety level 1 (BSL-1)

APPENDIX C: PFPA-PEG Modification of PDA Coated Surfaces SOP

C.1 Purpose

To modify PDA coated surfaces with PFPA-PEG.

C.2 Materials

- Hydrophilic polycarbonate track etch membranes (PC, d = 25mm, 0.01 μm pore) (Sterlitech Corporation, Kent, WA)
 - Samples cut into 8 triangles
- Glass samples (Haimen Aibende Experiment Equipment Co. LTD., Nantong, China)
- PDMS discs (see PDMS samples sop)
- Bovine serum albumin (>98% lyophilized powder) (Sigma-Aldrich, Oakville, ON)
- Dopamine (Sigma-Aldrich, Oakville, ON)
- NH_2 -PEG- NH_2 (MW 5000 Da) (JenKem Technology USA Inc., Plano, TX)
- 10X phosphate buffered saline (PBS), pH 7.4 (BioShop Canada Inc., Burlington, ON)
 - Diluted to 1X PBS using Milli-Q water (18.2 $\text{M}\Omega\cdot\text{cm}$) from Millipore Co.
 - 1X PBS adjusted to pH 8.5 using NaOH
- 100 mL Pyrex glass dishes
- Tweezers
- Graduated cylinder
- 96-well plates
- Milli-Q water
- Mineralight UV lamp UVG-11 ($\lambda = 254 \text{ nm}$, 1.12 mW/cm^2)
- Tin foil

C.3 Methods

C.3.1 PDA Modification

1. PC, PDMS, and glass samples were washed in 95% ethanol and rinsed thoroughly before use.
2. Prepare 100 mL of 2 mg/mL dopamine solution in PBS pH 8.5 at room temperature.
3. Dissolve dopamine powder then quickly pour 50 mL of dopamine solution into two glass dishes.
4. Add PC, PDMS, and glass samples to the dopamine solution. Make sure that the samples do not overlap and are submerged. Place PDMS samples one by one while stirring the dopamine solution to prevent PDMS samples from sticking together. Do not place PDMS and PC samples together in the same dish (since PC can stick to PDMS).
5. Place dishes in an open shaker. Allow samples to stir for 3 h at 200 RPM in room temperature. Do not cover the dish.
6. Discard PDA solution in the sink and flush with lots of water.
7. Rinse samples 3x thoroughly with Milli-Q water.
8. Store samples in 96-well plate (one sample per well).

C.3.2 PFPA-PEG Modification

C.3.3 *Work to be done in a dark room, protecting samples from light.*

1. In an eppendorf tube, prepare 10.5 mg/mL PFPA-PEG solution in 1 mL of Milli-Q water.
2. Dip samples one-by-one in the PFPA-PEG solution (~3 sec).
3. Place the samples in individual wells of a 96-well plate.
4. Use tin foil to cover the samples. Dry at 60°C for 3 h.
5. Place the dried samples flat onto the lid of a 96-well plate.
6. Use a rack to elevate the samples ~1.5” away from the UV lamp (254 nm).
7. Irradiate the samples using a UV-lamp for 5 min on each side.
8. Rinse the samples thoroughly using Milli-Q water.
9. Repeat steps 1-8.

C.4 Hazard Identification and Risk of Exposure to Hazards

- UV damage: cataracts, erythema, burns

C.5 Exposure Controls specific to Above Risk of Exposure

- Wear UV-blocking safety glasses
- Cover exposed skin by wearing appropriate PPE

C.6 Biological Waste Disposal Methods

- Dispose unused PFPA-PEG solution as chemical waste.

C.7 Spill Response Procedures

Use a chemical spill kit for PFPA-PEG solution spills.

C.8 Biosafety Training Requirements

- All required McMaster safety courses for workers.
- Biosafety level 1 (BSL-1)
- Laser safety training

APPENDIX D: I¹²⁵ Protein Radiolabeling SOP

D.1 Purpose

To radiolabel bovine serum albumin (BSA) and fibrinogen (Fg) with isotope (Iodide-125).

D.2 Materials

- Bovine serum albumin (>98% lyophilized powder) (Sigma-Aldrich, Oakville, ON)
- Slide-A-Lyzer dialysis cassettes (Thermo Fisher Scientific, Mississauga, ON)
- Float
- Human Fibrinogen (Fg; Enzyme Research laboratories, South Bend, IN)
- AG 1-X4 Resin (Bio-Rad, Mississauga, ON)
- 10X phosphate buffered saline (PBS), pH 7.4 (BioShop Canada Inc., Burlington, ON)
 - Prepared as 1X PBS by dilution in Milli-Q water
- Sodium iodide-125 (Na¹²⁵I) isotope (McMaster Nuclear Reactor, McMaster University, Hamilton, ON)
- Glycine buffer (pH 8.8)
- Trichloroacetic acid (TCA)
- Iodide chloride (ICl)
- Absorbent pads
- Beaker with magnetic stirrer
- 96-well plates
- Tweezers
- 1 mL syringe
- 1.5” 22 gauge needles
- 1.5 mL Eppendorf tubes
- Counting vials
- Filter paper
- Two tubes with stoppers
- UV Cuvette

D.3 Methods

D.3.1 Bovine Serum Albumin Radiolabeling

1. In a tube, prepare 10mg BSA solution in 1mL
2. Add 140 μ L glycine to BSA solution. Label the tube, Tube 1.
3. In another tube (Tube 2), add 176 μ L ICl and 42 μ L glycine.
4. Fill beaker with PBS buffer and hydrate dialysis cassette.
5. Sign the isotope inventory sheet on the door.
6. In the radioactivity labeling lab, sign the sign in sheet on the fume hood. Check that the fume hood is running.
7. Swab the hood with filter paper for contamination monitoring, starting from the ledge to the inside. Place the filter paper in a counting tube labeled “Start”.
8. Set up hood with absorbent pad, magnetic stirrer, rack, etc. Label the working station with the date, time, worker name, and contact number.

9. Add 10 μL of I-125 to the Tube 2 in the hood and cap immediately. Switch gloves immediately after. Swirl the tube.
10. Add tube 1 to 2 with the transfer pipette and cap immediately. Let it react for 2min.
11. Use syringe and needle to add the solution to the cassette. Remove the excess air.
12. Obtain 1mL PBS and wash the tube. Add it to the cassette.
13. Discard needle in the sharps waste. Do NOT recap!
14. Turn on stirrer and dialyze for 2 hours.
15. After 2 hours, discard PBS buffer in I-125 liquid waste container. Be careful as the solution contains free iodide.
16. Add new buffer and dialyze again for another 2 hours. Repeat step 15.
17. Parafilm the beaker and place it in the transport box. Dialyze again overnight in the fridge.
18. Swab the hood with filter paper for contamination monitoring, starting from the ledge to the inside. Place the filter paper in a counting tube labeled “End”. Place the Start and End counting vials on a gamma counter and determine the radioactivity. If the counts per minute (CPM) of the Start and End tubes differ by more than 50 CPM, decontaminate the hood by wiping the surfaces with extrand. Re-swab the hood and determine the new radioactivity. Repeat decontamination procedures until the $\text{CPM} < 50$.
19. The next morning, repeat step 16 for the fourth time in the fume hood.
20. Use another syringe and needle to obtain radiolabeled protein from the cassette. Place solution in a new tube labeled “BSA stock”.
21. Add 100 μL of stock solution and 900 μL of PBS to a 1 cm cuvette and measure the solution absorbance on a spectrophotometer at 280 nm to determine the protein concentration.

$$\text{Concentration} = \frac{A_{280}}{\text{Extinction Coefficient}} \times 10$$

Where the extinction coefficient for BSA = 0.667

D.3.2 Fibrinogen Radiolabeling

1. In a 50 mL tube, hydrate ~10 mL of resin with 40 mL PBS. Must be prepared at least one day prior to use.
2. Add 200 μL of Fg solution (10 mg/mL) and 70 μL glycine to a tube. Label the tube, Tube 1.
3. In another tube (Tube 2), add 8.75 μL ICl and 25 μL glycine.
4. Mix resin well then pack it into a 1 mL syringe by tapping the sides of the syringe to allow excess PBS to be discarded.
5. Equip the syringe with a needle. Place the resin column in a 50 mL tube filled with PBS. Keep the column hydrated by adding PBS to the top of the resin as needed.
6. Sign the isotope inventory sheet on the door.
7. In the radioactivity labeling lab, sign the sign in sheet on the fume hood. Check that the fume hood is running.
8. Swab the hood with filter paper for contamination monitoring, starting from the ledge to the inside. Place the filter paper in a counting tube labeled “Start”.

9. Set up hood with absorbent pad and resin column with a new tube to allow solution to drain into. Label the working station with the date, time, worker name, and contact number.
10. Add 5 μL of I-125 to the Tube 2 in the hood and cap immediately. Switch gloves immediately after. Swirl the tube.
11. Add tube 1 to 2 with the transfer pipette and cap immediately. Let it react for 2min.
12. Slowly add the radioactive protein solution to the resin column.
13. Add 1 mL of PBS to rinse Tube 2, then add the solution to the resin column.
14. Continue to add PBS to the column and allow solution to pass the resin column until a volume of 5 mL is collected.
15. Discard excess radioactive liquid in the radioactive liquid waste. Discard resin column in sharps waste.
16. Swab the hood with filter paper for contamination monitoring, starting from the ledge to the inside. Place the filter paper in a counting tube labeled “End”. Place the Start and End counting vials on a gamma counter and determine the radioactivity. If the counts per minute (CPM) of the Start and End tubes differ by more than 50 CPM, decontaminate the hood by wiping the surfaces with extrand. Re-swab the hood and determine the new radioactivity. Repeat decontamination procedures until the $\text{CPM} < 50$.
17. Add 100 μL of stock solution and 900 μL of PBS to a 1 cm cuvette and measure the solution absorbance on a spectrophotometer at 280 nm to determine the protein concentration (extinction coefficient for Fg is 1.55).

D.3.3 Free Iodide Test

1. Add 990 μL of 10 mg/mL BSA solution to six Eppendorf tubes.
2. Add 10 μL of radiolabeled protein stock solution to the same six Eppendorf tubes.
3. Place three of the tubes' solutions into counting vials (“STOCK”).
4. Carefully add 500 μL of TCA to three of the Eppendorf tubes. Close and mix well. Then allow for the solution to react for 5 min.
5. Centrifuge the protein precipitate for 5 min at 5000 RPM.
6. Add 500 μL of the supernatant to three counting vials. Add 500 μL of PBS to three counting vials (total volume = 1 mL). (“FREE”)
7. Place the 3 tubes of “STOCK” and three tubes of “FREE” on a gamma counter.
8. Discard radioactive waste appropriately.

$$\text{Free Iodide} = \frac{\text{Average of FREE} \times 3}{\text{Average of STOCK}} \times 100\%$$

Note: Acceptable levels of free iodide <1%

D.4 Hazard Identification and Risk of Exposure to Hazards

- Radioactive contamination by: skin absorption, ingestion, or inhalation
- Risk of exposure during: spills and radiolabeling
- Local effects: erythema, burns, cataracts
- Stochastic effects: cancer and genetic effect

D.5 Exposure Controls specific to Above Risk of Exposure

- All radioactive work must be conducted in facilities with radioactive permits.

- All radioactive work with free iodide must be conducted in the fume hood. Shielding using lead.
- Contamination monitoring of work areas must be conducted weekly.
- Health monitoring of the thyroid gland must be conducted within 5 days of radioactive labeling.
- All workers must wear an isotope monitoring badge when conducting work with radioactive samples.
- All doses must be maintained as low as reasonably achievable. Please review individual dose limits as specified on the radioactivity work permit.
- Pregnant female workers must stop work immediately and notify health physics as soon as pregnancy is confirmed.

D.6 Biological Waste Disposal Methods

- Solid radioactive waste must be disposed of in radioactive waste bins. Estimated radioactivity must be recorded and signed by the user.
- Liquid radioactive waste must be disposed of in chemical waste containers in the fume hood. Waste contents must be identified (ex. I-125, BSA)
- TCA waste must be disposed of in separate waste containers as marked (ex. I-125, BSA, TCA) in the fume hood.
- Radioactive needles must be disposed of in radioactive sharps waste container in the fume hood.

D.7 Spill Response Procedures

D.7.1 Small Spills

1. Notify workers in the area that a spill has occurred.
2. Wear appropriate PPE then wipe it up with paper towels or the absorbent pads using tweezers, working from the outside of the spill to the center.
3. Place waste in a ziplock bag.
4. Wash the contaminated surface with Extrand and wipe and bag again for disposal.
5. Monitor yourself and the area for contamination frequently.

D.7.2 Large Spills

For spills involving a large volume of radioactive liquids with bound isotope.

For spills of any volume involving free isotope.

Notify health physics promptly at x24226, or x88 (security) after hours.

D.8 Biosafety Training Requirements

- All required McMaster safety courses for workers.
- Biosafety level 1 (BSL-1)
- Radioactive Safety Training

D.9 References

McMaster Health Physics. (2017). Initial Radiation Safety Training at McMaster University [PowerPoint Slides]. Retrieved from <https://www.mcmaster.ca/healthphysics/Library/General%20Radiation%20Safety%20Training%20at%20McMaster%20-%20Online%20Material.pdf>

APPENDIX E: Quantifying I¹²⁵ Radiolabeled Protein Adsorption SOP

E.1 Purpose

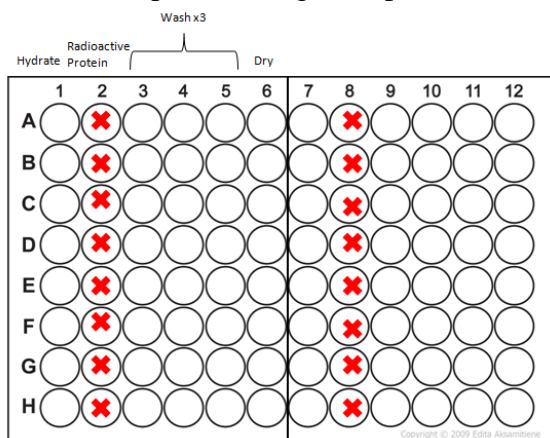
To quantify protein adsorption on surfaces using radiolabeled proteins.

E.2 Materials

- Modified PDMS, PC, and glass samples at n=3 per modification
- Bovine serum albumin (>98% lyophilized powder) (Sigma-Aldrich, Oakville, ON)
- Human Fibrinogen (Fg; Enzyme Research laboratories, South Bend, IN)
- 10X phosphate buffered saline (PBS), pH 7.4 (BioShop Canada Inc., Burlington, ON)
 - Prepared as 1X PBS by dilution in Milli-Q water
- 96-well Plates
- Transfer pipettes
- UV Cuvette
- Kim wipes
- Counting vials

E.3 Methods

1. In a 96-well plate, arrange samples in the following:



Where columns 1 and 7 contain samples in hydrated in PBS (hydrate samples the night before the experiment), columns 2 and 8 contain radioactive protein solution, columns 3-5 and 9-11 contain PBS for rinsing the samples, and columns 6 and 12 are empty to allow surfaces to dry.

2. Obtain stock solutions of BSA or Fg made in the I¹²⁵ protein radiolabeling SOP.
3. Prepare protein working solutions at 5% labeled.

Example: For adsorption in 1 mg/mL Fg and n=15 samples.
 $V \text{ needed} = 250 \mu\text{L} \times 15 = 3.75 \text{ mL} \dots \text{raise to } 5 \text{ mL}$
 Mix 5% of 5 mg = 0.25 mg of Fg* (Radioactive Fg) and 4.75 mg of Fg (non-radioactive Fg) to a total volume of 5 mL.
4. Check the concentration of the working solution using a spectrophotometer.
5. Add 250 μL of working solution to the wells in columns 2 and 8.
6. Using tweezers, transfer hydrated surfaces from columns 1 and 7 to columns 2 and 8.
7. Incubate samples for 2 h.

8. Fill columns 3-5 and 9-11 with PBS.
9. After 2 h, transfer surfaces into rinsing columns 3-5 and 9-11 for 5 min each. Wipe tweezers with a kim wipe after each transfer.
10. Transfer surfaces into dry wells in columns 6 and 12.
11. Prepare working solution counts by pipetting 10 μL of working solution into three counting vials. Cap the counting vials.
12. Transfer surfaces into individual counting vials.
13. Count the surface radiation on a gamma counter. Set program to I-125 1 min counts.
14. Dispose all radioactive liquid and solid waste appropriately.
15. Determine protein adsorption using the following formula:

$$\text{Adsorption } \mu\text{g}/\text{cm}^2 = \frac{\text{Sample (CPM)} \times [\text{working}] \left(\frac{\mu\text{g}}{\text{mL}}\right)}{\text{working} \left(\frac{\text{CPM}}{\text{mL}}\right) \times \text{surface area (cm}^2\text{)}}$$

E.4 Hazard Identification and Risk of Exposure to Hazards

- Radioactive contamination by: skin absorption, ingestion, or inhalation
- Risk of exposure during: spills and radiolabeling
- Local effects: erythema, burns, cataracts
- Stochastic effects: cancer and genetic effect

E.5 Exposure Controls specific to Above Risk of Exposure

- All radioactive work must be conducted in facilities with radioactive permits.
- All radioactive work with free iodide must be conducted in the fume hood. Shielding using lead.
- Contamination monitoring of work areas must be conducted weekly.
- Health monitoring of the thyroid gland must be conducted within 5 days of radioactive labeling.
- All workers must wear an isotope monitoring badge when conducting work with radioactive samples.
- All doses must be maintained as low as reasonably achievable. Please review individual dose limits as specified on the radioactivity work permit.
- Pregnant female workers must stop work immediately and notify health physics as soon as pregnancy is confirmed.

E.6 Biological Waste Disposal Methods

- Solid radioactive waste must be disposed of in radioactive waste bins. Estimated radioactivity must be recorded and signed by the user.
- Liquid radioactive waste must be disposed of in chemical waste containers in the fume hood. Waste contents must be identified (ex. I-125, BSA)
- TCA waste must be disposed of in separate waste containers as marked (ex. I-125, BSA, TCA) in the fume hood.
- Radioactive needles must be disposed of in radioactive sharps waste container in the fume hood.

E.7 Spill Response Procedures

E.7.1 Small Spills

1. Notify workers in the area that a spill has occurred.
2. Wear appropriate PPE then wipe it up with paper towels or the absorbent pads using tweezers, working from the outside of the spill to the center.
3. Place waste in a ziplock bag.
4. Wash the contaminated surface with Extrand and wipe and bag again for disposal.
5. Monitor yourself and the area for contamination frequently.

E.7.2 Large Spills

For spills involving a large volume of radioactive liquids with bound isotope.

For spills of any volume involving free isotope.

Notify health physics promptly at x24226, or x88 (security) after hours.

E.8 Biosafety Training Requirements

- All required McMaster safety courses for workers.
- Biosafety level 1 (BSL-1)
- Radioactive Safety Training

E.9 References

McMaster Health Physics. (2017). Initial Radiation Safety Training at McMaster University [PowerPoint Slides]. Retrieved from <https://www.mcmaster.ca/healthphysics/Library/General%20Radiation%20Safety%20Training%20at%20McMaster%20-%20Online%20Material.pdf>

APPENDIX F: Quantifying *E. coli* Adhesion SOP

F.1 Purpose

To quantify *E. coli* adhesion on modified surfaces.

F.2 Materials

- Modified PDMS, PC, and glass samples at n=3 per modification
- 10X phosphate buffered saline (PBS), pH 7.4 (BioShop Canada Inc., Burlington, ON)
 - Prepared as 1X PBS by dilution in Milli-Q water
- *E. coli* K-12 expressing GFP from plasmid (Courtesy of Dr. Schellhorn Lab)
- Eppendorf tubes
- 96-well plates
- 48-well plates
- Agar plates

F.3 Methods

1. Streak *E. coli* stock (from -80°C storage) onto an agar plate.
2. Incubate the agar plate at 37°C for 16 h.
3. Prepare kanamycin antibiotics by mixing 50 mL of water and 1.25 g of kanamycin. Mix well then filter.
4. Inoculate *E. coli* cultures from the agar plate in LB media supplemented with 25 µg/mL Kanamycin the night before (~13 h before use).
5. Sterilize surfaces with 70% EtOH and rinse with Milli-Q water.
6. Hydrate surfaces in PBS the night before in a 96-well plate.
7. The next morning, check the optical density (OD) of the culture on a spectrophotometer. Mix the culture well and add Allow the culture to grow until OD = 0.4-0.6.
8. Calculate the volume of *E. coli* stock needed (V_i) to obtain 1 mL of 10^9 cells/mL. (i.e. $OD_f = 1$ and $V_f = 1$)

$$OD_i V_i = OD_f V_f$$

9. In eppendorf tubes, add the calculated volume (V_i) of *E. coli* stock and centrifuge at 12 G for 2 min. Remove the supernatant. Resuspend in 1 mL of PBS.
10. Make seeding solutions of 2×10^7 cells/mL and 2×10^8 cells/mL *E. coli*.
11. Place PDMS and PC samples in eppendorf tubes. Place glass samples flat in 48-well plates. (n=3 per material, per modification).
12. Add 1 mL of 2×10^7 cells/mL to PDMS and glass. Add 1 mL of 2×10^8 cells/mL to PC.
13. Place PDMS and PC samples in an eppendorf rack. Secure the rack horizontally in a shaker at 37°C, 200 RPM. Incubate for 4 h.
14. Place glass samples in a stationary incubator at 37°C. Incubate for 5 h.
15. Fill a 96-well plate with PBS. Rinse PDMS and PC samples in 3 wells (3 rinses) for 5 min each. Do not rinse glass surfaces.
16. Image samples on an Evos FL Auto epifluorescence microscope (Life Technologies, United States) equipped with a YFP LED light cube (Ex. 500/24nm; Em. 524/27nm) at 20x objective.
17. Acquire 10 images per sample of highest cell density areas.
18. Count cells using ImageJ particle analysis software.

F.4 Hazard Identification and Risk of Exposure to Hazards

- Risk of contamination by: ingestion

F.5 Exposure Controls specific to Above Risk of Exposure

- Intestinal illness, fever, diarrhea

F.6 Biological Waste Disposal Methods

- Dispose all waste in biohazardous waste bins
- Bleach *E. coli* cultures with 10% bleach. Dispose bleached solutions in the sink with lots of running water.

F.7 Spill Response Procedures

Use a biological spill kit to wipe up the spill. Dispose paper towels in biohazardous waste. Clean surface with 70% EtOH.

F.8 Biosafety Training Requirements

- All required McMaster safety courses for workers.
- Biosafety level 1 (BSL-2)

F.9 References

Public Health Agency of Canada. (2017). Escherichia Coli Pathogen Safety Data Sheet – Infectious Substances. Retrieved from <http://www.phac-aspc.gc.ca/lab-bio/res/psds-ftss/escherichia-coli-eng.php>